



Search for events with a pair of displaced vertices from long-lived neutral particles decaying into hadronic jets in the ATLAS muon spectrometer in pp collisions at $\sqrt{s} = 13$ TeV

The ATLAS Collaboration

A search for events with two displaced vertices from long-lived particles (LLP) pairs using data collected by the ATLAS detector at the LHC is presented. This analysis uses 139 fb^{-1} of proton–proton collision data at $\sqrt{s} = 13$ TeV recorded in 2015–2018. The search employs techniques for reconstructing vertices of LLPs decaying to jets in the muon spectrometer displaced between 3 m and 14 m with respect to the primary interaction vertex. The observed numbers of events are consistent with the expected background and limits for several benchmark signals are determined. For the Higgs boson with a mass of 125 GeV, the paper reports the first exclusion limits for branching fractions into neutral long-lived particles below 0.1%, while branching fractions above 10% are excluded at 95% confidence level for LLP proper lifetimes ranging from 4 cm to 72.4 m. In addition, the paper present the first results for the decay of LLPs into into $t\bar{t}$ in the ATLAS muon spectrometer.

Contents

1	Introduction	2
2	ATLAS detector	3
3	Analysis strategy	4
4	Signal model	5
5	Data and MC simulation	6
6	Trigger selection and event reconstruction	7
6.1	Muon RoI Cluster trigger	8
6.2	Reconstruction of MS displaced vertices	9
6.3	Reconstruction of the primary vertex and prompt hadronic jets	9
7	Event selection	9
7.1	Baseline event selection	10
7.2	Signal displaced vertex selection	11
7.3	MS displaced vertex reconstruction efficiency	13
8	Background estimation	14
9	Systematic uncertainties	15
10	Results	16
11	Summary	19

1 Introduction

The discovery of the Higgs boson at the LHC completed the Standard Model (SM) of elementary particles and focused attention on the many central features of our universe that the SM does not address: dark matter, neutrino mass, matter–antimatter asymmetry, and the hierarchy problem (naturalness). Many beyond-the-SM (BSM) theoretical constructs that address these phenomena predict the existence of long-lived particles (LLPs), with macroscopic decay lengths.

Examples of these constructs include supersymmetric (SUSY) models such as mini split SUSY [1, 2], gauge-mediated SUSY breaking [3], R -parity-violating SUSY [4, 5] and Stealth SUSY [6, 7]; models addressing the hierarchy problem such as Neutral Naturalness [8–11] and Hidden Valley [12, 13]; models addressing dark matter [14–18], and the matter–antimatter asymmetry of the universe [19–21]; and models that generate neutrino masses [22, 23]. Many of these theoretical models result in neutral LLPs, which may be produced in the proton–proton collisions at the LHC and decay back into SM particles far from the interaction point (IP). Such LLP decays can result in secondary decays significantly displaced from the IP that are usually referred to as displaced vertices (DVs).

Searches for LLPs decaying into final states containing jets have been carried out at LEP by DELPHI [24], at the Tevatron by both the CDF [25] and D0 [26] collaborations, and at the LHC by the ATLAS, CMS and LHCb collaborations [27–43]. To date, no search has observed evidence of BSM, neutral LLPs.

This search focuses on DVs occurring in the ATLAS muon spectrometer (MS) and uses 139 fb^{-1} of 13 TeV pp collision data. The event selection criteria and vertex reconstruction algorithms choose candidate events with two MS DVs. The results are interpreted in terms of a scalar portal model, but the analysis may be sensitive to additional models. These results supersede those of a previous search [38] for events with two MS DVs in a smaller 13 TeV dataset. Furthermore, the current analysis uses an improved background estimation methodology, more advanced modeling of the trigger and vertex reconstruction in Monte Carlo (MC) simulation, as well as a refined signal efficiency extrapolation as a function of the LLP lifetime.

The paper describes the ATLAS detector in Section 2, followed by an overview of the analysis strategy in Section 3 and the theoretical models in Section 4. Details of the pp collision data and MC simulation are provided in Section 5, while those of the specialized trigger and the purpose-built displaced vertex reconstruction algorithm follow in Section 6. The baseline event selection is described in Section 7.1, while Section 7.2 describes the signal selection and Section 8 describes the background estimation. The systematic uncertainties are discussed in Section 9, and the results are presented in Section 10.

2 ATLAS detector

The ATLAS detector [44], which has nearly 4π steradian coverage,¹ is a multipurpose detector consisting of an inner tracking detector (ID) surrounded by a superconducting solenoid providing a 2 T axial magnetic field, electromagnetic and hadronic calorimeters, and a muon spectrometer (MS) based on three large air-core toroidal superconducting magnets, each with eight coils. The field integral of the toroids ranges between 2.0 and 6.0 T m across most of the detector.

The ID covers the pseudorapidity range $|\eta| < 2.5$. It consists of a silicon pixel detector, a silicon microstrip detector, and a straw-tube transition-radiation tracker.

The calorimeter system covers the pseudorapidity range $|\eta| < 4.9$. It consists of a high-granularity electromagnetic calorimeter (ECal) surrounded by a hadronic calorimeter (HCal). Within the region $|\eta| < 3.2$, the ECal comprises liquid-argon (LAr) barrel and endcap electromagnetic calorimeters with lead absorbers. An additional thin LAr presampler covering $|\eta| < 1.8$ is used to correct for energy loss in material upstream of the calorimeters. The ECal extends from 1.5 m to 2.0 m in r in the barrel and from 3.6 m to 4.25 m in $|z|$ in the endcaps. The HCal is a steel/scintillator-tile calorimeter that is segmented into three barrel structures within $|\eta| < 1.7$, and two copper/LAr hadronic calorimeters in the endcaps ($1.5 < |\eta| < 3.2$). The HCal covers the region from 2.25 m to 4.25 m in r in the barrel (although the HCal active material extends only up to 3.9 m) and from 4.3 m to 6.05 m in $|z|$ in the endcaps. The solid angle coverage is completed with forward copper/LAr and tungsten/LAr calorimeter modules optimized for electromagnetic and hadronic measurements, respectively. Together the ECal and HCal have a thickness of 9.7 interaction lengths at $\eta = 0$.

¹ ATLAS uses a right-handed coordinate system with its origin at the nominal IP in the center of the detector and the z -axis along the beam pipe. The x -axis points from the IP to the center of the LHC ring, and the y -axis points upwards. Cylindrical coordinates (r, ϕ) are used in the transverse plane, where ϕ is the azimuth angle around the z -axis. The pseudorapidity is defined in terms of the polar angle θ as $\eta = -\ln \tan(\theta/2)$. Angular distance is measured in units of $\Delta R \equiv \sqrt{(\Delta\eta)^2 + (\Delta\phi)^2}$.

The MS comprises three stations of separate trigger and tracking chambers that measure the deflection of muons in a magnetic field generated by the air-core toroid magnets. The barrel and endcap chamber systems are subdivided into 16 sectors: 8 large sectors and 8 small sectors. For the barrel, the small sectors are inside each of the 8 magnet coils and the large sectors are between the coils. The endcap TGC chambers are arranged into 24 or 48 sectors depending on their η and radial position. Three stations of resistive-plate chambers (RPC) and thin-gap chambers (TGC) are used for triggering in the MS barrel and endcaps, respectively. The first two RPC stations, which are radially separated by 0.5 m, begin at a radius of either 7 m (large sectors) or 8 m (small sectors). The third station is located at a radius of either 9 m (large sectors) or 10 m (small sectors). In the endcaps, the first TGC station is located at $|z| = 13$ m. The other two stations start at $|z| = 14$ m and $|z| = 14.5$ m, respectively. The muon trigger system covers the range $|\eta| < 2.4$. The muon tracking chamber system covers the region $|\eta| < 2.7$ with three stations of monitored drift tubes (MDT), complemented by cathode-strip chambers (CSC) in the forward region. The MDT chambers consist of two multilayers separated by a distance ranging from 6.5 mm to 317 mm. Each multilayer consists of three or four layers of drift tubes. The individual drift tubes are 30 mm in diameter and have lengths of 2–5 m (barrel) and 2–6.5 m (endcaps) depending on the location of the chamber in the spectrometer. In each multilayer, charged-particle track-segment reconstruction entails finding the line that is tangent to the drift circles. These single-multilayer segments are local measurements of the position and direction of the charged particle. Because of its design, the MDT measurement provides only a very coarse ϕ position of the track hit. In order to reconstruct the ϕ position and direction, the MDT measurements are combined with the ϕ -coordinate measurements from the trigger chambers.

The ATLAS trigger and data acquisition system [45] consists of a hardware-based first-level (L1) trigger followed by a software-based high-level trigger (HLT) that reduces the rate of events selected for offline storage to 1 kHz.

The implementation of the L1 muon trigger logic is similar for the RPC and TGC systems. Each of the three stations of the RPC system and the two outermost stations of the TGC system consist of a doublet of independent detector layers. The first TGC station contains a triplet of detector layers. The transverse momentum (p_T) of the muon candidate is measured by the L1 muon trigger, using different algorithms for low- p_T and high- p_T triggers. In the barrel, a low- p_T (< 10 GeV) muon region-of-interest (RoI) is generated by requiring a coincidence of hits in at least three of the four layers of the two inner RPC stations. In the endcaps, the trigger requires hits in the two outer TGC stations. A high- p_T muon RoI in the barrel requires additional hits in at least one of the two layers of the outer RPC station, while for the endcaps, additional hits in two of the three layers of the innermost TGC station are required. The muon RoIs have an angular extent of 0.2×0.2 in $\Delta\eta \times \Delta\phi$ in the MS barrel and 0.1×0.1 in $\Delta\eta \times \Delta\phi$ in the MS endcaps.

An extensive software suite [46] is used in the reconstruction and analysis of real and simulated data, in detector operations, and in the trigger and data acquisition systems of the experiment.

3 Analysis strategy

The analysis presented in this paper searches for events with two DVs in the MS. The benchmark models that motivate these strategies are discussed in detail in Section 4.

Candidate events are selected by the Muon RoI Cluster HLT trigger [47], and a dedicated algorithm is used to reconstruct DVs in the MS [48]. Additional selection criteria, optimized by comparing expected signal events with background events, are used to maximize the analysis sensitivity.

The main background to LLPs decaying into hadronic jets in the MS originates from hadronic or electromagnetic showers not fully contained in the calorimeter volume (*punch-through jets*) that result in tracks reconstructed in the MS. Multijet events that result in vertices in the MS will often have ID tracks and calorimeter jets that point towards the MS DV. To reduce the acceptance of such fake vertices from multijet events, vertices are required to be isolated in η and ϕ from ID tracks and calorimeter jets. Multijet events with mismeasured jets are another source of background as they will not be removed by the isolation criteria.

Additional background, referred to as *noncollision background*, can be generated by electronic noise in the MDT and RPC/TGC chambers, by cosmic-ray muons, and by the LHC beam (beam-induced background [49]). This last contribution is composed of hadronic and electromagnetic showers caused by beam protons interacting with collimators or residual gas molecules inside the vacuum pipe.

To avoid unintended biasing of the results during the development of the analysis, the number of events observed in the signal region was not measured until the entire set of selection criteria were optimized and all the systematic uncertainties completely evaluated.

4 Signal model

Although this analysis is sensitive to a large variety of models, this paper interprets the results in terms of a *scalar portal* model [13], where a Higgs boson with a mass of 125 GeV or a lower/higher-mass scalar boson, both indicated by the symbol Φ , decays into two long-lived scalars.

A standard way of introducing long-lived, neutral particles to the SM is through a hidden sector that weakly couples to the SM. Scalar portals, where a 125 GeV Higgs boson or a lower/higher-mass scalar boson mixes weakly with a hidden-sector scalar field, can result in pair production of long-lived hidden-sector scalars or pseudoscalars that carry no SM quantum numbers. An indirect upper limit on the BSM Higgs boson decays of the order of 20% can be derived from combined studies of the Higgs boson production and decay [50, 51] under several assumptions, potentially allowing sizable branching fractions for decays into non-SM particles.

Long-lived scalars with a mass from 5 to 30 GeV are also well motivated by naturalness models that are generic extensions of hidden-valley portal models [52].

The mechanism for LLP production is shown in Figure 1. Here, a scalar boson Φ decays with some effective coupling into a pair of long-lived scalars, s . The scalars s subsequently decay into SM particles. In this model the couplings of the scalar s to SM fermions are determined by the Higgs Yukawa coupling. Therefore, each long-lived scalar decays mainly into the heaviest fermion pair that is kinematically accessible. The branching fractions of $b\bar{b}$, $c\bar{c}$, and $\tau^+\tau^-$ decays depend on the mass of the scalar (m_s), and for $m_s \gtrsim 25$ GeV they are almost independent of its mass and equal to 85%, 5%, and 8%, respectively. While only these decay modes were considered in the previous ATLAS publication [38], this paper also considers the decay into $t\bar{t}$ as it is the dominant decay mode when it becomes kinematically available.

The branching fraction for Φ decaying into a pair of long-lived scalars is not constrained in these models. It is therefore interesting to focus on Φ decays into LLPs where Φ is a Higgs boson with a mass of 125 GeV or another scalar with a different mass.

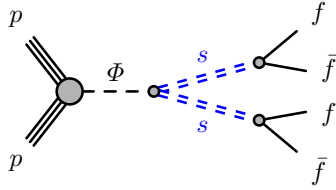


Figure 1: Diagram of the scalar portal model studied in this paper. The LLPs are represented by double lines and labeled s , and the final-state SM fermions are labeled as f [13].

The relative masses and lifetimes generated, as well as details about the Monte Carlo (MC) event generation are described in Section 5. Only the gluon–gluon fusion production mode is considered, as it is the dominant production mode.

5 Data and MC simulation

The analysis presented in this paper uses $\sqrt{s} = 13$ TeV pp collision data recorded by the ATLAS detector with stable LHC beams during the 2015–2018 data-taking periods [53]. Events are required to have been taken during stable beam conditions and when all the detector subsystems were operational. After data quality requirements [53], the total integrated luminosity is 139 fb^{-1} .

An unbiased random trigger (the zero-bias trigger) that fires on the bunch crossing occurring one LHC revolution after a low-threshold calorimeter-based trigger was used to collect data for background estimation with negligible signal contamination. The zero-bias trigger runs throughout the ATLAS data-taking, so the events are acquired with the same beam conditions present in normal physics data-taking and can be used to study the expected background. The zero-bias trigger was prescaled as a function of the instantaneous pileup to have a fixed output event rate throughout the data-taking period. Therefore, to estimate the correct number of background events, the pileup profile from the zero-bias trigger was rescaled to match that from the data used to select candidate events.

Signal MC simulation samples were produced using the Hidden Abelian Higgs Model [54], considering only the gluon–gluon fusion production mechanism. The masses, summarized in Table 1, were chosen to span the accessible parameter space. The mean proper lifetime in each sample was tuned to maximize the number of decays throughout the ATLAS detector volume and covers a range of 0.13–6 m, depending on the sample. All samples were generated at leading order using MADGRAPH5_AMC@NLO [55] interfaced to the PYTHIA 8 [56] parton shower model. The Φ transverse momentum distribution for the samples is reweighted to match that obtained for the corresponding next-to-leading order (NLO) Higgs samples generated using the MADGRAPH5_AMC@NLO merging approach [57]. A set of tuned parameters called the A14 tune [58] was used together with the NNPDF3.1LO parton distribution function (PDF) set [59]. The EVTGEN 1.2.0 program [60] was used to model b - and c -hadron decays. The generated events were processed through a full simulation of the ATLAS detector geometry and response [61] using the GEANT4 [62] toolkit. The simulation includes multiple pp interactions per bunch crossing (pileup), as well as the effect on the detector response due to interactions from bunch crossings before or after the one containing the hard interaction. Pileup was simulated with the soft strong-interaction processes of PYTHIA 8 using the A3 tune [63] and the NNPDF2.3LO [59] PDF set. Per-event weights were applied to the simulated events to match the distribution of the average number of interactions per bunch crossing measured in data.

A multijet background sample was generated using PYTHIA 8.230 [64] with leading-order matrix elements for dijet production which were matched to the parton shower. The NNPDF2.3_{LO} PDF set was used in the matrix element generation, the parton shower, and the simulation of the multiparton interactions. The A14 tune was used. Perturbative uncertainties were estimated through event weights [65] that encompass variations of the scales at which the strong coupling constant is evaluated in the initial- and final-state showers, as well as the PDF uncertainty in the shower and the nonsingular part of the splitting functions.

Table 1: Mass parameters for the simulated scalar portal based on the Hidden Abelian Higgs Model [54]. A second set of samples with a different lifetime was generated for some scalar masses to validate the lifetime-extrapolation procedure.

m_Φ [GeV]	m_s [GeV]	Proper lifetime [m]
125	5	0.127, 0.411
	16	0.580
	35	1.310, 2.630
	55	1.050, 5.320
60	5	0.217
	15	0.661
200	50	1.255
400	100	1.608
600	50	0.590
	150	1.840, 3.309
	275	4.288
1000	50	0.406
	275	2.399, 4.328
	475	6.039

Since the analysis is sensitive to a wide range of mean proper lifetimes, and the generation of many samples to cover a broad lifetime range would consume far too much CPU time, a toy MC method was adopted to extrapolate the expected number of events to the range of mean proper lifetimes between 0.01 and 1000 m. For each LLP in the MC sample, a random decay time, sampled from an exponential distribution of a chosen proper lifetime, was generated. The physical decay distance in the detector was then calculated for each simulated LLP using its four-momentum. The overall probability of the event to satisfy the signal selection criteria, parameterized as a function of the LLP decay position and boost, is then evaluated from the LLP trigger and vertex efficiencies described in Sections 6.1 and 7.3, respectively. In order to validate the lifetime-extrapolation procedure described above, a second set of samples with a different lifetime was generated for some scalar masses.

6 Trigger selection and event reconstruction

Hadronic LLP decays in the MS typically produce narrow, high-multiplicity hadronic showers. The track multiplicity and shower width vary with the mass and boost of the decaying LLP and the final states to which the LLP decays. Dedicated trigger [47] and vertex [48] algorithms were developed to select and reconstruct displaced decays in the MS. Due to the amount of material in the calorimeter, only decays occurring in or after the last sampling layer of the hadronic calorimeter produce enough hits in the MS to allow reconstruction of the DV.

6.1 Muon RoI Cluster trigger

The Muon RoI Cluster trigger is a signature-driven trigger that selects candidate events for decays of LLPs in the MS [47]. Events must contain at L1 two muon RoIs with a p_T higher than 10 GeV, and in the HLT a cluster of three (four) muon RoIs within a $\Delta R = 0.4$ cone centered on the L1 object in the barrel (endcaps). The isolation criteria for jets and tracks discussed in Ref. [47], used to reduce background DVs from punch-through jets, are not considered in the analysis presented in this paper. The trigger selects both isolated, signal-like events and nonisolated, background-like events used for data-driven background estimations.

The trigger efficiency, defined as the fraction of LLP decays in the MS fiducial volume that are selected by the trigger as a function of the LLP decay position, is shown in Figures 2(a) and 2(b) for four MC simulated benchmark samples with LLP decays in the MS barrel and endcap regions, respectively. The efficiency is parameterized as a function of the transverse decay radius (L_{xy}) in the barrel and the longitudinal decay position ($|L_z|$) in the endcaps. The events are required to pass the data quality requirements [53] and have a reconstructed primary vertex as described in Section 6.3. The trigger is efficient for hadronic decays of LLPs that occur anywhere from the outer regions of the HCal to the middle stations of the MS. These efficiencies are obtained from a subset of simulated signal events with only a single LLP decay in the muon spectrometer in order to ensure that the result of the trigger is due to a single burst of MS activity. The uncertainties shown are statistical only. The relative differences between the efficiencies of the benchmark samples are a result of the different masses of the LLPs, which in turn affect their momenta and consequently the opening angles of the decay products. The trigger efficiency increases as the LLPs decay closer to the end of the hadronic calorimeter, located at $r \approx 4$ m for the barrel and $|z| \approx 6$ m for the endcaps. The efficiency decreases rapidly as the decay occurs closer to the middle stations of the muon spectrometer (barrel: $r \approx 7$ m; endcaps: $|z| \approx 13$ m).

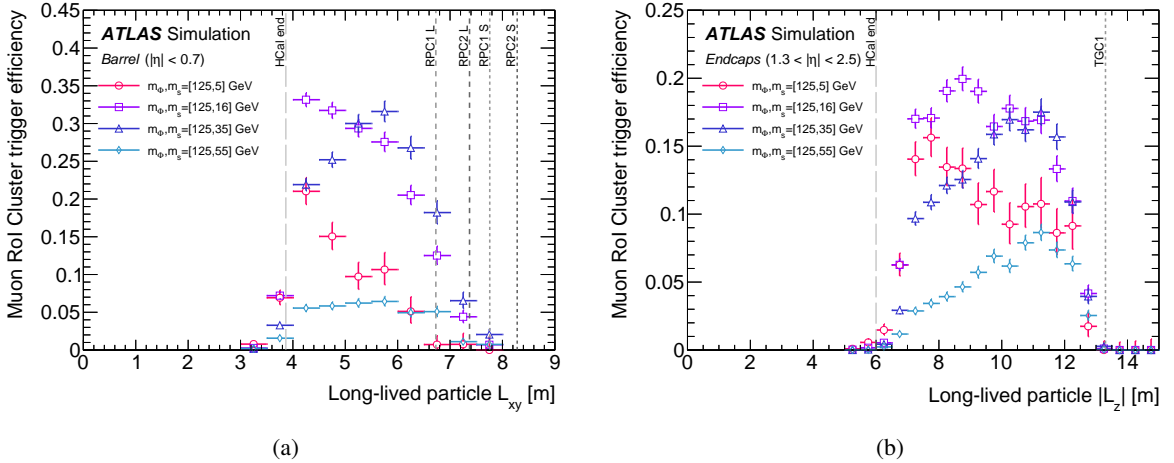


Figure 2: Efficiency for the Muon RoI Cluster trigger as a function of the decay position of the LLP for some scalar portal samples in the (a) MS barrel and (b) MS endcaps for events passing the data quality requirements and having a reconstructed primary vertex. These efficiency distributions are based solely on MC simulation, without any corrections applied for the mismodeling described in Section 6.1. The vertical lines show the relevant detector boundaries, where “HCal end” is the outer limit of the hadronic calorimeter, “RPC 1/2” represent the first/second stations of RPC chambers, “TGC 1” represents the first stations of TGC chambers and “L/S” indicate whether they are in the Large or Small sectors.

To quantify the mismodeling of the L1 muon trigger efficiency in MC simulation, the distributions of the number of muon-RoI clusters within a cone of $\Delta R = 0.4$ around the axis of a punch-through jet in multijet MC and data events are compared. High-energy jets in data were selected using jet triggers with a p_T threshold of 400 GeV or 420 GeV, depending on the data-taking period. MC simulation shows a rate of muon-RoI clusters that is 24% (20%) lower than in data in the barrel (endcaps). This mismodeling does not depend on the η , ϕ or p_T of the jet, and it is used as a systematic uncertainty on the signal trigger efficiency.

6.2 Reconstruction of MS displaced vertices

A dedicated algorithm [48], capable of reconstructing low-momentum tracks in a busy environment, is used to reconstruct the MS DV. This algorithm was also employed by previous searches for displaced decays in the MS [27, 29, 38]. The algorithm takes advantage of the spatial separation between the two multilayers inside a single MDT chamber. Single-multilayer straight-line segments that contain three or more MDT hits are reconstructed using a χ^2 fit. Segments from multilayer 1 are then matched with those from multilayer 2. The matched pair of a multilayer-1 segment with a multilayer-2 segment and their corresponding track parameters is called a *tracklet*. Tracklets that are spatially clustered within $|\Delta\eta| < 0.7$ and $|\Delta\phi| < \pi/3$ in the detector are extrapolated backwards to reconstruct the (η, ϕ) position of the MS DV with a χ^2 fit. At least three (four) tracklets are required to be used in the fit in the barrel (endcaps). Detectable vertices arise from decays that occur in the region between the outer edge of the HCal and the middle stations of muon chambers. Because their detector technology is different (no spatially separated multilayers), the CSC chambers are not used for the MS DV reconstruction.

6.3 Reconstruction of the primary vertex and prompt hadronic jets

Events are required to have a primary vertex (PV) with at least two tracks with $p_T > 500$ MeV. If more than one PV candidate is reconstructed, the candidate with the largest sum of the squares of the transverse momenta of all tracks associated with the vertex is selected.

Hadronic jets are constructed by using FastJet [66] to apply the anti- k_t jet algorithm [67] with a radius parameter $R = 0.4$. A collection of three-dimensional topological clusters of neighboring energy deposits in the calorimeter cells containing a significant energy above a noise threshold [68] provide input to the anti- k_t algorithm. After reconstruction, jets are calibrated using the procedure outlined in Refs. [69–75].

7 Event selection

All events considered in this search must pass an event-level selection to distinguish signal from background.

Table 2: Summary of the baseline selection criteria applied to data and simulated events. The variables $n_{\text{MDT}}/n_{\text{RPC}}/n_{\text{TGC}}$ are the numbers of MDT/RPC/TGC hits in the vertex cone, as described in the text, and η_{vx} is the pseudorapidity of the MS DV with respect to the IP.

Event passes data quality requirements and Muon RoI Cluster trigger	
Event has a PV with at least two tracks with $p_T > 500$ MeV	
Event has at least one MS DV	
MS DV is matched to the triggering muon-RoI cluster ($\Delta R(\text{DV}, \text{RoI cluster}) < 0.4$) In the case of two muon-RoI clusters, the second vertex must be matched to the second cluster	
$300 \leq n_{\text{MDT}} < 3000$	
<i>Barrel</i>	<i>Endcaps</i>
MS DV with $ \eta_{\text{vx}} < 0.7$	MS DV with $1.3 < \eta_{\text{vx}} < 2.5$
MS DV with $3 \text{ m} < L_{xy} < 8 \text{ m}$	MS DV with $L_{xy} < 10 \text{ m}$ and $5 \text{ m} < L_z < 15 \text{ m}$
$n_{\text{RPC}} \geq 250$	$n_{\text{TGC}} \geq 250$

7.1 Baseline event selection

A common baseline selection is applied to the events considered in this search and summarized in Table 2.

Events with at least one MS DV are required to pass the data quality requirements [53] and the Muon RoI Cluster trigger, and contain a PV. The PV selection has very little impact on the signal efficiency but it helps to reject background events; in simulation, the selected PV corresponds to the signal interaction in about 95%–99% of the cases, depending on the sample. Even though the LLPs are invisible in the ID, the scalar boson is produced with an average p_T of 20 GeV, and a number of tracks are left by recoiling particles produced in the same pp interaction.

An MS DV that arises from a displaced decay typically has many more hits than an MS DV from background. To take advantage of this difference, a minimum number of MDT (n_{MDT}) and RPC/TGC ($n_{\text{RPC}}/n_{\text{TGC}}$) hits is required. The n_{MDT} hits are counted in the MDT chambers that have their center within $\Delta\phi = 0.6$ and $\Delta\eta = 0.6$ of the DV (η, ϕ) direction. The n_{RPC} and n_{TGC} hits are the sum of hits that are within $\Delta R = 0.6$ of the DV position. A requirement on the maximum number of MDT hits is also applied to remove background events caused by coherent noise bursts in the MDT chambers. This selection has a negligible impact on the signal events.

A displaced decay that occurs in the transition region between the MS barrel and endcaps results in hits in both regions. Vertex reconstruction is performed separately in the barrel and endcaps, and only the barrel (endcap) hits are used in the barrel (endcap) vertex reconstruction algorithm. Therefore, MS vertices reconstructed from either of the two algorithms have fewer hits, as they are reconstructed from a subset of the full set of hits. This results in a decrease in the reconstruction efficiency, and occasionally two vertices being reconstructed from a single LLP decay. Therefore, the MS DVs with pseudorapidity $|\eta_{\text{vx}}|$ between 0.8 and 1.3 are not considered in the analysis. This has a negligible effect on the total signal efficiency, because the average MS DV reconstruction efficiency in this region is less than 2%. Moreover, in the transition region between the barrel and the endcap hadronic calorimeters, $0.7 < |\eta_{\text{vx}}| < 1.2$, the probability of having a jet that does not fulfill the minimal selection criteria to be considered for isolation

and also punches through into the MS is much higher than in other regions of the detector. This region overlaps the already excluded MS transition region, except for $0.7 < |\eta_{\text{vx}}| < 0.8$. Therefore, vertices reconstructed with pseudorapidity in the range $0.7 < |\eta_{\text{vx}}| < 0.8$ are also not considered.

The number of events passing the baseline selection is 1,385,587 and 5,138,794 in the barrel and endcaps, respectively. After these requirements, the main background contribution is from punch-through jets.

7.2 Signal displaced vertex selection

To reject background vertices created by punch-through jets, a set of *vertex isolation criteria* was established. These criteria are based on the angular distance, ΔR , between the direction of the tracks or jets and the vertex axis, defined as the line from the IP to the DV. No jets or tracks should be present in a ΔR cone around the MS DV axis. For isolation from tracks, two criteria are used. One is for isolation from tracks with $p_T > 5$ GeV (high- p_T tracks). The other takes the vector p_T sum of all tracks associated with the primary vertex (PV) that have $500 \text{ MeV} < p_T < 5$ GeV (low- p_T tracks) and are in a cone of $\Delta R = 0.2$ around the MS DV axis. The use of two different isolation criteria stems from the fact that some jets have most of their energy in a few hadrons, while others can consist of multiple low- p_T tracks. The isolation criteria are summarized in Table 3. An MS DV that satisfies these criteria is considered in the analysis.

Table 3: Summary of the vertex isolation criteria used to select signal DVs in the barrel and endcap regions.

Isolation requirements	Barrel	Endcaps
Isolation from high- p_T tracks ($p_T > 5$ GeV)	$\Delta R > 0.3$	$\Delta R > 0.6$
Isolation from low- p_T tracks ($\Sigma p_T(\Delta R < 0.2)$)	$\Sigma p_T < 10$ GeV	$\Sigma p_T < 10$ GeV
Isolation from jets	$\Delta R > 0.3$	$\Delta R > 0.6$

The isolation criteria were optimized for the MC benchmark samples by comparing simulated signal events with simulated multijet events. Figure 3 shows the cumulative vertex efficiency as a function of the isolation requirements in the barrel for data events and simulated multijet and signal events.

All jets considered for DV isolation must satisfy $p_T > 30$ GeV and $\log_{10}(E_{\text{HAD}}/E_{\text{EM}}) < 0.5$, where E_{HAD} is the jet energy deposited in the HCal, and E_{EM} the energy deposited in the ECal. The latter criterion is commonly used to identify the decay of a neutral LLP in the hadronic calorimeter [41] that results in little or no energy deposited in the electromagnetic calorimeter and consequently in an anomalously large value of the hadronic to electromagnetic energy ratio. It ensures that vertices originating from LLPs that decay near the outer edge of the hadronic calorimeter and also have significant MS activity are not rejected by the isolation requirement. In addition, in order to reduce the probability that pileup jets prevent a signal vertex from meeting the isolation criteria, jets with $20 < E_T < 60$ GeV must be matched to the PV by using a jet vertex tagger (JVT) discriminant [71]. Standard jet-quality criteria [76] are not applied because jets that do not fulfill these requirements can also produce a background MS DV, and therefore need to be considered when computing the isolation.

At least two isolated MS DVs must be present in the event. One MS DV must be matched to the trigger-level muon-RoI cluster by satisfying $\Delta R(\text{cluster}, \text{vertex}) < 0.4$. If there are two distinct clusters, each MS DV must be matched to a different cluster. To ensure that the two MS DVs and/or two muon-RoI clusters do not come from the same background activity, the two vertices are required to be separated by at least $\Delta R = 1.0$, which has minimal impact ($\lesssim 3\%$) on the overall signal acceptance. After the vertex isolation criteria are

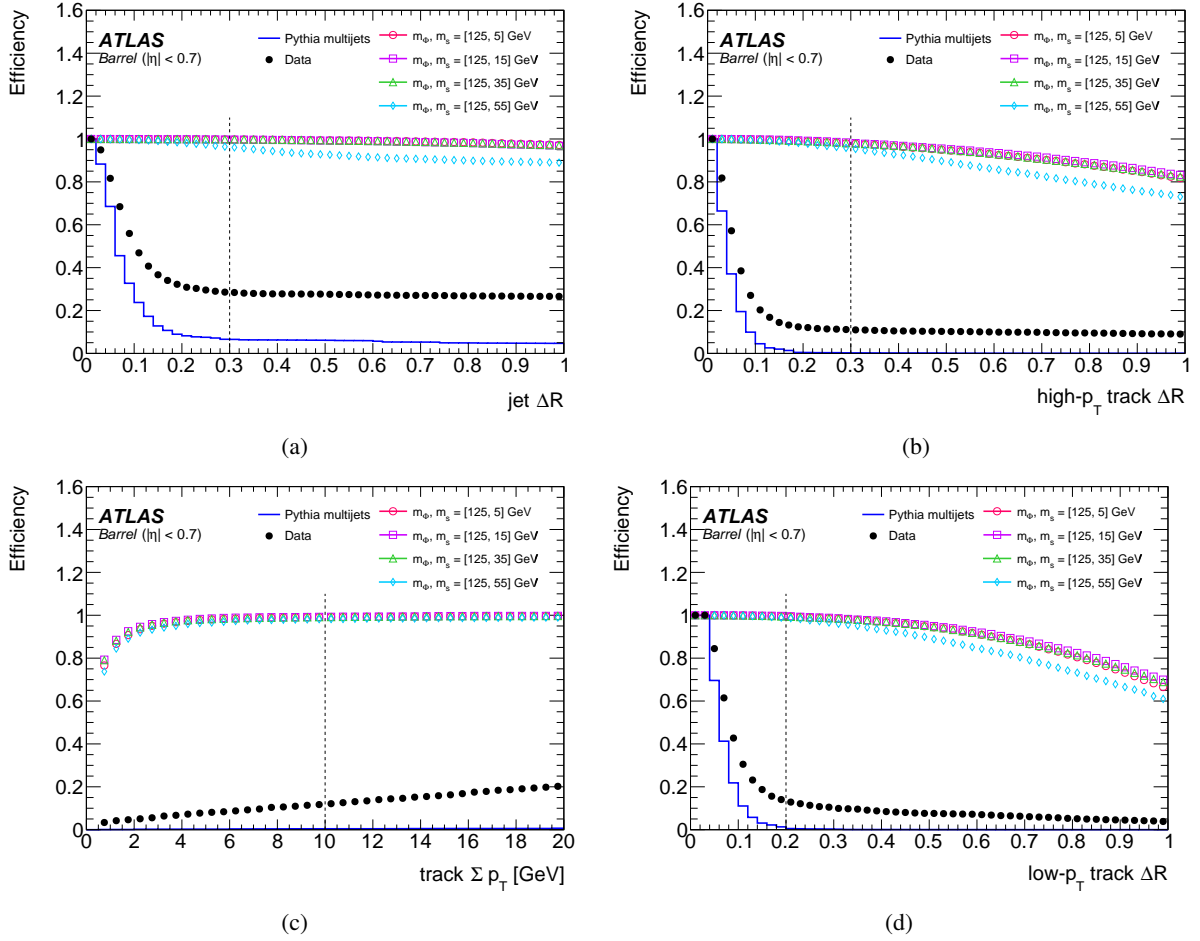


Figure 3: Cumulative efficiency of vertices in the barrel where the vertex is required to be isolated from (a) jets and (b) high- p_T tracks, as a function of the selected ΔR , when the sum of low- p_T tracks in a $\Delta R = 0.2$ cone around the vertex direction is required to be less than a specified cut in p_T (c), and when the sum of low- p_T tracks in a ΔR cone around the vertex is required to be less than 10 GeV, as a function of the ΔR value (d). The vertical lines show the selected ΔR value that is used in analysis. The differences between Pythia multijet and data distributions are attributable to the noncollision background, which is not present in MC simulations.

applied, most vertices from punch-through jets are eliminated, and the main background contribution is from noncollision backgrounds.

7.3 MS displaced vertex reconstruction efficiency

The efficiency for vertex reconstruction [48] is defined as the fraction of simulated LLP decays in the MS fiducial volume that correspond to a reconstructed vertex passing the baseline event selection reported in Table 2 and satisfying the vertex isolation criteria summarized in Table 3. A reconstructed vertex is considered matched to a displaced decay if the vertex is within $\Delta R = 0.4$ of the simulated decay position. The MS DV efficiency is parameterized as a function of the L_{xy} and $|L_z|$ LLP decay position in the barrel and endcaps, respectively. Figure 4(a) shows the efficiency for reconstructing a vertex in the MS barrel for a selection of benchmark samples. Figure 4(b) shows the efficiency for reconstructing a vertex in the MS endcaps.

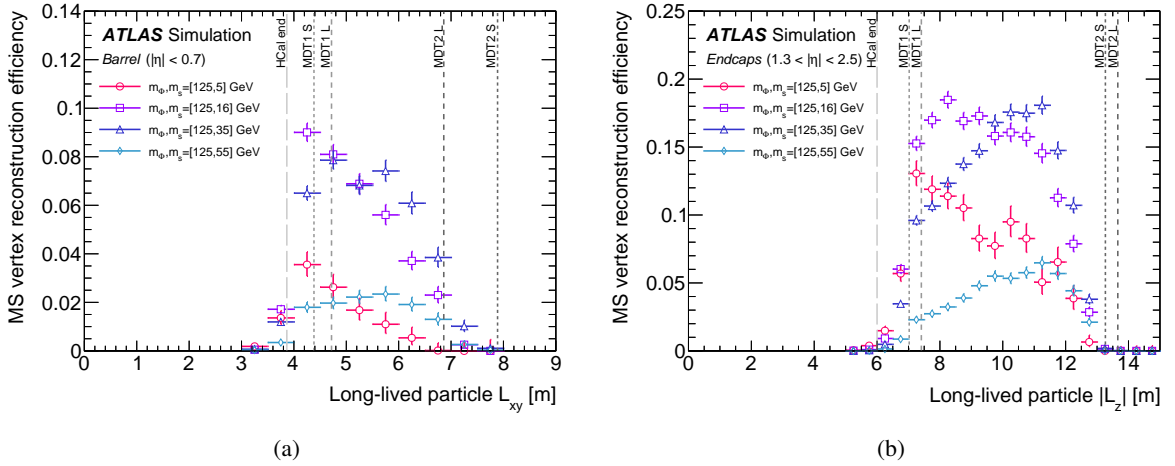


Figure 4: Efficiency to reconstruct an MS DV for scalar portal samples with $m_\phi = 125$ GeV for vertices that pass the baseline event selection and satisfy the vertex isolation criteria. (a): Barrel MS DV reconstruction efficiency as a function of the transverse decay position of the LLP. (b): Endcap MS DV reconstruction efficiency as a function of the longitudinal decay position of the LLP relative to the center of the detector. The efficiency distributions are corrected for the mismodeling described in Section 7.3. The vertical lines show the relevant detector boundaries, where “HCal end” is the outer limit of the hadronic calorimeter, “MDT 1/2” represent the first/second stations of MDT chambers and “L/S” indicate whether they are in Large or Small sectors.

For the MC samples considered in this paper, the MS barrel vertex reconstruction efficiency is $O(2 - 15)\%$ near the outer edge of the hadronic calorimeter ($r \approx 4$ m) and decreases substantially as the decay occurs closer to the middle stations ($r \approx 7$ m). The decrease occurs because the charged hadrons and photons are not spatially separated and overlap when they traverse the middle stations. This results in a reduction of the efficiencies for tracklet reconstruction and, consequently, vertex reconstruction. The efficiencies are also shaped by the mass and boost of the LLP. The efficiency for reconstructing vertices is higher in the MS endcaps due to a more efficient selection and vertex reconstruction, and it reaches 40% for higher-mass benchmark models. Since the magnetic field in the region in which endcap tracklets are reconstructed is very weak, the vertex reconstruction does not have the curvature constraints on the tracklets from the charge and momentum measurements that are present in the barrel. Therefore, in the endcaps, the vertex reconstruction algorithm uses straight-line fits so that low-momentum tracks are not rejected,

while in the barrel the curvature plus combinatorics provide better rejection of misreconstructed tracks. Consequently, the vertex reconstruction in the endcaps is more efficient for signal, but also less robust in rejecting background events. More details are provided in Ref. [48].

Potential MC simulation inaccuracies in the DV reconstruction are estimated by comparing the distribution of the number of tracklets in a punch-through jet ΔR cone of 0.4 in data and MC events using a strategy similar to the one used for the trigger, which was described in Section 6.1. MC simulation shows a rate of tracklets that is 20% (15%) higher than in data in the barrel (endcaps). This mismodeling does not depend on the η , ϕ or p_T of the jet. Its impact on the DV reconstruction efficiency is estimated by randomly dropping tracklets used to reconstruct the vertex in accordance with the measured mismodeling factor in the barrel and endcaps and counting the number of reconstructed vertices. The efficiency variation between the nominal reconstruction and the one considering the mismodeling factors, averaged over the MC benchmark samples, is 27% in the barrel, and 9% in the endcaps. The corrected efficiencies are used to compute the expected number of signal events. The systematic uncertainty associated to this correction is discussed in Section 9.

Over the range of the extrapolated lifetimes, the maximum acceptance times efficiency for vertices passing the signal selection ranges from 0.005% (for the MC sample with $m_\Phi = 60$ GeV, $m_s = 5$ GeV at a proper lifetime of 0.5 m) to 0.3% (for the MC sample with $m_\Phi = 600$ GeV, $m_s = 50$ GeV at a proper lifetime of 1.1 m).

8 Background estimation

The two-MS-vertex strategy is designed to be sensitive to models where two LLPs are produced and decay hadronically between the outer region of the HCal and the middle stations of the MS. Requiring two MS DVs significantly reduces the background. In addition, background from punch-through jets is further reduced using the isolation criteria described in Section 7.2.

Residual background can arise from collision or noncollision processes and cannot be simulated accurately. Thus, a data-driven method is used to estimate the expected background. This has the advantage of avoiding the systematic uncertainties related to simulation accuracy present when using MC-based background estimates.

As described in Section 7.1, the signal selection requires that one vertex is always matched to a RoI cluster, and only in the case of two RoI clusters the second vertex is also required to be matched. Therefore, we can naturally factorize the background estimation into three terms:

$$N_{2Vx} = N^{1cl} \cdot P_{\text{noMStrig}}^{Vx} + N_{1UMBcl}^{2cl} \cdot P_{Bcl}^{Vx} + N_{1UMEcl}^{2cl} \cdot P_{Ecl}^{Vx} . \quad (1)$$

The first term in Eq. (1) gives the number of background events that contain one vertex-cluster pair anywhere in the detector fiducial region and one other isolated MS vertex anywhere in the same fiducial region. The second and third terms estimate the number of background events that contain one vertex-cluster pair anywhere in the detector fiducial region and an additional vertex-cluster pair in the barrel or endcap region. The background from events with one muon-RoI cluster (first term in Eq. (1)) is estimated by multiplying the number of events with one muon-RoI cluster (N^{1cl}) by the probability of finding an isolated MS DV vertex in events not selected by the Muon RoI Cluster trigger (P_{noMStrig}^{Vx}). The probability P_{noMStrig}^{Vx} is determined using data collected with the zero-bias trigger and it is found by dividing the number of events

with an isolated MS DV (N^{1Vx}) by the total number of zero-bias events that satisfy standard event-quality requirements (N_{Events}). The background from events with two muon-RoI clusters (second and third terms in Eq. (1)) is estimated by multiplying the number of events with two muon-RoI clusters where one of the two clusters is not matched to an isolated vertex in the barrel (N_{IUMBcl}^{2cl}) or endcaps (N_{IUMEcl}^{2cl}) by the probability of finding an MS DV vertex given a muon-RoI cluster in the barrel or endcaps respectively (P_{Bcl}^{Vx} and P_{Ecl}^{Vx}). The probabilities P_{Bcl}^{Vx} and P_{Ecl}^{Vx} are found by dividing the number of events with an isolated MS DV matched to a muon-RoI cluster (N^{1BclVx} and N^{1EclVx}) by the number of events with a muon-RoI cluster (N^{1Bcl} and N^{1Ecl}).

All the numbers of events and probabilities used in Eq. (1) are reported in Table 4.

Table 4: Numbers of events in the 13 TeV dataset passing the zero-bias and Muon RoI Cluster triggers.

Stream	Quantity	Value
Zero-bias	N_{Events}	$115,709,000 \pm 11,000$
	N^{1Vx}	53 ± 7
	$\rightarrow P_{\text{noMStrig}}^{Vx}$	$(4.58 \pm 0.63) \times 10^{-7}$
Muon RoI Cluster	N^{1cl}	$674,800 \pm 800$
	N_{IUMBcl}^{2cl}	$3^{+2.43}_{-1.17}$
	N_{IUMEcl}^{2cl}	$0^{+1.35}_{-0.00}$
	N^{1Bcl}	$38,509,000 \pm 6000$
	N^{1BclVx}	$124,650 \pm 350$
	$\rightarrow P_{\text{Bcl}}^{Vx}$	$(3.24 \pm 0.01) \times 10^{-3}$
	N^{1Ecl}	$15,599,000 \pm 4000$
	N^{1EclVx}	$550,100 \pm 700$
	$\rightarrow P_{\text{Ecl}}^{Vx}$	$(3.53 \pm 0.01) \times 10^{-2}$

All events used for the background estimation are orthogonal to the signal region that requires two isolated DVs. Therefore, events that pass the Muon RoI Cluster trigger and have only one isolated MS DV are assumed to be fake vertices not due to displaced decays. Potential signal contamination would result in an overestimation of the background rates, but its contribution has been estimated to be smaller than 0.02% for injected signal with rates of the order of the observed 95% CL upper limits.

The background estimation strategy was validated using an orthogonal signal-free data sample obtained by inverting the isolation criteria used to define the signal region. In this validation region, the expected number of background events was calculated to be 0.99 ± 0.20 and 1.56 ± 0.27 for one-cluster and two-cluster events, respectively, where the uncertainty is purely statistical. One event, which contained two clusters, was observed. Therefore, no systematic error is assigned to the background estimation.

The number of expected background events with two MS DVs is 0.32 ± 0.05 , where the uncertainty is statistical only.

9 Systematic uncertainties

The signal efficiency systematic uncertainties are dominated by the modeling of the signal physics processes, pileup and detector response and the extrapolation of the expected number of signal events as a function of

the LLP proper lifetime.

One of the sources of systematic uncertainty associated with the Muon RoI Cluster trigger is the modeling of the minimum-bias interactions used to simulate pileup; another stems from the systematic uncertainty due to the PDF used to generate signal MC events. These were estimated by varying the pileup and PDF weights in accord with the respective $\pm 1\sigma$ systematic uncertainties and evaluating the resultant change in the trigger efficiency. For the latter, uncertainties in the nominal PDF set were evaluated using 100 replica variations. In each case, the systematic uncertainty was determined to be negligible. The systematic uncertainty from the pileup and PDF contributions to the MS DV reconstruction efficiency for signal was evaluated with a procedure similar to that for the trigger, and again the systematic uncertainties were determined to be negligible.

The mismodeling of the L1 muon trigger efficiency in MC simulation described in Section 6 contributes a systematic uncertainty of 20% (24%) in the barrel (endcaps). Another source of systematic uncertainty is the uncertainty in the corrected efficiencies that is due to the MC mismodeling in the vertex reconstruction described in Section 7.3. The corrected vertex reconstruction efficiencies were also estimated with a second method, in which events are weighted such that the MC distribution of the number of reconstructed tracklets matches the data distribution. The efficiency was re-evaluated after reweighting each vertex according to how many tracklets are associated with it. The average efficiency variation is computed and its difference from the variation calculated using the nominal method described in Section 7.3 is taken as the systematic uncertainty, which is 11% in the barrel and 13% in the endcaps.

A systematic uncertainty associated with the efficiency extrapolation method was estimated by comparing the signal efficiency computed using the fully simulated MC samples with the one extrapolated (using toy MC samples) at the same proper lifetime. The difference between the two efficiencies is used as the systematic uncertainty, and it varies from 1.9% to 30%, depending on the kinematics of the sample. For several of the signal samples, two proper lifetime points were fully simulated: one nominal sample and a secondary sample with longer proper lifetime, as described in Section 5. The secondary sample was used to cross-check the lifetime-extrapolation procedure, and good closure was found.

An uncertainty on the NLO-reweighting of the signal samples is obtained by comparing the 125-GeV mediator NLO MADGRAPH predictions to next-to-next-to-leading-order (NNLO) accuracy in QCD using POWHEG Box v2 [77–81]. This results in an additional uncertainty on the signal efficiency ranging from 0.1 to 4%.

The uncertainty in the combined 2015–2018 integrated luminosity is 1.7% [82], obtained using the LUCID-2 detector [83] for the primary luminosity measurements.

The systematic uncertainties described above change the production cross-section limits by about 15% on average.

10 Results

In ATLAS Run 2 data, 0.32 ± 0.05 background events are expected for this analysis. Zero events are observed in the signal region.

Upper limits on the production cross-section times branching fraction are derived using the CL_s prescription [84], implemented with the pyhf [85, 86] package using a profile likelihood function [87]. The likelihood includes a Poisson probability term describing the total number of observed events. Background and

signal uncertainties are taken into account using Gaussian terms, as commonly done in these cases. Pseudo-experiments which sample the distribution of the profile likelihood ratio are generated to compute the p -value and derive the exclusion limits.

For scalar boson benchmark samples with $m_\Phi \neq 125$ GeV, upper limits are set on $\sigma \times B$, where B represents the branching fraction for $\Phi \rightarrow ss$ assuming 100% branching fraction of s into the heaviest fermion pairs kinematically accessible. As discussed in Section 4, the long-lived scalar mainly decays into $b\bar{b}$, except when $m_s > 2m_t$ (i.e. for the sample with $m_\Phi = 1000$ GeV and $m_s = 475$ GeV) where the dominant decay is into $t\bar{t}$. For scalar boson benchmark samples with $m_\Phi = 125$ GeV, upper limits are set on $(\sigma/\sigma_{\text{SM}}) \times B$, where $\sigma_{\text{SM}} = 48.61$ pb [88] is the SM Higgs boson gluon–gluon fusion production cross-section.

Figure 5 shows a comparison between the expected and observed 95% CL upper limits for one representative sample as well as the observed 95% CL limits for all the MC benchmark samples. Observed limits are consistent with the expected ones within the uncertainty. For $m_\Phi = 125$ GeV the limits are stronger for intermediate LLP masses, while they become weaker for very low and very high masses. Moreover, the mean proper lifetime $c\tau_s$ at which the upper limit is strongest increases with the long-lived scalar mass. These patterns of behavior are correlated with changes in the trigger and reconstruction efficiencies that depend mainly on the kinematics of the LLP decay.

Table 5 summarizes the lifetime ranges excluded by the analysis for branching fractions $B(\Phi(125) \rightarrow ss) = 10\%$, 1% and 0.1% for the scalar boson with $m_\Phi = 125$ GeV decaying into two long-lived scalars.

Table 5: Ranges of mean proper lifetime excluded at 95% CL for scalar boson benchmark models with $m_\Phi = 125$ GeV, assuming a production cross-section times branching fraction equal to 10%, 1% and 0.1% of the SM Higgs boson production cross-section [88].

$\Phi(125) \rightarrow ss$ m_s [GeV]	Excluded $c\tau_s$ range for s [m]		
	$B = 0.1\%$	$B = 1\%$	$B = 10\%$
5	–	0.08–1.6	0.04–5.9
16	0.48–2.6	0.19–12.2	0.12–36.7
35	1.4–4.0	0.49–22.8	0.31–72.4
55	–	2.0–11.0	0.92–47.6

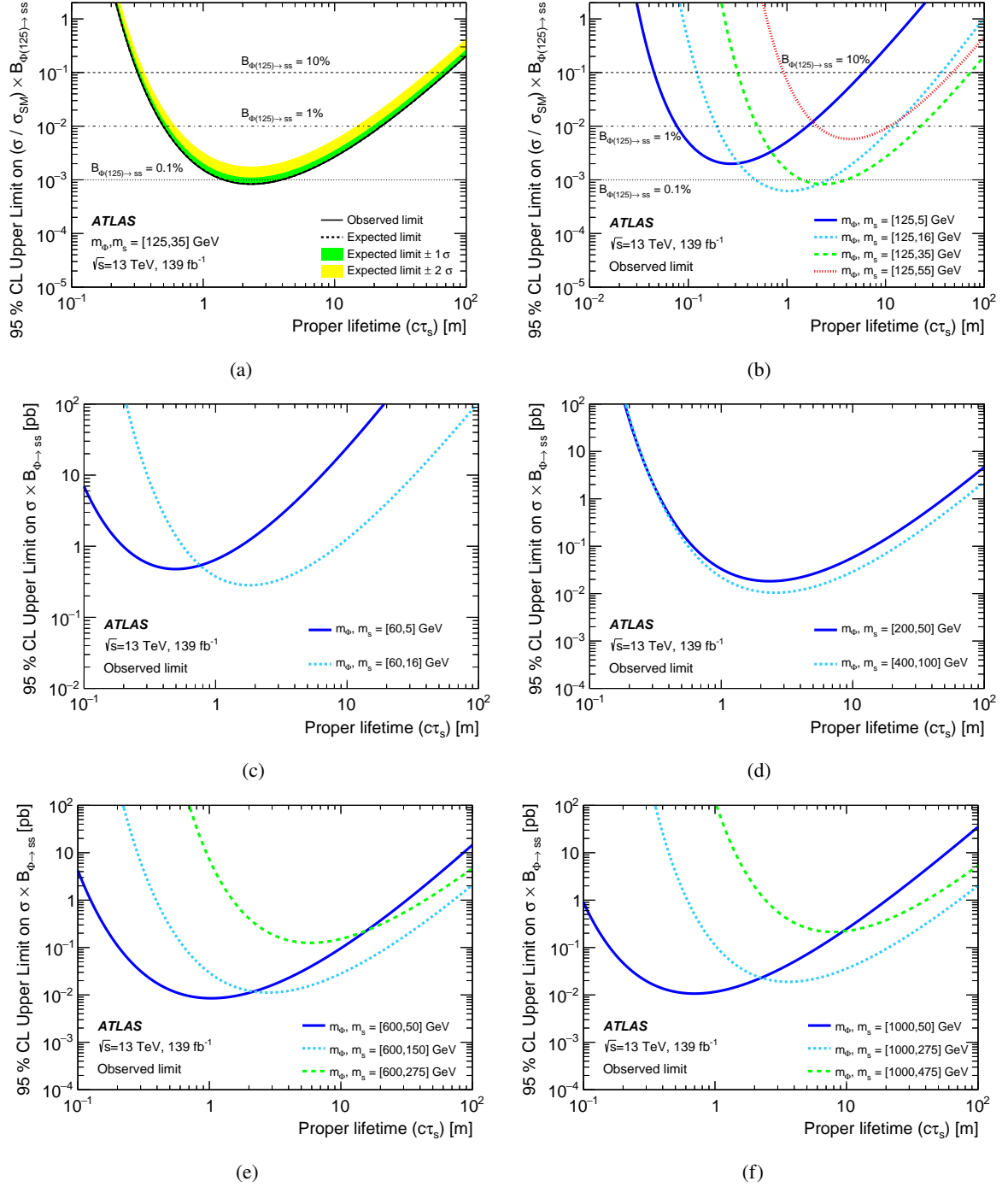


Figure 5: Comparison between observed and expected 95% CL limits (a) on $(\sigma/\sigma_{\text{SM}}) \times B$ for $m_\Phi = 125$ GeV and $m_s = 35$ GeV. Observed 95% CL limits (b) on $(\sigma/\sigma_{\text{SM}}) \times B$ for $m_\Phi = 125$ GeV, and (c)–(f) on $\sigma \times B$ for $m_\Phi \neq 125$ GeV.

11 Summary

This paper presents a search for events with two displaced vertices from pair-produced long-lived particles decaying into hadronic jets using 139 fb^{-1} of proton–proton collisions at $\sqrt{s} = 13 \text{ TeV}$ recorded at the LHC by the ATLAS detector during 2015–2018 data-taking period. The search is performed with the same strategy that ATLAS adopted in Run 1 and in a Run 2 search using 2015–2016 data, and benefits from very low background. A data-driven method is used to estimate the expected background in the signal region. No events with two reconstructed displaced vertices in the muon spectrometer are observed in the signal region, and exclusion limits on the LLP production cross-section as a function of its proper lifetime are computed for a scalar portal model where a Higgs boson with a mass of 125 GeV or another short-lived scalar can decay into two long-lived scalars. For the 125 GeV Higgs boson, the paper reports the first exclusion limits for branching fractions below 0.1%, while branching fractions above 10% are excluded at 95% confidence level for LLP mean proper lifetimes ranging from 4 cm to 72.4 m. In addition, the paper presents the first results for the decay of LLPs into $t\bar{t}$ in the ATLAS muon spectrometer.

Acknowledgments

We thank CERN for the very successful operation of the LHC, as well as the support staff from our institutions without whom ATLAS could not be operated efficiently.

We acknowledge the support of ANPCyT, Argentina; YerPhI, Armenia; ARC, Australia; BMWFW and FWF, Austria; ANAS, Azerbaijan; SSTC, Belarus; CNPq and FAPESP, Brazil; NSERC, NRC and CFI, Canada; CERN; ANID, Chile; CAS, MOST and NSFC, China; Minciencias, Colombia; MEYS CR, Czech Republic; D NRF and DNSRC, Denmark; IN2P3-CNRS and CEA-DRF/IRFU, France; SRNSFG, Georgia; BMBF, HGF and MPG, Germany; GSRI, Greece; RGC and Hong Kong SAR, China; ISF and Benozziyo Center, Israel; INFN, Italy; MEXT and JSPS, Japan; CNRST, Morocco; NWO, Netherlands; RCN, Norway; MEiN, Poland; FCT, Portugal; MNE/IFA, Romania; JINR; MES of Russia and NRC KI, Russian Federation; MESTD, Serbia; MSSR, Slovakia; ARRS and MIZŠ, Slovenia; DSI/NRF, South Africa; MICINN, Spain; SRC and Wallenberg Foundation, Sweden; SERI, SNSF and Cantons of Bern and Geneva, Switzerland; MOST, Taiwan; TENMAK, Türkiye; STFC, United Kingdom; DOE and NSF, United States of America. In addition, individual groups and members have received support from BCKDF, CANARIE, Compute Canada and CRC, Canada; COST, ERC, ERDF, Horizon 2020 and Marie Skłodowska-Curie Actions, European Union; Investissements d’Avenir Labex, Investissements d’Avenir Idex and ANR, France; DFG and AvH Foundation, Germany; Herakleitos, Thales and Aristeia programmes co-financed by EU-ESF and the Greek NSRF, Greece; BSF-NSF and GIF, Israel; Norwegian Financial Mechanism 2014–2021, Norway; NCN and NAWA, Poland; La Caixa Banking Foundation, CERCA Programme Generalitat de Catalunya and PROMETEO and GenT Programmes Generalitat Valenciana, Spain; Göran Gustafssons Stiftelse, Sweden; The Royal Society and Leverhulme Trust, United Kingdom.

The crucial computing support from all WLCG partners is acknowledged gratefully, in particular from CERN, the ATLAS Tier-1 facilities at TRIUMF (Canada), NDGF (Denmark, Norway, Sweden), CC-IN2P3 (France), KIT/GridKA (Germany), INFN-CNAF (Italy), NL-T1 (Netherlands), PIC (Spain), ASGC (Taiwan), RAL (UK) and BNL (USA), the Tier-2 facilities worldwide and large non-WLCG resource providers. Major contributors of computing resources are listed in Ref. [89].

References

- [1] A. Arvanitaki, N. Craig, S. Dimopoulos, and G. Villadoro, *Mini-Split*, *JHEP* **02** (2013) 126, arXiv: [1210.0555 \[hep-ph\]](#).
- [2] N. Arkani-Hamed, A. Gupta, D. E. Kaplan, N. Weiner, and T. Zorawski, *Simply Unnatural Supersymmetry*, arXiv: [1212.6971 \[hep-ph\]](#).
- [3] G. F. Giudice and R. Rattazzi, *Theories with gauge-mediated supersymmetry breaking*, *Phys. Rept.* **322** (1999) 419, arXiv: [hep-ph/9801271 \[hep-ph\]](#).
- [4] R. Barbier et al., *R-Parity-violating supersymmetry*, *Phys. Rept.* **420** (2005) 1, arXiv: [hep-ph/0406039 \[hep-ph\]](#).
- [5] C. Csaki, E. Kuflik, and T. Volansky, *Dynamical R-Parity Violation*, *Phys. Rev. Lett.* **112** (2014) 131801, arXiv: [1309.5957 \[hep-ph\]](#).
- [6] J. Fan, M. Reece, and J. T. Ruderman, *Stealth supersymmetry*, *JHEP* **11** (2011) 012, arXiv: [1105.5135](#).
- [7] J. Fan, M. Reece, and J. T. Ruderman, *A stealth supersymmetry sampler*, *JHEP* **07** (2012) 196, arXiv: [1201.4875](#).
- [8] Z. Chacko, D. Curtin, and C. B. Verhaaren, *A quirky probe of neutral naturalness*, *Phys. Rev. D* **94** (2016) 011504, arXiv: [1512.05782](#).
- [9] G. Burdman, Z. Chacko, H.-S. Goh, and R. Harnik, *Folded supersymmetry and the LEP paradox*, *JHEP* **0702** (2007) 009, arXiv: [hep-ph/0609152 \[hep-ph\]](#).
- [10] H. Cai, H.-C. Cheng, and J. Terning, *A quirky little Higgs model*, *JHEP* **0905** (2009) 045, arXiv: [0812.0843 \[hep-ph\]](#).
- [11] Z. Chacko, H.-S. Goh, and R. Harnik, *Natural Electroweak Breaking from a Mirror Symmetry*, *Phys. Rev. Lett.* **96** (2006) 231802, arXiv: [hep-ph/0506256 \[hep-ph\]](#).
- [12] M. J. Strassler and K. M. Zurek, *Echoes of a hidden valley at hadron colliders*, *Phys. Lett. B* **651** (2007) 374, arXiv: [hep-ph/0604261](#).
- [13] M. J. Strassler and K. M. Zurek, *Discovering the Higgs through highly-displaced vertices*, *Phys. Lett. B* **661** (2008) 263, arXiv: [hep-ph/0605193](#).
- [14] M. Baumgart, C. Cheung, J. T. Ruderman, L.-T. Wang, and I. Yavin, *Non-abelian dark sectors and their collider signatures*, *JHEP* **04** (2009) 014, arXiv: [0901.0283 \[hep-ph\]](#).
- [15] D. E. Kaplan, M. A. Luty, and K. M. Zurek, *Asymmetric dark matter*, *Phys. Rev. D* **79** (2009) 115016, arXiv: [0901.4117 \[hep-ph\]](#).
- [16] Y. F. Chan, M. Low, D. E. Morrissey, and A. P. Spray, *LHC signatures of a minimal supersymmetric hidden valley*, *JHEP* **05** (2012) 155, arXiv: [1112.2705 \[hep-ph\]](#).
- [17] K. R. Dienes and B. Thomas, *Dynamical dark matter: I. Theoretical overview*, *Phys. Rev. D* **85** (2012) 083523, arXiv: [1106.4546 \[hep-ph\]](#).
- [18] K. R. Dienes, S. Su, and B. Thomas, *Distinguishing dynamical dark matter at the LHC*, *Phys. Rev. D* **86** (2012) 054008, arXiv: [1204.4183 \[hep-ph\]](#).
- [19] Y. Cui and R. Sundrum, *Baryogenesis for weakly interacting massive particles*, *Phys. Rev. D* **87** (2013) 116013, arXiv: [1212.2973 \[hep-ph\]](#).

- [20] Y. Cui, *Natural baryogenesis from unnatural supersymmetry*, [JHEP **12** \(2013\) 067](#), arXiv: [1309.2952 \[hep-ph\]](#).
- [21] Y. Cui and B. Shuve, *Probing baryogenesis with displaced vertices at the LHC*, [JHEP **02** \(2015\) 049](#), arXiv: [1409.6729 \[hep-ph\]](#).
- [22] J. C. Helo, M. Hirsch, and S. Kovalenko, *Heavy neutrino searches at the LHC with displaced vertices*, [Phys. Rev. D **89** \(2014\) 073005](#), arXiv: [1312.2900 \[hep-ph\]](#), Erratum: [Phys. Rev. D **93** \(2016\) 099902](#).
- [23] B. Batell, M. Pospelov, and B. Shuve, *Shedding light on neutrino masses with dark forces*, [JHEP **08** \(2016\) 052](#), arXiv: [1604.06099 \[hep-ph\]](#).
- [24] DELPHI Collaboration, *Search for neutral heavy leptons produced in Z decays*, [Z. Phys. C **74** \(1997\) 57](#), Erratum: [Z. Phys. C **75** \(1997\) 580](#).
- [25] CDF Collaboration, *Search for heavy metastable particles decaying to jet pairs in $p\bar{p}$ collisions at $\sqrt{s} = 1.96$ TeV*, [Phys. Rev. D **85** \(2012\) 012007](#), arXiv: [1109.3136](#).
- [26] D0 Collaboration, *Search for Resonant Pair Production of Neutral Long-Lived Particles Decaying to $b\bar{b}$ in $p\bar{p}$ Collisions at $\sqrt{s} = 1.96$ TeV*, [Phys. Rev. Lett. **103** \(2009\) 071801](#), arXiv: [0906.1787](#).
- [27] ATLAS Collaboration, *Search for a Light Higgs Boson Decaying to Long-Lived Weakly Interacting Particles in Proton-Proton Collisions at $\sqrt{s} = 7$ TeV with the ATLAS Detector*, [Phys. Rev. Lett. **108** \(2012\) 251801](#), arXiv: [1203.1303](#).
- [28] LHCb Collaboration, *Search for long-lived particles decaying to jet pairs*, [Eur. Phys. J. C **75** \(2015\) 152](#), arXiv: [1412.3021](#).
- [29] ATLAS Collaboration, *Search for long-lived, weakly interacting particles that decay to displaced hadronic jets in proton-proton collisions at $\sqrt{s} = 8$ TeV with the ATLAS detector*, [Phys. Rev. D. **92** \(2015\) 012010](#), arXiv: [1504.03634](#).
- [30] ATLAS Collaboration, *Search for massive, long-lived particles using multitrack displaced vertices or displaced lepton pairs in pp collisions at $\sqrt{s} = 8$ TeV with the ATLAS detector*, [Phys. Rev. D **92** \(2015\) 072004](#), arXiv: [1504.05162 \[hep-ex\]](#).
- [31] CMS Collaboration, *Search for long-lived neutral particles decaying to quark-antiquark pairs in proton-proton collisions at $\sqrt{s} = 8$ TeV*, [Phys. Rev. D **91** \(2015\) 012007](#), arXiv: [1411.6530](#).
- [32] ATLAS Collaboration, *Search for pair-produced long-lived neutral particles decaying to jets in the ATLAS hadronic calorimeter in pp collisions at $\sqrt{s} = 8$ TeV*, [Phys. Lett. B **743** \(2015\) 15](#), arXiv: [1501.04020](#).
- [33] LHCb Collaboration, *Updated search for long-lived particles decaying to jet pairs*, [Eur. Phys. J. C **77** \(2017\) 812](#), arXiv: [1705.07332 \[hep-ex\]](#).
- [34] LHCb Collaboration, *Search for massive long-lived particles decaying semileptonically in the LHCb detector*, [Eur. Phys. J. C **77** \(2017\) 224](#), arXiv: [1612.00945 \[hep-ex\]](#).
- [35] CMS Collaboration, *Search for new long-lived particles at $\sqrt{s} = 13$ TeV*, [Phys. Lett. B **780** \(2018\) 432](#), arXiv: [1711.09120 \[hep-ex\]](#).
- [36] CMS Collaboration, *Search for long-lived particles with displaced vertices in multijet events in proton-proton collisions at $\sqrt{s} = 13$ TeV*, [Phys. Rev. D **98** \(2018\) 092011](#), arXiv: [1808.03078 \[hep-ex\]](#).

- [37] CMS Collaboration, *Search for long-lived particles decaying into displaced jets in proton–proton collisions at $\sqrt{s} = 13$ TeV*, *Phys. Rev. D* **99** (2019) 032011, arXiv: [1811.07991 \[hep-ex\]](#).
- [38] ATLAS Collaboration, *Search for long-lived particles produced in pp collisions at $\sqrt{s} = 13$ TeV that decay into displaced hadronic jets in the ATLAS muon spectrometer*, *Phys. Rev. D* **99** (2019) 052005, arXiv: [1811.07370 \[hep-ex\]](#).
- [39] ATLAS Collaboration, *Search for the Production of a Long-Lived Neutral Particle Decaying within the ATLAS Hadronic Calorimeter in Association with a Z Boson from pp Collisions at $\sqrt{s} = 13$ TeV*, *Phys. Rev. Lett.* **122** (2019) 151801, arXiv: [1811.02542 \[hep-ex\]](#).
- [40] ATLAS Collaboration, *Search for long-lived, massive particles in events with displaced vertices and missing transverse momentum in $\sqrt{s} = 13$ TeV pp collisions with the ATLAS detector*, *Phys. Rev. D* **97** (2018) 052012, arXiv: [1710.04901 \[hep-ex\]](#).
- [41] ATLAS Collaboration, *Search for long-lived neutral particles in pp collisions at $\sqrt{s} = 13$ TeV that decay into displaced hadronic jets in the ATLAS calorimeter*, *Eur. Phys. J. C* **79** (2019) 481, arXiv: [1902.03094 \[hep-ex\]](#).
- [42] LHCb Collaboration, *Search for heavy neutral leptons in $W^+ \rightarrow \mu^+ \mu^\pm$ jet decays*, *Eur. Phys. J. C* **81** (2020) 248, arXiv: [2011.05263 \[hep-ex\]](#).
- [43] LHCb Collaboration, *Updated search for long-lived particles decaying to jet pairs*, *Eur. Phys. J. C* **77** (2017) 812, arXiv: [1705.07332 \[hep-ex\]](#).
- [44] ATLAS Collaboration, *The ATLAS Experiment at the CERN Large Hadron Collider*, *JINST* **3** (2008) S08003.
- [45] ATLAS Collaboration, *Performance of the ATLAS trigger system in 2015*, *Eur. Phys. J. C* **77** (2017) 317, arXiv: [1611.09661 \[hep-ex\]](#).
- [46] ATLAS Collaboration, *The ATLAS Collaboration Software and Firmware*, ATL-SOFT-PUB-2021-001, 2021, URL: <https://cds.cern.ch/record/2767187>.
- [47] ATLAS Collaboration, *Triggers for displaced decays of long-lived neutral particles in the ATLAS detector*, *JINST* **8** (2013) P07015, arXiv: [1305.2284](#).
- [48] ATLAS Collaboration, *Standalone vertex finding in the ATLAS muon spectrometer*, *JINST* **9** (2014) P02001, arXiv: [1311.7070 \[hep-ex\]](#).
- [49] R. Bruce et al., *Sources of machine-induced background in the ATLAS and CMS detectors at the CERN Large Hadron Collider*, *Nucl. Instrum. Meth. A* **729** (2013) 825.
- [50] ATLAS Collaboration, *Combined measurements of Higgs boson production and decay using up to 80fb^{-1} of proton–proton collision data at $\sqrt{s} = 13$ TeV collected with the ATLAS experiment*, *Phys. Rev. D* **101** (2020) 012002, arXiv: [1909.02845 \[hep-ex\]](#).
- [51] CMS Collaboration, *Search for invisible decays of a Higgs boson produced through vector boson fusion in proton–proton collisions at $\sqrt{s} = 13$ TeV*, *Phys. Lett. B* **793** (2019) 520, arXiv: [1809.05937 \[hep-ex\]](#).
- [52] D. Curtin and C. B. Verhaaren, *Discovering Uncolored Naturalness in Exotic Higgs Decays*, *JHEP* **12** (2015) 072, arXiv: [1506.06141](#).
- [53] ATLAS Collaboration, *ATLAS data quality operations and performance for 2015–2018 data-taking*, *JINST* **15** (2020) P04003, arXiv: [1911.04632 \[physics.ins-det\]](#).

- [54] D. Curtin et al., *Exotic decays of the 125 GeV Higgs boson*, *Phys. Rev. D* **90** (2014) 075004, arXiv: [1312.4992](#).
- [55] J. Alwall and et al., *The automated computation of tree-level and next-to-leading order differential cross sections, and their matching to parton shower simulations*, *JHEP* **7** (2014) 79, arXiv: [1405.0301](#).
- [56] T. Sjostrand, S. Mrenna, and P. Z. Skands, *A brief introduction to PYTHIA 8.1*, *Comput. Phys. Commun.* **178** (2008) 852, arXiv: [0710.3820](#).
- [57] R. Frederix and S. Frixione, *Merging meets matching in MC@NLO*, *JHEP* **12** (2012) 061, arXiv: [1209.6215](#) [[hep-ph](#)].
- [58] ATLAS Collaboration, *ATLAS Pythia 8 tunes to 7 TeV data*, ATL-PHYS-PUB-2014-021, 2014, URL: <https://cds.cern.ch/record/1966419>.
- [59] R. D. Ball et al., *Parton distributions with LHC data*, *Nucl. Phys. B* **867** (2013) 244, arXiv: [1207.1303](#) [[hep-ph](#)].
- [60] D. J. Lange, *The EvtGen particle decay simulation package*, *Nucl. Instr. Meth. A* **462** (2001) 152.
- [61] ATLAS Collaboration, *The ATLAS Simulation Infrastructure*, *Eur. Phys. J. C* **70** (2010) 823, arXiv: [1005.4568](#).
- [62] S. Agostinelli et al., *GEANT4— a simulation toolkit*, *Nucl. Instrum. Meth. A* **506** (2003) 250.
- [63] ATLAS Collaboration, *The Pythia 8 A3 tune description of ATLAS minimum bias and inelastic measurements incorporating the Donnachie–Landshoff diffractive model*, ATL-PHYS-PUB-2016-017, 2016, URL: <https://cds.cern.ch/record/2206965>.
- [64] T. Sjöstrand et al., *An introduction to PYTHIA 8.2*, *Comput. Phys. Commun.* **191** (2015) 159, arXiv: [1410.3012](#) [[hep-ph](#)].
- [65] S. Mrenna and P. Skands, *Automated parton-shower variations in PYTHIA 8*, *Phys. Rev. D* **94** (2016) 074005, arXiv: [1605.08352](#) [[hep-ph](#)].
- [66] M. Cacciari, G. P. Salam, and G. Soyez, *FastJet user manual*, *Eur. Phys. J. C* **72** (2012) 1896, arXiv: [1111.6097](#) [[hep-ph](#)].
- [67] M. Cacciari, G. P. Salam, and G. Soyez, *The anti- k_t jet clustering algorithm*, *JHEP* **04** (2008) 063, arXiv: [0802.1189](#) [[hep-ph](#)].
- [68] ATLAS Collaboration, *Topological cell clustering in the ATLAS calorimeters and its performance in LHC Run 1*, *Eur. Phys. J. C* **77** (2017) 490, arXiv: [1603.02934](#) [[hep-ex](#)].
- [69] ATLAS Collaboration, *Jet energy measurement and its systematic uncertainty in proton–proton collisions at $\sqrt{s} = 7$ TeV with the ATLAS detector*, *Eur. Phys. J. C* **75** (2015) 17, arXiv: [1406.0076](#) [[hep-ex](#)].
- [70] ATLAS Collaboration, *Jet energy measurement with the ATLAS detector in proton–proton collisions at $\sqrt{s} = 7$ TeV*, *Eur. Phys. J. C* **73** (2013) 2304, arXiv: [1112.6426](#) [[hep-ex](#)].
- [71] ATLAS Collaboration, *Performance of pile-up mitigation techniques for jets in pp collisions at $\sqrt{s} = 8$ TeV using the ATLAS detector*, *Eur. Phys. J. C* **76** (2016) 581, arXiv: [1510.03823](#) [[hep-ex](#)].

- [72] ATLAS Collaboration, *Jet global sequential corrections with the ATLAS detector in proton–proton collisions at $\sqrt{s} = 8$ TeV*, ATLAS-CONF-2015-002, 2015, URL: <https://cds.cern.ch/record/2001682>.
- [73] ATLAS Collaboration, *ATLAS b -jet identification performance and efficiency measurement with $t\bar{t}$ events in pp collisions at $\sqrt{s} = 13$ TeV*, *Eur. Phys. J. C* **79** (2019) 970, arXiv: [1907.05120](https://arxiv.org/abs/1907.05120) [hep-ex].
- [74] ATLAS Collaboration, *Jet Calibration and Systematic Uncertainties for Jets Reconstructed in the ATLAS Detector at $\sqrt{s} = 13$ TeV*, ATL-PHYS-PUB-2015-015, 2015, URL: <https://cds.cern.ch/record/2037613>.
- [75] ATLAS Collaboration, *Jet energy scale measurements and their systematic uncertainties in proton–proton collisions at $\sqrt{s} = 13$ TeV with the ATLAS detector*, *Phys. Rev. D* **96** (2017) 072002, arXiv: [1703.09665](https://arxiv.org/abs/1703.09665) [hep-ex].
- [76] ATLAS Collaboration, *Selection of jets produced in 13 TeV proton–proton collisions with the ATLAS detector*, ATLAS-CONF-2015-029, 2015, URL: <https://cds.cern.ch/record/2037702>.
- [77] K. Hamilton, P. Nason, E. Re, and G. Zanderighi, *NNLOPS simulation of Higgs boson production*, *JHEP* **10** (2013) 222, arXiv: [1309.0017](https://arxiv.org/abs/1309.0017) [hep-ph].
- [78] K. Hamilton, P. Nason, and G. Zanderighi, *Finite quark-mass effects in the NNLOPS POWHEG+MiNLO Higgs generator*, *JHEP* **05** (2015) 140, arXiv: [1501.04637](https://arxiv.org/abs/1501.04637) [hep-ph].
- [79] S. Alioli, P. Nason, C. Oleari, and E. Re, *A general framework for implementing NLO calculations in shower Monte Carlo programs: the POWHEG BOX*, *JHEP* **06** (2010) 043, arXiv: [1002.2581](https://arxiv.org/abs/1002.2581) [hep-ph].
- [80] P. Nason, *A new method for combining NLO QCD with shower Monte Carlo algorithms*, *JHEP* **11** (2004) 040, arXiv: [hep-ph/0409146](https://arxiv.org/abs/hep-ph/0409146).
- [81] S. Frixione, P. Nason, and C. Oleari, *Matching NLO QCD computations with parton shower simulations: the POWHEG method*, *JHEP* **11** (2007) 070, arXiv: [0709.2092](https://arxiv.org/abs/0709.2092) [hep-ph].
- [82] ATLAS Collaboration, *Luminosity determination in pp collisions at $\sqrt{s} = 13$ TeV using the ATLAS detector at the LHC*, ATLAS-CONF-2019-021, 2019, URL: <https://cds.cern.ch/record/2677054>.
- [83] ATLAS Collaboration, *The LUCID-2 detector*, *Nucl. Instrum. Meth. A* **936** (2019) 152.
- [84] A. L. Read, *Presentation of search results: The CL_s technique*, *J. Phys. G* **28** (2002) 2693.
- [85] L. Heinrich, M. Feickert, and G. Stark, *pyhf: v0.6.2*, version 0.6.2, <https://github.com/scikit-hep/pyhf/releases/tag/v0.6.2>, URL: <https://doi.org/10.5281/zenodo.1169739>.
- [86] L. Heinrich, M. Feickert, G. Stark, and K. Cranmer, *pyhf: pure-Python implementation of HistFactory statistical models*, *Journal of Open Source Software* **6** (2021) 2823, URL: <https://doi.org/10.21105/joss.02823>.
- [87] G. Cowan, K. Cranmer, E. Gross, and O. Vitells, *Asymptotic formulae for likelihood-based tests of new physics*, *Eur. Phys. J. C* **71** (2011) 1554, arXiv: [1007.1727](https://arxiv.org/abs/1007.1727) [physics.data-an], Erratum: *Eur. Phys. J. C* **73** (2013) 2501.

- [88] Working Group 2 on the Physics of the HL-LHC, and Perspectives at the HE-LHC, *Higgs Physics at the HL-LHC and HE-LHC*, (2019), arXiv: [1902.00134](https://arxiv.org/abs/1902.00134).
- [89] ATLAS Collaboration, *ATLAS Computing Acknowledgements*, ATL-SOFT-PUB-2021-003, URL: <https://cds.cern.ch/record/2776662>.

The ATLAS Collaboration

G. Aad⁹⁸, B. Abbott¹²⁴, D.C. Abbott⁹⁹, A. Abed Abud³⁴, K. Abeling⁵¹, D.K. Abhayasinghe⁹¹, S.H. Abidi²⁷, A. Aboulhorma^{33e}, H. Abramowicz¹⁵⁷, H. Abreu¹⁵⁶, Y. Abulaiti⁵, A.C. Abusleme Hoffman^{142a}, B.S. Acharya^{64a,64b,o}, B. Achkar⁵¹, L. Adam⁹⁶, C. Adam Bourdarios⁴, L. Adamczyk^{81a}, L. Adamek¹⁶², S.V. Addepalli²⁴, J. Adelman¹¹⁶, A. Adiguzel^{11c,ac}, S. Adorni⁵², T. Adye¹³⁹, A.A. Affolder¹⁴¹, Y. Afik³⁴, C. Agapopoulou⁶², M.N. Agaras¹², J. Agarwala^{68a,68b}, A. Aggarwal¹¹⁴, C. Agheorghiesei^{25c}, J.A. Aguilar-Saavedra^{135f,135a,ab}, A. Ahmad³⁴, F. Ahmadov^{77,z}, W.S. Ahmed¹⁰⁰, X. Ai⁴⁴, G. Aielli^{71a,71b}, I. Aizenberg¹⁷⁵, S. Akatsuka⁸³, M. Akbiyik⁹⁶, T.P.A. Åkesson⁹⁴, A.V. Akimov¹⁰⁷, K. Al Khoury³⁷, G.L. Alberghi^{21b}, J. Albert¹⁷¹, P. Albicocco⁴⁹, M.J. Alconada Verzini⁸⁶, S. Alderweireldt⁴⁸, M. Aleksa³⁴, I.N. Aleksandrov⁷⁷, C. Alexa^{25b}, T. Alexopoulos⁹, A. Alfonsi¹¹⁵, F. Alfonsi^{21b}, M. Alhroob¹²⁴, B. Ali¹³⁷, S. Ali¹⁵⁴, M. Aliev¹⁶¹, G. Alimonti^{66a}, C. Allaire³⁴, B.M.M. Allbrooke¹⁵², P.P. Allport¹⁹, A. Aloisio^{67a,67b}, F. Alonso⁸⁶, C. Alpigiani¹⁴⁴, E. Alunno Camelia^{71a,71b}, M. Alvarez Estevez⁹⁵, M.G. Alvigi^{67a,67b}, Y. Amaral Coutinho^{78b}, A. Ambler¹⁰⁰, L. Ambroz¹³⁰, C. Amelung³⁴, D. Amidei¹⁰², S.P. Amor Dos Santos^{135a}, S. Amoroso⁴⁴, K.R. Amos¹⁶⁹, C.S. Amrouche⁵², V. Ananiev¹²⁹, C. Anastopoulos¹⁴⁵, N. Andari¹⁴⁰, T. Andeen¹⁰, J.K. Anders¹⁸, S.Y. Andread^{43a,43b}, A. Andreazza^{66a,66b}, S. Angelidakis⁸, A. Angerami³⁷, A.V. Anisenkov^{117b,117a}, A. Annovi^{69a}, C. Antel⁵², M.T. Anthony¹⁴⁵, E. Antipov¹²⁵, M. Antonelli⁴⁹, D.J.A. Antrim¹⁶, F. Anulli^{70a}, M. Aoki⁷⁹, J.A. Aparisi Pozo¹⁶⁹, M.A. Aparo¹⁵², L. Aperio Bella⁴⁴, N. Aranzabal³⁴, V. Araujo Ferraz^{78a}, C. Arcangeletti⁴⁹, A.T.H. Arce⁴⁷, E. Arena⁸⁸, J-F. Arguin¹⁰⁶, S. Argyropoulos⁵⁰, J.-H. Arling⁴⁴, A.J. Armbruster³⁴, A. Armstrong¹⁶⁶, O. Arnaez¹⁶², H. Arnold³⁴, Z.P. Arrubarrena Tame¹¹⁰, G. Artoni¹³⁰, H. Asada¹¹², K. Asai¹²², S. Asai¹⁵⁹, N.A. Asbah⁵⁷, E.M. Asimakopoulou¹⁶⁷, L. Asquith¹⁵², J. Assahsah^{33d}, K. Assamagan²⁷, R. Astalos^{26a}, R.J. Atkin^{31a}, M. Atkinson¹⁶⁸, N.B. Atlay¹⁷, H. Atmani^{58b}, P.A. Atlasiddha¹⁰², K. Augsten¹³⁷, S. Auricchio^{67a,67b}, V.A. Austrup¹⁷⁷, G. Avner¹⁵⁶, G. Avolio³⁴, M.K. Ayoub^{13c}, G. Azuelos^{106,aj}, D. Babal^{26a}, H. Bachacou¹⁴⁰, K. Bachas¹⁵⁸, A. Bachiu³², F. Backman^{43a,43b}, A. Badea⁵⁷, P. Bagnaia^{70a,70b}, H. Bahrasemani¹⁴⁸, A.J. Bailey¹⁶⁹, V.R. Bailey¹⁶⁸, J.T. Baines¹³⁹, C. Bakalis⁹, O.K. Baker¹⁷⁸, P.J. Bakker¹¹⁵, E. Bakos¹⁴, D. Bakshi Gupta⁷, S. Balaji¹⁵³, R. Balasubramanian¹¹⁵, E.M. Baldin^{117b,117a}, P. Balek¹³⁸, E. Ballabene^{66a,66b}, F. Balli¹⁴⁰, L.M. Baltés^{59a}, W.K. Balunas¹³⁰, J. Balz⁹⁶, E. Banas⁸², M. Bandieramonte¹³⁴, A. Bandyopadhyay²², S. Bansal²², L. Barak¹⁵⁷, E.L. Barberio¹⁰¹, D. Barberis^{53b,53a}, M. Barbero⁹⁸, G. Barbour⁹², K.N. Barends^{31a}, T. Barillari¹¹¹, M-S. Barisits³⁴, J. Barkeloo¹²⁷, T. Barklow¹⁴⁹, B.M. Barnett¹³⁹, R.M. Barnett¹⁶, A. Baroncelli^{58a}, G. Barone²⁷, A.J. Barr¹³⁰, L. Barranco Navarro^{43a,43b}, F. Barreiro⁹⁵, J. Barreiro Guimarães da Costa^{13a}, U. Barron¹⁵⁷, S. Barsov¹³³, F. Bartels^{59a}, R. Bartoldus¹⁴⁹, G. Bartolini⁹⁸, A.E. Barton⁸⁷, P. Bartos^{26a}, A. Basalae⁴⁴, A. Basan⁹⁶, M. Baselga⁴⁴, I. Bashta^{72a,72b}, A. Bassalat^{62,ag}, M.J. Basso¹⁶², C.R. Basson⁹⁷, R.L. Bates⁵⁵, S. Batlamous^{33e}, J.R. Batley³⁰, B. Batool¹⁴⁷, M. Battaglia¹⁴¹, M. Bauge^{70a,70b}, F. Bauer^{140,*}, P. Bauer²², H.S. Bawa²⁹, A. Bayirli^{11c}, J.B. Beacham⁴⁷, T. Beau¹³¹, P.H. Beauchemin¹⁶⁵, F. Becherer⁵⁰, P. Bechtel²², H.P. Beck^{18,q}, K. Becker¹⁷³, C. Becot⁴⁴, A.J. Beddall^{11a}, V.A. Bednyakov⁷⁷, C.P. Bee¹⁵¹, T.A. Beermann³⁴, M. Begalli^{78b}, M. Beger²⁷, A. Behera¹⁵¹, J.K. Behr⁴⁴, C. Beirao Da Cruz E Silva³⁴, J.F. Beirer^{51,34}, F. Beisiegel²², M. Belfkir⁴, G. Bella¹⁵⁷, L. Bellagamba^{21b}, A. Bellerive³², P. Bellos¹⁹, K. Beloborodov^{117b,117a}, K. Belotskiy¹⁰⁸, N.L. Belyaev¹⁰⁸, D. Benchebkroun^{33a}, Y. Benhammou¹⁵⁷,

D.P. Benjamin²⁷, M. Benoit²⁷, J.R. Bensinger²⁴, S. Bentvelsen¹¹⁵, L. Beresford³⁴, M. Beretta⁴⁹,
 D. Berge¹⁷, E. Bergeaas Kuutmann¹⁶⁷, N. Berger⁴, B. Bergmann¹³⁷, L.J. Bergsten²⁴, J. Beringer¹⁶,
 S. Berlendis⁶, G. Bernardi¹³¹, C. Bernius¹⁴⁹, F.U. Bernlochner²², T. Berry⁹¹, P. Berta¹³⁸, A. Berthold⁴⁶,
 I.A. Bertram⁸⁷, O. Bessidskaia Bylund¹⁷⁷, S. Bethke¹¹¹, A. Betti⁴⁰, A.J. Bevan⁹⁰, S. Bhatta¹⁵¹,
 D.S. Bhattacharya¹⁷², P. Bhattarai²⁴, V.S. Bhopatkar⁵, R. Bi¹³⁴, R.M. Bianchi¹³⁴, O. Biebel¹¹⁰,
 R. Bielski¹²⁷, N.V. Biesuz^{69a,69b}, M. Biglietti^{72a}, T.R.V. Billoud¹³⁷, M. Bindi⁵¹, A. Bingul^{11d},
 C. Bini^{70a,70b}, S. Biondi^{21b,21a}, A. Biondini⁸⁸, C.J. Birch-sykes⁹⁷, G.A. Bird^{19,139}, M. Birman¹⁷⁵,
 T. Bisanz³⁴, J.P. Biswal², D. Biswas^{176j}, A. Bitadze⁹⁷, C. Bittrich⁴⁶, K. Bjørke¹²⁹, I. Bloch⁴⁴, C. Blocker²⁴,
 A. Blue⁵⁵, U. Blumenschein⁹⁰, J. Blumenthal⁹⁶, G.J. Bobbink¹¹⁵, V.S. Bobrovnikov^{117b,117a}, M. Boehler⁵⁰,
 D. Bogavac¹², A.G. Bogdanchikov^{117b,117a}, C. Bohm^{43a}, V. Boisvert⁹¹, P. Bokan⁴⁴, T. Bold^{81a},
 M. Bomben¹³¹, M. Bona⁹⁰, M. Boonekamp¹⁴⁰, C.D. Booth⁹¹, A.G. Borbély⁵⁵, H.M. Borecka-Bielska¹⁰⁶,
 L.S. Borgna⁹², G. Borissov⁸⁷, D. Bortoletto¹³⁰, D. Boscherini^{21b}, M. Bosman¹², J.D. Bossio Sola³⁴,
 K. Bouaouda^{33a}, J. Boudreau¹³⁴, E.V. Bouhova-Thacker⁸⁷, D. Boumediene³⁶, R. Bouquet¹³¹, A. Boveia¹²³,
 J. Boyd³⁴, D. Boye²⁷, I.R. Boyko⁷⁷, A.J. Bozson⁹¹, J. Bracinik¹⁹, N. Brahimi^{58d,58c}, G. Brandt¹⁷⁷,
 O. Brandt³⁰, F. Braren⁴⁴, B. Brau⁹⁹, J.E. Brau¹²⁷, W.D. Breaden Madden⁵⁵, K. Brendlinger⁴⁴, R. Brenner¹⁷⁵,
 L. Brenner³⁴, R. Brenner¹⁶⁷, S. Bressler¹⁷⁵, B. Brickwedde⁹⁶, D.L. Briglin¹⁹, D. Britton⁵⁵, D. Britzger¹¹¹,
 I. Brock²², R. Brock¹⁰³, G. Brooijmans³⁷, W.K. Brooks^{142e}, E. Brost²⁷, P.A. Bruckman de Renstrom⁸²,
 B. Brüers⁴⁴, D. Bruncko^{26b}, A. Bruni^{21b}, G. Bruni^{21b}, M. Bruschi^{21b}, N. Brusino^{70a,70b},
 L. Bryngemark¹⁴⁹, T. Buanes¹⁵, Q. Buat¹⁵¹, P. Buchholz¹⁴⁷, A.G. Buckley⁵⁵, I.A. Budagov⁷⁷,
 M.K. Bugge¹²⁹, O. Bulekov¹⁰⁸, B.A. Bullard⁵⁷, S. Burdin⁸⁸, C.D. Burgard⁴⁴, A.M. Burger¹²⁵,
 B. Burghgrave⁷, J.T.P. Burr⁴⁴, C.D. Burton¹⁰, J.C. Burzynski¹⁴⁸, E.L. Busch³⁷, V. Büscher⁹⁶,
 P.J. Bussey⁵⁵, J.M. Butler²³, C.M. Buttar⁵⁵, J.M. Butterworth⁹², W. Buttinger¹³⁹, C.J. Buxo Vazquez¹⁰³,
 A.R. Buzykaev^{117b,117a}, G. Cabras^{21b}, S. Cabrera Urbán¹⁶⁹, D. Caforio⁵⁴, H. Cai¹³⁴, V.M.M. Cairo¹⁴⁹,
 O. Cakir^{3a}, N. Calace³⁴, P. Calafiura¹⁶, G. Calderini¹³¹, P. Calfayan⁶³, G. Callea⁵⁵, L.P. Caloba^{78b},
 D. Calvet³⁶, S. Calvet³⁶, T.P. Calvet⁹⁸, M. Calvetti^{69a,69b}, R. Camacho Toro¹³¹, S. Camarda³⁴,
 D. Camarero Munoz⁹⁵, P. Camarri^{71a,71b}, M.T. Camerlingo^{72a,72b}, D. Cameron¹²⁹, C. Camincher¹⁷¹,
 M. Campanelli⁹², A. Camplani³⁸, V. Canale^{67a,67b}, A. Canesse¹⁰⁰, M. Cano Bret⁷⁵, J. Cantero¹²⁵,
 Y. Cao¹⁶⁸, F. Capocasa²⁴, M. Capua^{39b,39a}, A. Carbone^{66a,66b}, R. Cardarelli^{71a}, J.C.J. Cardenas⁷,
 F. Cardillo¹⁶⁹, G. Carducci^{39b,39a}, T. Carli³⁴, G. Carlino^{67a}, B.T. Carlson¹³⁴, E.M. Carlson^{171,163a},
 L. Carminati^{66a,66b}, M. Carnesale^{70a,70b}, R.M.D. Carney¹⁴⁹, S. Caron¹¹⁴, E. Carquin^{142e}, S. Carrá⁴⁴,
 G. Carratta^{21b,21a}, J.W.S. Carter¹⁶², T.M. Carter⁴⁸, D. Casadei^{31c}, M.P. Casado^{12g}, A.F. Casha¹⁶²,
 E.G. Castiglia¹⁷⁸, F.L. Castillo^{59a}, L. Castillo Garcia¹², V. Castillo Gimenez¹⁶⁹, N.F. Castro^{135a,135e},
 A. Catinaccio³⁴, J.R. Catmore¹²⁹, A. Cattai³⁴, V. Cavaliere²⁷, N. Cavalli^{21b,21a}, V. Cavasinni^{69a,69b},
 E. Celebi^{11b}, F. Celli¹³⁰, M.S. Centonze^{65a,65b}, K. Cerny¹²⁶, A.S. Cerqueira^{78a}, A. Cerri¹⁵²,
 L. Cerrito^{71a,71b}, F. Cerutti¹⁶, A. Cervelli^{21b}, S.A. Cetin^{11b}, Z. Chadi^{33a}, D. Chakraborty¹¹⁶, M. Chala^{135f},
 J. Chan¹⁷⁶, W.S. Chan¹¹⁵, W.Y. Chan⁸⁸, J.D. Chapman³⁰, B. Chargeishvili^{155b}, D.G. Charlton¹⁹,
 T.P. Charman⁹⁰, M. Chatterjee¹⁸, S. Chekanov⁵, S.V. Chekulaev^{163a}, G.A. Chelkov^{77,ae}, A. Chen¹⁰²,
 B. Chen¹⁵⁷, B. Chen¹⁷¹, C. Chen^{58a}, C.H. Chen⁷⁶, H. Chen^{13c}, H. Chen²⁷, J. Chen^{58c}, J. Chen²⁴,
 S. Chen¹³², S.J. Chen^{13c}, X. Chen^{58c}, X. Chen^{13b}, Y. Chen^{58a}, Y-H. Chen⁴⁴, C.L. Cheng¹⁷⁶,
 H.C. Cheng^{60a}, A. Cheplakov⁷⁷, E. Cheremushkina⁴⁴, E. Cherepanova⁷⁷, R. Cherkaoui El Moursli^{33e},
 E. Cheu⁶, K. Cheung⁶¹, L. Chevalier¹⁴⁰, V. Chiarella⁴⁹, G. Chiarelli^{69a}, G. Chiodini^{65a}, A.S. Chisholm¹⁹,
 A. Chitan^{25b}, Y.H. Chiu¹⁷¹, M.V. Chizhov^{77,s}, K. Choi¹⁰, A.R. Chomont^{70a,70b}, Y. Chou⁹⁹, Y.S. Chow¹¹⁵,
 T. Chowdhury^{31f}, L.D. Christopher^{31f}, M.C. Chu^{60a}, X. Chu^{13a,13d}, J. Chudoba¹³⁶, J.J. Chwastowski⁸²,
 D. Cieri¹¹¹, K.M. Ciesla⁸², V. Cindro⁸⁹, I.A. Cioară^{25b}, A. Ciocio¹⁶, F. Ciotto^{67a,67b}, Z.H. Citron^{175,k},
 M. Citterio^{66a}, D.A. Ciubotaru^{25b}, B.M. Ciungu¹⁶², A. Clark⁵², P.J. Clark⁴⁸, J.M. Clavijo Columbie⁴⁴,
 S.E. Clawson⁹⁷, C. Clement^{43a,43b}, L. Clissa^{21b,21a}, Y. Coadou⁹⁸, M. Cobal^{64a,64c}, A. Coccaro^{53b},
 J. Cochran⁷⁶, R.F. Coelho Barrue^{135a}, R. Coelho Lopes De Sa⁹⁹, S. Coelli^{66a}, H. Cohen¹⁵⁷,

A.E.C. Coimbra³⁴, B. Cole³⁷, J. Collot⁵⁶, P. Conde Muiño^{135a,135g}, S.H. Connell^{31c}, I.A. Connelly⁵⁵, E.I. Conroy¹³⁰, F. Conventi^{67a,ak}, H.G. Cooke¹⁹, A.M. Cooper-Sarkar¹³⁰, F. Cormier¹⁷⁰, L.D. Corpe³⁴, M. Corradi^{70a,70b}, E.E. Corrigan⁹⁴, F. Corriveau^{100,y}, M.J. Costa¹⁶⁹, F. Costanza⁴, D. Costanzo¹⁴⁵, B.M. Cote¹²³, G. Cowan⁹¹, J.W. Cowley³⁰, K. Cranmer¹²¹, S. Crépe-Renaudin⁵⁶, F. Crescioli¹³¹, M. Cristinziani¹⁴⁷, M. Cristoforetti^{73a,73b,b}, V. Croft¹⁶⁵, G. Crosetti^{39b,39a}, A. Cueto³⁴, T. Cuhadar Donszelmann¹⁶⁶, H. Cui^{13a,13d}, A.R. Cukierman¹⁴⁹, W.R. Cunningham⁵⁵, F. Curcio^{39b,39a}, P. Czodrowski³⁴, M.M. Czurylo^{59b}, M.J. Da Cunha Sargedas De Sousa^{58a}, J.V. Da Fonseca Pinto^{78b}, C. Da Via⁹⁷, W. Dabrowski^{81a}, T. Dado⁴⁵, S. Dahbi^{31f}, T. Dai¹⁰², C. Dallapiccola⁹⁹, M. Dam³⁸, G. D'amen²⁷, V. D'Amico^{72a,72b}, J. Damp⁹⁶, J.R. Dandoy¹³², M.F. Daneri²⁸, M. Danninger¹⁴⁸, V. Dao³⁴, G. Darbo^{53b}, S. Darmora⁵, A. Dattagupta¹²⁷, S. D'Auria^{66a,66b}, C. David^{163b}, T. Davidek¹³⁸, D.R. Davis⁴⁷, B. Davis-Purcell³², I. Dawson⁹⁰, K. De⁷, R. De Asmundis^{67a}, M. De Beurs¹¹⁵, S. De Castro^{21b,21a}, N. De Groot¹¹⁴, P. de Jong¹¹⁵, H. De la Torre¹⁰³, A. De Maria^{13c}, D. De Pedis^{70a}, A. De Salvo^{70a}, U. De Sanctis^{71a,71b}, M. De Santis^{71a,71b}, A. De Santo¹⁵², J.B. De Vivie De Regie⁵⁶, D.V. Dedovich⁷⁷, J. Degens¹¹⁵, A.M. Deiana⁴⁰, J. Del Peso⁹⁵, Y. Delabat Diaz⁴⁴, F. Deliot¹⁴⁰, C.M. Delitzsch⁶, M. Della Pietra^{67a,67b}, D. Della Volpe⁵², A. Dell'Acqua³⁴, L. Dell'Asta^{66a,66b}, M. Delmastro⁴, P.A. Delsart⁵⁶, S. Demers¹⁷⁸, M. Demichev⁷⁷, S.P. Denisov¹¹⁸, L. D'Eramo¹¹⁶, D. Derendarz⁸², J.E. Derkaoui^{33d}, F. Derue¹³¹, P. Dervan⁸⁸, K. Desch²², K. Dette¹⁶², C. Deutsch²², P.O. Deviveiros³⁴, F.A. Di Bello^{70a,70b}, A. Di Ciaccio^{71a,71b}, L. Di Ciaccio⁴, A. Di Domenico^{70a,70b}, C. Di Donato^{67a,67b}, A. Di Girolamo³⁴, G. Di Gregorio^{69a,69b}, A. Di Luca^{73a,73b}, B. Di Micco^{72a,72b}, R. Di Nardo^{72a,72b}, C. Diaconu⁹⁸, F.A. Dias¹¹⁵, T. Dias Do Vale^{135a}, M.A. Diaz^{142a}, F.G. Diaz Capriles²², J. Dickinson¹⁶, M. Didenko¹⁶⁹, E.B. Diehl¹⁰², J. Dietrich¹⁷, S. Díez Cornell⁴⁴, C. Díez Pardos¹⁴⁷, A. Dimitrievska¹⁶, W. Ding^{13b}, J. Dingfelder²², I.M. Dinu^{25b}, S.J. Dittmeier^{59b}, F. Dittus³⁴, F. Djama⁹⁸, T. Djobava^{155b}, J.I. Djuvsland¹⁵, M.A.B. Do Vale¹⁴³, D. Dodsworth²⁴, C. Doglioni⁹⁴, J. Dolejsi¹³⁸, Z. Dolezal¹³⁸, M. Donadelli^{78c}, B. Dong^{58c}, J. Donini³⁶, A. D'onofrio^{13c}, M. D'Onofrio⁸⁸, J. Dopke¹³⁹, A. Doria^{67a}, M.T. Dova⁸⁶, A.T. Doyle⁵⁵, E. Drechsler¹⁴⁸, E. Dreyer¹⁴⁸, T. Dreyer⁵¹, A.S. Drobac¹⁶⁵, D. Du^{58a}, T.A. du Pree¹¹⁵, F. Dubinin¹⁰⁷, M. Dubovsky^{26a}, A. Dubreuil⁵², E. Duchovni¹⁷⁵, G. Duckeck¹¹⁰, O.A. Ducu^{34,25b}, D. Duda¹¹¹, A. Dudarev³⁴, M. D'uffizi⁹⁷, L. Dufлот⁶², M. Dührssen³⁴, C. Dülsen¹⁷⁷, A.E. Dumitriu^{25b}, M. Dunford^{159a}, S. Dungs⁴⁵, K. Dunne^{43a,43b}, A. Duperrin⁹⁸, H. Duran Yildiz^{3a}, M. Düren⁵⁴, A. Durglishvili^{155b}, B. Dutta⁴⁴, B.L. Dwyer¹¹⁶, G.I. Dyckes¹⁶, M. Dyndal^{81a}, S. Dysch⁹⁷, B.S. Dziedzic⁸², B. Eckerova^{26a}, M.G. Eggleston⁴⁷, E. Egidio Purcino De Souza^{78b}, L.F. Ehrke⁵², T. Eifert⁷, G. Eigen¹⁵, K. Einsweiler¹⁶, T. Ekelof¹⁶⁷, Y. El Ghazali^{33b}, H. El Jarrari^{33e}, A. El Moussaouy^{33a}, V. Ellajosyula¹⁶⁷, M. Ellert¹⁶⁷, F. Ellinghaus¹⁷⁷, A.A. Elliot⁹⁰, N. Ellis³⁴, J. Elmsheuser²⁷, M. Elsing³⁴, D. Emelianov¹³⁹, A. Emerman³⁷, Y. Enari¹⁵⁹, J. Erdmann⁴⁵, A. Ereditato¹⁸, P.A. Erland⁸², M. Errenst¹⁷⁷, M. Escalier⁶², C. Escobar¹⁶⁹, O. Estrada Pastor¹⁶⁹, E. Etzion¹⁵⁷, G. Evans^{135a}, H. Evans⁶³, M.O. Evans¹⁵², A. Ezhilov¹³³, F. Fabbri⁵⁵, L. Fabbri^{21b,21a}, G. Facini¹⁷³, V. Fadeyev¹⁴¹, R.M. Fakhruddinov¹¹⁸, S. Falciano^{70a}, P.J. Falke²², S. Falke³⁴, J. Faltova¹³⁸, Y. Fan^{13a}, Y. Fang^{13a}, G. Fanourakis⁴², M. Fanti^{66a,66b}, M. Faraj^{58c}, A. Farbin⁷, A. Farilla^{72a}, E.M. Farina^{68a,68b}, T. Farooque¹⁰³, S.M. Farrington⁴⁸, P. Farthouat³⁴, F. Fassi^{33e}, D. Fassouliotis⁸, M. Fauci Giannelli^{71a,71b}, W.J. Fawcett³⁰, L. Fayard⁶², O.L. Fedin^{133,p}, M. Feickert¹⁶⁸, L. Felgioni⁹⁸, A. Fell¹⁴⁵, C. Feng^{58b}, M. Feng^{13b}, M.J. Fenton¹⁶⁶, A.B. Fenyuk¹¹⁸, S.W. Ferguson⁴¹, J. Ferrando⁴⁴, A. Ferrari¹⁶⁷, P. Ferrari¹¹⁵, R. Ferrari^{68a}, D. Ferrere⁵², C. Ferretti¹⁰², F. Fiedler⁹⁶, A. Filipčič⁸⁹, F. Filthaut¹¹⁴, M.C.N. Fiolhais^{135a,135c,a}, L. Fiorini¹⁶⁹, F. Fischer¹⁴⁷, W.C. Fisher¹⁰³, T. Fitschen¹⁹, I. Fleck¹⁴⁷, P. Fleischmann¹⁰², T. Flick¹⁷⁷, B.M. Flierl¹¹⁰, L. Flores¹³², M. Flores^{31d}, L.R. Flores Castillo^{60a}, F.M. Follega^{73a,73b}, N. Fomin¹⁵, J.H. Foo¹⁶², B.C. Forland⁶³, A. Formica¹⁴⁰, F.A. Förster¹², A.C. Forti⁹⁷, E. Fortin⁹⁸, M.G. Foti¹³⁰, L. Fountas⁸, D. Fournier⁶², H. Fox⁸⁷, P. Francavilla^{69a,69b}, S. Francescato⁵⁷, M. Franchini^{21b,21a}, S. Franchino^{59a}, D. Francis³⁴, L. Franco⁴, L. Franconi¹⁸, M. Franklin⁵⁷, G. Frattari^{70a,70b}, A.C. Freegard⁹⁰, P.M. Freeman¹⁹, W.S. Freund^{78b}, E.M. Freundlich⁴⁵, D. Froidevaux³⁴, J.A. Frost¹³⁰, Y. Fu^{58a},

M. Fujimoto¹²², E. Fullana Torregrosa¹⁶⁹, J. Fuster¹⁶⁹, A. Gabrielli^{21b,21a}, A. Gabrielli³⁴, P. Gadow⁴⁴,
G. Gagliardi^{53b,53a}, L.G. Gagnon¹⁶, G.E. Gallardo¹³⁰, E.J. Gallas¹³⁰, B.J. Gallop¹³⁹, R. Gamboa Goni⁹⁰,
K.K. Gan¹²³, S. Ganguly¹⁵⁹, J. Gao^{58a}, Y. Gao⁴⁸, Y.S. Gao^{29,m}, F.M. Garay Walls^{142a}, C. García¹⁶⁹,
J.E. García Navarro¹⁶⁹, J.A. García Pascual^{13a}, M. Garcia-Sciveres¹⁶, R.W. Gardner³⁵, D. Garg⁷⁵,
R.B. Garg¹⁴⁹, S. Gargiulo⁵⁰, C.A. Garner¹⁶², V. Garonne¹²⁹, S.J. Gasiorowski¹⁴⁴, P. Gaspar^{78b},
G. Gaudio^{68a}, P. Gauzzi^{70a,70b}, I.L. Gavrilenko¹⁰⁷, A. Gavrilyuk¹¹⁹, C. Gay¹⁷⁰, G. Gaycken⁴⁴, E.N. Gazis⁹,
A.A. Geanta^{25b}, C.M. Gee¹⁴¹, C.N.P. Gee¹³⁹, J. Geisen⁹⁴, M. Geisen⁹⁶, C. Gemme^{53b}, M.H. Genest⁵⁶,
S. Gentile^{70a,70b}, S. George⁹¹, W.F. George¹⁹, T. Geralis⁴², L.O. Gerlach⁵¹, P. Gessinger-Befurt³⁴,
M. Ghasemi Bostanabad¹⁷¹, A. Ghosh¹⁶⁶, A. Ghosh⁷⁵, B. Giacobbe^{21b}, S. Giagu^{70a,70b},
N. Giangiacomi¹⁶², P. Giannetti^{69a}, A. Giannini^{67a,67b}, S.M. Gibson⁹¹, M. Gignac¹⁴¹, D.T. Gil^{81b},
B.J. Gilbert³⁷, D. Gillberg³², G. Gilles¹¹⁵, N.E.K. Gillwald⁴⁴, D.M. Gingrich^{2,aj}, M.P. Giordani^{64a,64c},
P.F. Giraud¹⁴⁰, G. Giugliarelli^{64a,64c}, D. Giugni^{66a}, F. Giuli^{71a,71b}, I. Gkialas^{8,h}, P. Gkoutoumis⁹,
L.K. Gladilin¹⁰⁹, C. Glasman⁹⁵, G.R. Gledhill¹²⁷, M. Glisic¹²⁷, I. Gnesi^{39b,d}, M. Goblirsch-Kolb²⁴,
D. Godin¹⁰⁶, S. Goldfarb¹⁰¹, T. Golling⁵², D. Golubkov¹¹⁸, J.P. Gombas¹⁰³, A. Gomes^{135a,135b},
R. Goncalves Gama⁵¹, R. Gonçalo^{135a,135c}, G. Gonella¹²⁷, L. Gonella¹⁹, A. Gongadze⁷⁷, F. Gonnella¹⁹,
J.L. Gonski³⁷, S. González de la Hoz¹⁶⁹, S. Gonzalez Fernandez¹², R. Gonzalez Lopez⁸⁸,
C. Gonzalez Renteria¹⁶, R. Gonzalez Suarez¹⁶⁷, S. Gonzalez-Sevilla⁵², G.R. Gonzalvo Rodriguez¹⁶⁹,
R.Y. González Andana^{142a}, L. Goossens³⁴, N.A. Gorasia¹⁹, P.A. Gorbounov¹¹⁹, H.A. Gordon²⁷,
B. Gorini³⁴, E. Gorini^{65a,65b}, A. Gorišek⁸⁹, A.T. Goshaw⁴⁷, M.I. Gostkin⁷⁷, C.A. Gottardo¹¹⁴,
M. Gouighri^{33b}, V. Goumarre⁴⁴, A.G. Goussiou¹⁴⁴, N. Govender^{31c}, C. Goy⁴, I. Grabowska-Bold^{81a},
K. Graham³², E. Gramstad¹²⁹, S. Grancagnolo¹⁷, M. Grandi¹⁵², V. Gratchev¹³³, P.M. Gravila^{25f},
F.G. Gravili^{65a,65b}, H.M. Gray¹⁶, C. Grefe²², I.M. Gregor⁴⁴, P. Grenier¹⁴⁹, K. Grevtsov⁴⁴, C. Grieco¹²,
N.A. Grieser¹²⁴, A.A. Grillo¹⁴¹, K. Grimm^{29,1}, S. Grinstein^{12,v}, J.-F. Grivaz⁶², S. Groh⁹⁶, E. Gross¹⁷⁵,
J. Grosse-Knetter⁵¹, C. Grud¹⁰², A. Grummer¹¹³, J.C. Grundy¹³⁰, L. Guan¹⁰², W. Guan¹⁷⁶, C. Gubbels¹⁷⁰,
J. Guenther³⁴, J.G.R. Guerrero Rojas¹⁶⁹, F. Guescini¹¹¹, D. Guest¹⁷, R. Gugel⁹⁶, A. Guida⁴⁴,
T. Guillemain⁴, S. Guindon³⁴, J. Guo^{58c}, L. Guo⁶², Y. Guo¹⁰², R. Gupta⁴⁴, S. Gurbuz²², G. Gustavino¹²⁴,
M. Guth⁵², P. Gutierrez¹²⁴, L.F. Gutierrez Zagazeta¹³², C. Gutschow⁹², C. Guyot¹⁴⁰, C. Gwenlan¹³⁰,
C.B. Gwilliam⁸⁸, E.S. Haaland¹²⁹, A. Haas¹²¹, M. Habedank⁴⁴, C. Haber¹⁶, H.K. Hadavand⁷, A. Hade⁹⁶,
S. Hadzic¹¹¹, M. Haleem¹⁷², J. Haley¹²⁵, J.J. Hall¹⁴⁵, G. Halladjian¹⁰³, G.D. Hallewell⁹⁸, L. Halser¹⁸,
K. Hamano¹⁷¹, H. Hamdaoui^{33e}, M. Hamer²², G.N. Hamity⁴⁸, K. Han^{58a}, L. Han^{13c}, L. Han^{58a}, S. Han¹⁶,
Y.F. Han¹⁶², K. Hanagaki^{79,t}, M. Hance¹⁴¹, M.D. Hank³⁵, R. Hankache⁹⁷, E. Hansen⁹⁴, J.B. Hansen³⁸,
J.D. Hansen³⁸, M.C. Hansen²², P.H. Hansen³⁸, K. Hara¹⁶⁴, T. Harenberg¹⁷⁷, S. Harkusha¹⁰⁴,
Y.T. Harris¹³⁰, P.F. Harrison¹⁷³, N.M. Hartman¹⁴⁹, N.M. Hartmann¹¹⁰, Y. Hasegawa¹⁴⁶, A. Hasib⁴⁸,
S. Hassani¹⁴⁰, S. Haug¹⁸, R. Hauser¹⁰³, M. Havranek¹³⁷, C.M. Hawkes¹⁹, R.J. Hawkings³⁴,
S. Hayashida¹¹², D. Hayden¹⁰³, C. Hayes¹⁰², R.L. Hayes¹⁷⁰, C.P. Hays¹³⁰, J.M. Hays⁹⁰, H.S. Hayward⁸⁸,
S.J. Haywood¹³⁹, F. He^{58a}, Y. He¹⁶⁰, Y. He¹³¹, M.P. Heath⁴⁸, V. Hedberg⁹⁴, A.L. Heggelund¹²⁹,
N.D. Hehir⁹⁰, C. Heidegger⁵⁰, K.K. Heidegger⁵⁰, W.D. Heidorn⁷⁶, J. Heilman³², S. Heim⁴⁴, T. Heim¹⁶,
B. Heinemann^{44,ah}, J.G. Heinlein¹³², J.J. Heinrich¹²⁷, L. Heinrich³⁴, J. Hejbal¹³⁶, L. Helary⁴⁴, A. Held¹²¹,
C.M. Helling¹⁴¹, S. Hellman^{43a,43b}, C. Helsens³⁴, R.C.W. Henderson⁸⁷, L. Henkelmann³⁰,
A.M. Henriques Correia³⁴, H. Herde¹⁴⁹, Y. Hernández Jiménez¹⁵¹, H. Herr⁹⁶, M.G. Herrmann¹¹⁰,
T. Herrmann⁴⁶, G. Herten⁵⁰, R. Hertenberger¹¹⁰, L. Hervas³⁴, N.P. Hessey^{163a}, H. Hibi⁸⁰, S. Higashino⁷⁹,
E. Higón-Rodríguez¹⁶⁹, K.H. Hiller⁴⁴, S.J. Hillier¹⁹, M. Hils⁴⁶, I. Hinchliffe¹⁶, F. Hinterkeuser²²,
M. Hirose¹²⁸, S. Hirose¹⁶⁴, D. Hirschebuehl¹⁷⁷, B. Hiti⁸⁹, O. Hladik¹³⁶, J. Hobbs¹⁵¹, R. Hobincu^{25e},
N. Hod¹⁷⁵, M.C. Hodgkinson¹⁴⁵, B.H. Hodgkinson³⁰, A. Hoecker³⁴, J. Hofer⁴⁴, D. Hohn⁵⁰, T. Holm²²,
T.R. Holmes³⁵, M. Holzbock¹¹¹, L.B.A.H. Hommels³⁰, B.P. Honan⁹⁷, J. Hong^{58c}, T.M. Hong¹³⁴,
Y. Hong⁵¹, J.C. Honig⁵⁰, A. Hönle¹¹¹, B.H. Hooberman¹⁶⁸, W.H. Hopkins⁵, Y. Horii¹¹², L.A. Horyn³⁵,
S. Hou¹⁵⁴, J. Howarth⁵⁵, J. Hoya⁸⁶, M. Hrabovsky¹²⁶, A. Hrynevich¹⁰⁵, T. Hryn'ova⁴, P.J. Hsu⁶¹,

S.-C. Hsu¹⁴⁴, Q. Hu³⁷, S. Hu^{58c}, Y.F. Hu^{13a,13d,al}, D.P. Huang⁹², X. Huang^{13c}, Y. Huang^{58a}, Y. Huang^{13a}, Z. Hubacek¹³⁷, F. Hubaut⁹⁸, M. Huebner²², F. Huegging²², T.B. Huffman¹³⁰, M. Huhtinen³⁴, S.K. Huiberts¹⁵, R. Hulsken⁵⁶, N. Huseynov^{77,z}, J. Huston¹⁰³, J. Huth⁵⁷, R. Hyneman¹⁴⁹, S. Hyrych^{26a}, G. Iacobucci⁵², G. Iakovidis²⁷, I. Ibragimov¹⁴⁷, L. Iconomidou-Fayard⁶², P. Iengo³⁴, R. Iguchi¹⁵⁹, T. Iizawa⁵², Y. Ikegami⁷⁹, A. Ilg¹⁸, N. Ilic¹⁶², H. Imam^{33a}, T. Ingebretsen Carlson^{43a,43b}, G. Introzzi^{68a,68b}, M. Iodice^{72a}, V. Ippolito^{70a,70b}, M. Ishino¹⁵⁹, W. Islam¹⁷⁶, C. Issever^{17,44}, S. Istin^{11c,am}, J.M. Iturbe Ponce^{60a}, R. Iuppa^{73a,73b}, A. Ivina¹⁷⁵, J.M. Izen⁴¹, V. Izzo^{67a}, P. Jacka¹³⁶, P. Jackson¹, R.M. Jacobs⁴⁴, B.P. Jaeger¹⁴⁸, C.S. Jagfeld¹¹⁰, G. Jäkel¹⁷⁷, K. Jakobs⁵⁰, T. Jakoubek¹⁷⁵, J. Jamieson⁵⁵, K.W. Janas^{81a}, G. Jarlskog⁹⁴, A.E. Jaspan⁸⁸, N. Javadov^{77,z}, T. Javûrek³⁴, M. Javurkova⁹⁹, F. Jeanneau¹⁴⁰, L. Jeanty¹²⁷, J. Jejelava^{155a,aa}, P. Jenni^{50,e}, S. Jézéquel⁴, J. Jia¹⁵¹, Z. Jia^{13c}, Y. Jiang^{58a}, S. Jiggins⁴⁸, J. Jimenez Pena¹¹¹, S. Jin^{13c}, A. Jinaru^{25b}, O. Jinnouchi¹⁶⁰, H. Jivan^{31f}, P. Johansson¹⁴⁵, K.A. Johns⁶, C.A. Johnson⁶³, D.M. Jones³⁰, E. Jones¹⁷³, R.W.L. Jones⁸⁷, T.J. Jones⁸⁸, J. Jovicevic¹⁴, X. Ju¹⁶, J.J. Junggeburth³⁴, A. Juste Rozas^{12,v}, S. Kabana^{142d}, A. Kaczmarska⁸², M. Kado^{70a,70b}, H. Kagan¹²³, M. Kagan¹⁴⁹, A. Kahn³⁷, A. Kahn¹³², C. Kahra⁹⁶, T. Kaji¹⁷⁴, E. Kajomovitz¹⁵⁶, C.W. Kalderon²⁷, A. Kamenshchikov¹¹⁸, M. Kaneda¹⁵⁹, N.J. Kang¹⁴¹, S. Kang⁷⁶, Y. Kano¹¹², D. Kar^{31f}, K. Karava¹³⁰, M.J. Kareem^{163b}, I. Karkaniyas¹⁵⁸, S.N. Karpov⁷⁷, Z.M. Karpova⁷⁷, V. Kartvelishvili⁸⁷, A.N. Karyukhin¹¹⁸, E. Kasimi¹⁵⁸, C. Kato^{58d}, J. Katzy⁴⁴, K. Kawade¹⁴⁶, K. Kawagoe⁸⁵, T. Kawaguchi¹¹², T. Kawamoto¹⁴⁰, G. Kawamura⁵¹, E.F. Kay¹⁷¹, F.I. Kaya¹⁶⁵, S. Kazakos¹², V.F. Kazanin^{117b,117a}, Y. Ke¹⁵¹, J.M. Keaveney^{31a}, R. Keeler¹⁷¹, J.S. Keller³², A.S. Kelly⁹², D. Kelsey¹⁵², J.J. Kempster¹⁹, J. Kendrick¹⁹, K.E. Kennedy³⁷, O. Kepka¹³⁶, S. Kersten¹⁷⁷, B.P. Kerševan⁸⁹, S. Ketabchi Haghghat¹⁶², M. Khandoga¹³¹, A. Khanov¹²⁵, A.G. Kharlamov^{117b,117a}, T. Kharlamova^{117b,117a}, E.E. Khoda¹⁴⁴, T.J. Khoo¹⁷, G. Khorauli¹⁷², E. Khramov⁷⁷, J. Khubua^{155b}, S. Kido⁸⁰, M. Kiehn³⁴, A. Kilgallon¹²⁷, E. Kim¹⁶⁰, Y.K. Kim³⁵, N. Kimura⁹², A. Kirchhoff⁵¹, D. Kirchmeier⁴⁶, C. Kirfel²², J. Kirk¹³⁹, A.E. Kiryunin¹¹¹, T. Kishimoto¹⁵⁹, D.P. Kisliuk¹⁶², C. Kitsaki⁹, O. Kivernyk²², T. Klapdor-Kleingrothaus⁵⁰, M. Klassen^{59a}, C. Klein³², L. Klein¹⁷², M.H. Klein¹⁰², M. Klein⁸⁸, U. Klein⁸⁸, P. Klimek³⁴, A. Klimentov²⁷, F. Klimpel¹¹¹, T. Klingl²², T. Klioutchnikova³⁴, F.F. Klitzner¹¹⁰, P. Kluit¹¹⁵, S. Kluth¹¹¹, E. Kneringer⁷⁴, T.M. Knight¹⁶², A. Knue⁵⁰, D. Kobayashi⁸⁵, R. Kobayashi⁸³, M. Kobel⁴⁶, M. Kocian¹⁴⁹, T. Kodama¹⁵⁹, P. Kodys¹³⁸, D.M. Koeck¹⁵², P.T. Koenig²², T. Koffas³², N.M. Köhler³⁴, M. Kolb¹⁴⁰, I. Koletsou⁴, T. Komarek¹²⁶, K. Köneke⁵⁰, A.X.Y. Kong¹, T. Kono¹²², V. Konstantinides⁹², N. Konstantinidis⁹², B. Konya⁹⁴, R. Kopeliansky⁶³, S. Koperny^{81a}, K. Korcyl⁸², K. Kordas¹⁵⁸, G. Koren¹⁵⁷, A. Korn⁹², S. Korn⁵¹, I. Korolkov¹², E.V. Korolkova¹⁴⁵, N. Korotkova¹⁰⁹, B. Kortman¹¹⁵, O. Kortner¹¹¹, S. Kortner¹¹¹, W.H. Kostecka¹¹⁶, V.V. Kostyukhin^{147,161}, A. Kotskechagia⁶², A. Kotwal⁴⁷, A. Koulouris³⁴, A. Kourkoumeli-Charalampidi^{68a,68b}, C. Kourkoumelis⁸, E. Kourlitis⁵, O. Kovanda¹⁵², R. Kowalewski¹⁷¹, W. Kozanecki¹⁴⁰, A.S. Kozhin¹¹⁸, V.A. Kramarenko¹⁰⁹, G. Kramberger⁸⁹, P. Kramer⁹⁶, D. Krasnopevtsev^{58a}, M.W. Krasny¹³¹, A. Krasznahorkay³⁴, J.A. Kremer⁹⁶, J. Kretzschmar⁸⁸, K. Kreul¹⁷, P. Krieger¹⁶², F. Krieter¹¹⁰, S. Krishnamurthy⁹⁹, A. Krishnan^{59b}, M. Krivos¹³⁸, K. Krizka¹⁶, K. Kroeninger⁴⁵, H. Kroha¹¹¹, J. Kroll¹³⁶, J. Kroll¹³², K.S. Krowpman¹⁰³, U. Kruchonak⁷⁷, H. Krüger²², N. Krumnack⁷⁶, M.C. Kruse⁴⁷, J.A. Krzysiak⁸², A. Kubota¹⁶⁰, O. Kuchinskaia¹⁶¹, S. Kuday^{3a}, D. Kuechler⁴⁴, J.T. Kuechler⁴⁴, S. Kuehn³⁴, T. Kuhl⁴⁴, V. Kukhtin⁷⁷, Y. Kulchitsky^{104,ad}, S. Kuleshov^{142c}, M. Kumar^{31f}, N. Kumari⁹⁸, M. Kuna⁵⁶, A. Kupco¹³⁶, T. Kupfer⁴⁵, O. Kuprash⁵⁰, H. Kurashige⁸⁰, L.L. Kurchaninov^{163a}, Y.A. Kurochkin¹⁰⁴, A. Kurova¹⁰⁸, M.G. Kurth^{13a,13d}, E.S. Kuwertz³⁴, M. Kuze¹⁶⁰, A.K. Kvam¹⁴⁴, J. Kvita¹²⁶, T. Kwan¹⁰⁰, K.W. Kwok^{60a}, C. Lacasta¹⁶⁹, F. Lacava^{70a,70b}, H. Lacker¹⁷, D. Lacour¹³¹, N.N. Lad⁹², E. Ladygin⁷⁷, R. Lafaye⁴, B. Laforge¹³¹, T. Lagouri^{142d}, S. Lai⁵¹, I.K. Lakomic^{81a}, N. Lalloue⁵⁶, J.E. Lambert¹²⁴, S. Lammers⁶³, W. Lamp¹⁶, C. Lampoudis¹⁵⁸, E. Lançon²⁷, U. Landgraf⁵⁰, M.P.J. Landon⁹⁰, V.S. Lang⁵⁰, J.C. Lange⁵¹, R.J. Langenberg⁹⁹, A.J. Lankford¹⁶⁶, F. Lanni²⁷, K. Lantzsch²², A. Lanza^{68a}, A. Lapertosa^{53b,53a}, J.F. Laporte¹⁴⁰, T. Lari^{66a}, F. Lasagni Manghi^{21b}, M. Lassnig³⁴, V. Latonova¹³⁶, T.S. Lau^{60a}, A. Laudrain⁹⁶, A. Laurier³²,

M. Lavorgna^{67a,67b}, S.D. Lawlor⁹¹, Z. Lawrence⁹⁷, M. Lazzaroni^{66a,66b}, B. Le⁹⁷, B. Leban⁸⁹,
A. Lebedev⁷⁶, M. LeBlanc³⁴, T. LeCompte⁵, F. Ledroit-Guillon⁵⁶, A.C.A. Lee⁹², G.R. Lee¹⁵, L. Lee⁵⁷,
S.C. Lee¹⁵⁴, S. Lee⁷⁶, L.L. Leeuw^{31c}, B. Lefebvre^{163a}, H.P. Lefebvre⁹¹, M. Lefebvre¹⁷¹, C. Leggett¹⁶,
K. Lehmann¹⁴⁸, N. Lehmann¹⁸, G. Lehmann Miotto³⁴, W.A. Leight⁴⁴, A. Leisos^{158,u}, M.A.L. Leite^{78c},
C.E. Leitgeb⁴⁴, R. Leitner¹³⁸, K.J.C. Leney⁴⁰, T. Lenz²², S. Leone^{69a}, C. Leonidopoulos⁴⁸, A. Leopold¹⁵⁰,
C. Leroy¹⁰⁶, R. Les¹⁰³, C.G. Lester³⁰, M. Levchenko¹³³, J. Levêque⁴, D. Levin¹⁰², L.J. Levinson¹⁷⁵,
D.J. Lewis¹⁹, B. Li^{13b}, B. Li^{58b}, C. Li^{58a}, C-Q. Li^{58c,58d}, H. Li^{58a}, H. Li^{58b}, H. Li^{58b}, J. Li^{58c}, K. Li¹⁴⁴,
L. Li^{58c}, M. Li^{13a,13d}, Q.Y. Li^{58a}, S. Li^{58d,58c,c}, T. Li^{58b}, X. Li⁴⁴, Y. Li⁴⁴, Z. Li^{58b}, Z. Li¹³⁰, Z. Li¹⁰⁰,
Z. Li⁸⁸, Z. Liang^{13a}, M. Liberatore⁴⁴, B. Liberti^{71a}, K. Lie^{60c}, J. Lieber Marin^{78b}, K. Lin¹⁰³, R.A. Linck⁶³,
R.E. Lindley⁶, J.H. Lindon², A. Linss⁴⁴, E. Lipeles¹³², A. Lipniacka¹⁵, T.M. Liss^{168,ai}, A. Lister¹⁷⁰,
J.D. Little⁷, B. Liu^{13a}, B.X. Liu¹⁴⁸, J.B. Liu^{58a}, J.K.K. Liu³⁵, K. Liu^{58d,58c}, M. Liu^{58a}, M.Y. Liu^{58a},
P. Liu^{13a}, X. Liu^{58a}, Y. Liu⁴⁴, Y. Liu^{13c,13d}, Y.L. Liu¹⁰², Y.W. Liu^{58a}, M. Livan^{68a,68b},
J. Llorente Merino¹⁴⁸, S.L. Lloyd⁹⁰, E.M. Lobodzinska⁴⁴, P. Loch⁶, S. Loffredo^{71a,71b}, T. Lohse¹⁷,
K. Lohwasser¹⁴⁵, M. Lokajicek¹³⁶, J.D. Long¹⁶⁸, I. Longarini^{70a,70b}, L. Longo³⁴, R. Longo¹⁶⁸,
I. Lopez Paz¹², A. Lopez Solis⁴⁴, J. Lorenz¹¹⁰, N. Lorenzo Martinez⁴, A.M. Lory¹¹⁰, A. Lösle⁵⁰,
X. Lou^{43a,43b}, X. Lou^{13a}, A. Lounis⁶², J. Love⁵, P.A. Love⁸⁷, J.J. Lozano Bahilo¹⁶⁹, G. Lu^{13a}, M. Lu^{58a},
S. Lu¹³², Y.J. Lu⁶¹, H.J. Lubatti¹⁴⁴, C. Luci^{70a,70b}, F.L. Lucio Alves^{13c}, A. Lucotte⁵⁶, F. Luehring⁶³,
I. Luise¹⁵¹, L. Luminari^{70a}, O. Lundberg¹⁵⁰, B. Lund-Jensen¹⁵⁰, N.A. Luongo¹²⁷, M.S. Lutz¹⁵⁷, D. Lynn²⁷,
H. Lyons⁸⁸, R. Lysak¹³⁶, E. Lytken⁹⁴, F. Lyu^{13a}, V. Lyubushkin⁷⁷, T. Lyubushkina⁷⁷, H. Ma²⁷, L.L. Ma^{58b},
Y. Ma⁹², D.M. Mac Donnell¹⁷¹, G. Maccarrone⁴⁹, C.M. Macdonald¹⁴⁵, J.C. MacDonald¹⁴⁵, R. Madar³⁶,
W.F. Mader⁴⁶, M. Madugoda Ralalage Don¹²⁵, N. Madysa⁴⁶, J. Maeda⁸⁰, T. Maeno²⁷, M. Maerker⁴⁶,
V. Magerl⁵⁰, J. Magro^{64a,64c}, D.J. Mahon³⁷, C. Maidantchik^{78b}, A. Maio^{135a,135b,135d}, K. Maj^{81a},
O. Majersky^{26a}, S. Majewski¹²⁷, N. Makovec⁶², V. Maksimovic¹⁴, B. Malaescu¹³¹, Pa. Malecki⁸²,
V.P. Maleev¹³³, F. Malek⁵⁶, D. Malito^{39b,39a}, U. Mallik⁷⁵, C. Malone³⁰, S. Maltezos⁹, S. Malyukov⁷⁷,
J. Mamuzic¹⁶⁹, G. Mancini⁴⁹, J.P. Mandalia⁹⁰, I. Mandić⁸⁹, L. Manhaes de Andrade Filho^{78a},
I.M. Maniatis¹⁵⁸, M. Manisha¹⁴⁰, J. Manjarres Ramos⁴⁶, K.H. Mankinen⁹⁴, A. Mann¹¹⁰, A. Manousos⁷⁴,
B. Mansoulie¹⁴⁰, I. Manthos¹⁵⁸, S. Manzoni¹¹⁵, A. Marantis^{158,u}, G. Marchiori¹³¹, M. Marcisovsky¹³⁶,
L. Marcoccia^{71a,71b}, C. Marcon⁹⁴, M. Marjanovic¹²⁴, Z. Marshall¹⁶, S. Marti-Garcia¹⁶⁹, T.A. Martin¹⁷³,
V.J. Martin⁴⁸, B. Martin dit Latour¹⁵, L. Martinelli^{70a,70b}, M. Martinez^{12,v}, P. Martinez Agullo¹⁶⁹,
V.I. Martinez Outschoorn⁹⁹, S. Martin-Haugh¹³⁹, V.S. Martoiu^{25b}, A.C. Martyniuk⁹², A. Marzin³⁴,
S.R. Maschek¹¹¹, L. Masetti⁹⁶, T. Mashimo¹⁵⁹, J. Masik⁹⁷, A.L. Maslennikov^{117b,117a}, L. Massa^{21b},
P. Massarotti^{67a,67b}, P. Mastrandrea^{69a,69b}, A. Mastroberardino^{39b,39a}, T. Masubuchi¹⁵⁹, D. Matakias²⁷,
T. Mathisen¹⁶⁷, A. Matic¹¹⁰, N. Matsuzawa¹⁵⁹, J. Maurer^{25b}, B. Maček⁸⁹, D.A. Maximov^{117b,117a},
R. Mazini¹⁵⁴, I. Maznas¹⁵⁸, S.M. Mazza¹⁴¹, C. Mc Ginn²⁷, J.P. Mc Gowan¹⁰⁰, S.P. Mc Kee¹⁰²,
T.G. McCarthy¹¹¹, W.P. McCormack¹⁶, E.F. McDonald¹⁰¹, A.E. McDougall¹¹⁵, J.A. Mcfayden¹⁵²,
G. Mchedlidze^{155b}, M.A. McKay⁴⁰, K.D. McLean¹⁷¹, S.J. McMahon¹³⁹, P.C. McNamara¹⁰¹,
R.A. McPherson^{171,y}, J.E. Mdhluli^{31f}, Z.A. Meadows⁹⁹, S. Meehan³⁴, T. Megy³⁶, S. Mehlhase¹¹⁰,
A. Mehta⁸⁸, B. Meirose⁴¹, D. Melini¹⁵⁶, B.R. Mellado Garcia^{31f}, A.H. Melo⁵¹, F. Meloni⁴⁴, A. Melzer²²,
E.D. Mendes Gouveia^{135a}, A.M. Mendes Jacques Da Costa¹⁹, H.Y. Meng¹⁶², L. Meng³⁴, S. Menke¹¹¹,
M. Mentink³⁴, E. Meoni^{39b,39a}, C. Merlassino¹³⁰, P. Mermod^{52,*}, L. Merola^{67a,67b}, C. Meroni^{66a},
G. Merz¹⁰², O. Meshkov^{107,109}, J.K.R. Meshreki¹⁴⁷, J. Metcalfe⁵, A.S. Mete⁵, C. Meyer⁶³, J-P. Meyer¹⁴⁰,
M. Michetti¹⁷, R.P. Middleton¹³⁹, L. Mijović⁴⁸, G. Mikenberg¹⁷⁵, M. Mikesikova¹³⁶, M. Mikuž⁸⁹,
H. Mildner¹⁴⁵, A. Milic¹⁶², C.D. Milke⁴⁰, D.W. Miller³⁵, L.S. Miller³², A. Milov¹⁷⁵, D.A. Milstead^{43a,43b},
T. Min^{13c}, A.A. Minaenko¹¹⁸, I.A. Minashvili^{155b}, L. Mince⁵⁵, A.I. Mincer¹²¹, B. Mindur^{81a}, M. Mineev⁷⁷,
Y. Minegishi¹⁵⁹, Y. Mino⁸³, L.M. Mir¹², M. Miralles Lopez¹⁶⁹, M. Mironova¹³⁰, T. Mitani¹⁷⁴,
V.A. Mitsou¹⁶⁹, M. Mittal^{58c}, O. Miu¹⁶², P.S. Miyagawa⁹⁰, Y. Miyazaki⁸⁵, A. Mizukami⁷⁹,
J.U. Mjörnmark⁹⁴, T. Mkrtchyan^{59a}, M. Mlynarikova¹¹⁶, T. Moe^{43a,43b}, S. Mobius⁵¹, K. Mochizuki¹⁰⁶,

P. Moder⁴⁴, P. Mogg¹¹⁰, A.F. Mohammed^{13a}, S. Mohapatra³⁷, G. Mokgatitswane^{31f}, B. Mondal¹⁴⁷,
 S. Mondal¹³⁷, K. Mönig⁴⁴, E. Monnier⁹⁸, L. Monsonis Romero¹⁶⁹, A. Montalbano¹⁴⁸,
 J. Montejo Berlingen³⁴, M. Montella¹²³, F. Monticelli⁸⁶, N. Morange⁶², A.L. Moreira De Carvalho^{135a},
 M. Moreno Llácer¹⁶⁹, C. Moreno Martinez¹², P. Moretini^{53b}, S. Morgenstern¹⁷³, D. Mori¹⁴⁸, M. Morii⁵⁷,
 M. Morinaga¹⁵⁹, V. Morisbak¹²⁹, A.K. Morley³⁴, A.P. Morris⁹², L. Morvaj³⁴, P. Moschovakos³⁴,
 B. Moser¹¹⁵, M. Mosidze^{155b}, T. Moskalets⁵⁰, P. Moskvitina¹¹⁴, J. Moss^{29,n}, E.J.W. Moyse⁹⁹, S. Muanza⁹⁸,
 J. Mueller¹³⁴, R. Mueller¹⁸, D. Muenstermann⁸⁷, G.A. Mullier⁹⁴, J.J. Mullin¹³², D.P. Mungo^{66a,66b},
 J.L. Munoz Martinez¹², F.J. Munoz Sanchez⁹⁷, M. Murin⁹⁷, P. Murin^{26b}, W.J. Murray^{173,139},
 A. Murrone^{66a,66b}, J.M. Muse¹²⁴, M. Muškinja¹⁶, C. Mwewa²⁷, A.G. Myagkov^{118,ae}, A.J. Myers⁷,
 A.A. Myers¹³⁴, G. Myers⁶³, M. Myska¹³⁷, B.P. Nachman¹⁶, O. Nackenhorst⁴⁵, A.Nag Nag⁴⁶, K. Nagai¹³⁰,
 K. Nagano⁷⁹, J.L. Nagle²⁷, E. Nagy⁹⁸, A.M. Nairz³⁴, Y. Nakahama¹¹², K. Nakamura⁷⁹, H. Nanjo¹²⁸,
 F. Napolitano^{59a}, R. Narayan⁴⁰, E.A. Narayanan¹¹³, I. Naryshkin¹³³, M. Naseri³², C. Nass²², T. Naumann⁴⁴,
 G. Navarro^{20a}, J. Navarro-Gonzalez¹⁶⁹, R. Nayak¹⁵⁷, P.Y. Nechaeva¹⁰⁷, F. Nechansky⁴⁴, T.J. Neep¹⁹,
 A. Negri^{68a,68b}, M. Negrini^{21b}, C. Nellist¹¹⁴, C. Nelson¹⁰⁰, K. Nelson¹⁰², S. Nemecek¹³⁶, M. Nessi^{34,f},
 M.S. Neubauer¹⁶⁸, F. Neuhaus⁹⁶, J. Neundorff⁴⁴, R. Newhouse¹⁷⁰, P.R. Newman¹⁹, C.W. Ng¹³⁴, Y.S. Ng¹⁷,
 Y.W.Y. Ng¹⁶⁶, B. Ngair^{33e}, H.D.N. Nguyen¹⁰⁶, R.B. Nickerson¹³⁰, R. Nicolaidou¹⁴⁰, D.S. Nielsen³⁸,
 J. Nielsen¹⁴¹, M. Niemeier⁵¹, N. Nikiforou¹⁰, V. Nikolaenko^{118,ae}, I. Nikolic-Audit¹³¹, K. Nikolopoulos¹⁹,
 P. Nilsson²⁷, H.R. Nindhito⁵², A. Nisati^{70a}, N. Nishu², R. Nisius¹¹¹, T. Nitta¹⁷⁴, T. Nobe¹⁵⁹, D.L. Noel³⁰,
 Y. Noguchi⁸³, I. Nomidis¹³¹, M.A. Nomura²⁷, M.B. Norfolk¹⁴⁵, R.R.B. Norisam⁹², J. Novak⁸⁹, T. Novak⁴⁴,
 O. Novgorodova⁴⁶, L. Novotny¹³⁷, R. Novotny¹¹³, L. Nozka¹²⁶, K. Ntekas¹⁶⁶, E. Nurse⁹²,
 F.G. Oakham^{32,aj}, J. Ocariz¹³¹, A. Ochi⁸⁰, I. Ochoa^{135a}, J.P. Ochoa-Ricoux^{142a}, S. Oda⁸⁵, S. Odaka⁷⁹,
 S. Oerdek¹⁶⁷, A. Ogrodnik^{81a}, A. Oh⁹⁷, C.C. Ohm¹⁵⁰, H. Oide¹⁶⁰, R. Oishi¹⁵⁹, M.L. Ojeda⁴⁴,
 Y. Okazaki⁸³, M.W. O'Keefe⁸⁸, Y. Okumura¹⁵⁹, A. Olariu^{25b}, L.F. Oleiro Seabra^{135a},
 S.A. Olivares Pino^{142d}, D. Oliveira Damazio²⁷, D. Oliveira Goncalves^{78a}, J.L. Oliver¹⁶⁶, M.J.R. Olsson¹⁶⁶,
 A. Olszewski⁸², J. Olszowska⁸², Ö.O. Öncel²², D.C. O'Neil¹⁴⁸, A.P. O'Neill¹³⁰, A. Onofre^{135a,135e},
 P.U.E. Onyisi¹⁰, R.G. Oreamuno Madriz¹¹⁶, M.J. Oreglia³⁵, G.E. Orellana⁸⁶, D. Orestano^{72a,72b},
 N. Orlando¹², R.S. Orr¹⁶², V. O'Shea⁵⁵, R. Ospanov^{58a}, G. Otero y Garzon²⁸, H. Otono⁸⁵, P.S. Ott^{59a},
 G.J. Ottino¹⁶, M. Ouchrif^{33d}, J. Ouellette²⁷, F. Ould-Saada¹²⁹, A. Ouraou^{140,*}, Q. Ouyang^{13a}, M. Owen⁵⁵,
 R.E. Owen¹³⁹, K.Y. Oyulmaz^{11c}, V.E. Ozcan^{11c}, N. Ozturk⁷, S. Ozturk^{11c}, J. Pacalt¹²⁶, H.A. Pacey³⁰,
 K. Pachal⁴⁷, A. Pacheco Pages¹², C. Padilla Aranda¹², S. Pagan Griso¹⁶, G. Palacino⁶³, S. Palazzo⁴⁸,
 S. Palestini³⁴, M. Palka^{81b}, P. Palni^{81a}, D.K. Panchal¹⁰, C.E. Pandini⁵², J.G. Panduro Vazquez⁹¹, P. Pani⁴⁴,
 G. Panizzo^{64a,64c}, L. Paolozzi⁵², C. Papadatos¹⁰⁶, S. Parajuli⁴⁰, A. Paramonov⁵, C. Paraskevopoulos⁹,
 D. Paredes Hernandez^{60b}, S.R. Paredes Saenz¹³⁰, B. Parida¹⁷⁵, T.H. Park¹⁶², A.J. Parker²⁹, M.A. Parker³⁰,
 F. Parodi^{53b,53a}, E.W. Parrish¹¹⁶, J.A. Parsons³⁷, U. Parzefall⁵⁰, L. Pascual Dominguez¹⁵⁷, V.R. Pascuzzi¹⁶,
 F. Pasquali¹¹⁵, E. Pasqualucci^{70a}, S. Passaggio^{53b}, F. Pastore⁹¹, P. Pasuwan^{43a,43b}, J.R. Pater⁹⁷,
 A. Pathak¹⁷⁶, J. Patton⁸⁸, T. Pauly³⁴, J. Pearkes¹⁴⁹, M. Pedersen¹²⁹, L. Pedraza Diaz¹¹⁴, R. Pedro^{135a},
 T. Peiffer⁵¹, S.V. Peleganchuk^{117b,117a}, O. Penc¹³⁶, C. Peng^{60b}, H. Peng^{58a}, M. Penzin¹⁶¹, B.S. Peralva^{78a},
 A.P. Pereira Peixoto^{135a}, L. Pereira Sanchez^{43a,43b}, D.V. Perepelitsa²⁷, E. Perez Codina^{163a}, M. Perganti⁹,
 L. Perini^{66a,66b}, H. Pernegger³⁴, S. Perrella³⁴, A. Perrevoort¹¹⁵, K. Peters⁴⁴, R.F.Y. Peters⁹⁷,
 B.A. Petersen³⁴, T.C. Petersen³⁸, E. Petit⁹⁸, V. Petousis¹³⁷, C. Petridou¹⁵⁸, P. Petroff⁶², F. Petrucci^{72a,72b},
 A. Petrukhin¹⁴⁷, M. Pettee¹⁷⁸, N.E. Pettersson³⁴, K. Petukhova¹³⁸, A. Peyaud¹⁴⁰, R. Pezoa^{142e},
 L. Pezzotti³⁴, G. Pezzullo¹⁷⁸, T. Pham¹⁰¹, P.W. Phillips¹³⁹, M.W. Phipps¹⁶⁸, G. Piacquadio¹⁵¹, E. Pianori¹⁶,
 F. Piazza^{66a,66b}, A. Picazio⁹⁹, R. Piegai²⁸, D. Pietreanu^{25b}, J.E. Pilcher³⁵, A.D. Pilkington⁹⁷,
 M. Pinamonti^{64a,64c}, J.L. Pinfold², C. Pitman Donaldson⁹², D.A. Pizzi³², L. Pizzimento^{71a,71b},
 A. Pizzini¹¹⁵, M.-A. Pleier²⁷, V. Plesanovs⁵⁰, V. Pleskot¹³⁸, E. Plotnikova⁷⁷, P. Podberezko^{117b,117a},
 R. Poettgen⁹⁴, R. Poggi⁵², L. Poggioli¹³¹, I. Pogrebnyak¹⁰³, D. Pohl²², I. Pokharel⁵¹, G. Polesello^{68a},
 A. Poley^{148,163a}, A. Policicchio^{70a,70b}, R. Polifka¹³⁸, A. Polini^{21b}, C.S. Pollard¹³⁰, Z.B. Pollock¹²³,

V. Polychronakos²⁷, D. Ponomarenko¹⁰⁸, L. Pontecorvo³⁴, S. Popa^{25a}, G.A. Popeneciu^{25d}, L. Portales⁴, D.M. Portillo Quintero^{163a}, S. Pospisil¹³⁷, P. Postolache^{25c}, K. Potamianos¹³⁰, I.N. Potrap⁷⁷, C.J. Potter³⁰, H. Potti¹, T. Poulsen⁴⁴, J. Poveda¹⁶⁹, T.D. Powell¹⁴⁵, G. Pownall⁴⁴, M.E. Pozo Astigarraga³⁴, A. Prades Ibanez¹⁶⁹, P. Pralavorio⁹⁸, M.M. Prapa⁴², S. Prell⁷⁶, D. Price⁹⁷, M. Primavera^{65a}, M.A. Principe Martin⁹⁵, M.L. Proffitt¹⁴⁴, N. Proklova¹⁰⁸, K. Prokofiev^{60c}, F. Prokoshin⁷⁷, S. Protopopescu²⁷, J. Proudfoot⁵, M. Przybycien^{81a}, D. Pudzha¹³³, P. Puza⁶², D. Pyatiizbyantseva¹⁰⁸, J. Qian¹⁰², Y. Qin⁹⁷, T. Qiu⁹⁰, A. Quadt⁵¹, M. Queitsch-Maitland³⁴, G. Rabanal Bolanos⁵⁷, F. Ragusa^{66a,66b}, J.A. Raine⁵², S. Rajagopalan²⁷, K. Ran^{13a,13d}, D.F. Rassloff^{59a}, D.M. Rauch⁴⁴, S. Rave⁹⁶, B. Ravina⁵⁵, I. Ravinovich¹⁷⁵, M. Raymond³⁴, A.L. Read¹²⁹, N.P. Readioff¹⁴⁵, D.M. Rebutti^{68a,68b}, G. Redlinger²⁷, K. Reeves⁴¹, D. Reikher¹⁵⁷, A. Reiss⁹⁶, A. Rej¹⁴⁷, C. Rembser³⁴, A. Renardi⁴⁴, M. Renda^{25b}, M.B. Rendel¹¹¹, A.G. Rennie⁵⁵, S. Resconi^{66a}, M. Ressegotti^{53b,53a}, E.D. Resseguie¹⁶, S. Rettie⁹², B. Reynolds¹²³, E. Reynolds¹⁹, M. Rezaei Estabragh¹⁷⁷, O.L. Rezanova^{117b,117a}, P. Reznicek¹³⁸, E. Ricci^{73a,73b}, R. Richter¹¹¹, S. Richter⁴⁴, E. Richter-Was^{81b}, M. Ridel¹³¹, P. Rieck¹¹¹, P. Riedler³⁴, O. Rifki⁴⁴, M. Rijssenbeek¹⁵¹, A. Rimoldi^{68a,68b}, M. Rimoldi⁴⁴, L. Rinaldi^{21b,21a}, T.T. Rinn¹⁶⁸, M.P. Rinnagel¹¹⁰, G. Ripellino¹⁵⁰, I. Riu¹², P. Rivadeneira⁴⁴, J.C. Rivera Vergara¹⁷¹, F. Rizatdinova¹²⁵, E. Rizvi⁹⁰, C. Rizzi⁵², B.A. Roberts¹⁷³, B.R. Roberts¹⁶, S.H. Robertson^{100,y}, M. Robin⁴⁴, D. Robinson³⁰, C.M. Robles Gajardo^{142e}, M. Robles Manzano⁹⁶, A. Robson⁵⁵, A. Rocchi^{71a,71b}, C. Roda^{69a,69b}, S. Rodriguez Bosca^{59a}, A. Rodriguez Rodriguez⁵⁰, A.M. Rodriguez Vera^{163b}, S. Roe³⁴, A.R. Roepe¹²⁴, J. Roggel¹⁷⁷, O. Røhne¹²⁹, R.A. Rojas¹⁷¹, B. Roland⁵⁰, C.P.A. Roland⁶³, J. Roloff²⁷, A. Romaniouk¹⁰⁸, M. Romano^{21b}, A.C. Romero Hernandez¹⁶⁸, N. Rompotis⁸⁸, M. Ronzani¹²¹, L. Roos¹³¹, S. Rosati^{70a}, B.J. Rosser¹³², E. Rossi¹⁶², E. Rossi⁴, E. Rossi^{67a,67b}, L.P. Rossi^{53b}, L. Rossini⁴⁴, R. Rosten¹²³, M. Rotaru^{25b}, B. Rottler⁵⁰, D. Rousseau⁶², D. Rousso³⁰, G. Rovelli^{68a,68b}, A. Roy¹⁰, A. Rozanov⁹⁸, Y. Rozen¹⁵⁶, X. Ruan^{31f}, A.J. Ruby⁸⁸, T.A. Ruggeri¹, F. Rühr⁵⁰, A. Ruiz-Martinez¹⁶⁹, A. Rummler³⁴, Z. Rurikova⁵⁰, N.A. Rusakovich⁷⁷, H.L. Russell³⁴, L. Rustige³⁶, J.P. Rutherford⁶, E.M. Rüttinger¹⁴⁵, M. Rybar¹³⁸, E.B. Rye¹²⁹, A. Ryzhov¹¹⁸, J.A. Sabater Iglesias⁴⁴, P. Sabatini¹⁶⁹, L. Sabetta^{70a,70b}, H.F-W. Sadrozinski¹⁴¹, R. Sadykov⁷⁷, F. Safai Tehrani^{70a}, B. Safarzadeh Samani¹⁵², M. Safdari¹⁴⁹, S. Saha¹⁰⁰, M. Sahinsoy¹¹¹, A. Sahu¹⁷⁷, M. Saimpert¹⁴⁰, M. Saito¹⁵⁹, T. Saito¹⁵⁹, D. Salamani³⁴, G. Salamanna^{72a,72b}, A. Salnikov¹⁴⁹, J. Salt¹⁶⁹, A. Salvador Salas¹², D. Salvatore^{39b,39a}, F. Salvatore¹⁵², A. Salzburger³⁴, D. Sammel⁵⁰, D. Sampsonidis¹⁵⁸, D. Sampsonidou^{58d,58c}, J. Sánchez¹⁶⁹, A. Sanchez Pineda⁴, V. Sanchez Sebastian¹⁶⁹, H. Sandaker¹²⁹, C.O. Sander⁴⁴, I.G. Sanderswood⁸⁷, J.A. Sandesara⁹⁹, M. Sandhoff¹⁷⁷, C. Sandoval^{20b}, D.P.C. Sankey¹³⁹, M. Sannino^{53b,53a}, A. Sansoni⁴⁹, C. Santoni³⁶, H. Santos^{135a,135b}, S.N. Santpur¹⁶, A. Santra¹⁷⁵, K.A. Saoucha¹⁴⁵, A. Sapronov⁷⁷, J.G. Saraiva^{135a,135d}, J. Sardain⁹⁸, O. Sasaki⁷⁹, K. Sato¹⁶⁴, C. Sauer^{59b}, F. Sauerburger⁵⁰, E. Sauvan⁴, P. Savard^{162,aj}, R. Sawada¹⁵⁹, C. Sawyer¹³⁹, L. Sawyer⁹³, I. Sayago Galvan¹⁶⁹, C. Sbarra^{21b}, A. Sbrizzi^{21b,21a}, T. Scanlon⁹², J. Schaarschmidt¹⁴⁴, P. Schacht¹¹¹, D. Schaefer³⁵, U. Schäfer⁹⁶, A.C. Schaffer⁶², D. Schaile¹¹⁰, R.D. Schamberger¹⁵¹, E. Schanet¹¹⁰, C. Scharf¹⁷, N. Scharmberg⁹⁷, V.A. Schegelsky¹³³, D. Scheirich¹³⁸, F. Schenck¹⁷, M. Schernau¹⁶⁶, C. Schiavi^{53b,53a}, L.K. Schildgen²², Z.M. Schillaci²⁴, E.J. Schioppa^{65a,65b}, M. Schioppa^{39b,39a}, B. Schlag⁹⁶, K.E. Schleicher⁵⁰, S. Schlenker³⁴, K. Schmieden⁹⁶, C. Schmitt⁹⁶, S. Schmitt⁴⁴, L. Schoeffel¹⁴⁰, A. Schoening^{59b}, P.G. Scholer⁵⁰, E. Schopf¹³⁰, M. Schott⁹⁶, J. Schovancova³⁴, S. Schramm⁵², F. Schroeder¹⁷⁷, H-C. Schultz-Coulon^{59a}, M. Schumacher⁵⁰, B.A. Schumm¹⁴¹, Ph. Schune¹⁴⁰, A. Schwartzman¹⁴⁹, T.A. Schwarz¹⁰², Ph. Schwemling¹⁴⁰, R. Schwienhorst¹⁰³, A. Sciandra¹⁴¹, G. Sciolla²⁴, F. Scuri^{69a}, F. Scutti¹⁰¹, C.D. Sebastiani⁸⁸, K. Sedlaczek⁴⁵, P. Seema¹⁷, S.C. Seidel¹¹³, A. Seiden¹⁴¹, B.D. Seidlitz²⁷, T. Seiss³⁵, C. Seitz⁴⁴, J.M. Seixas^{78b}, G. Sekhniaidze^{67a}, S.J. Sekula⁴⁰, L. Selem⁴, N. Semprini-Cesari^{21b,21a}, S. Sen⁴⁷, C. Serfon²⁷, L. Serin⁶², L. Serkin^{64a,64b}, M. Sessa^{72a,72b}, H. Severini¹²⁴, S. Sevova¹⁴⁹, F. Sforza^{53b,53a}, A. Sfyrla⁵², E. Shabalina⁵¹, R. Shaheen¹⁵⁰, J.D. Shahinian¹³², N.W. Shaikh^{43a,43b}, D. Shaked Renous¹⁷⁵, L.Y. Shan^{13a}, M. Shapiro¹⁶, A. Sharma³⁴,

A.S. Sharma¹, S. Sharma⁴⁴, P.B. Shatalov¹¹⁹, K. Shaw¹⁵², S.M. Shaw⁹⁷, P. Sherwood⁹², L. Shi⁹²,
 C.O. Shimmin¹⁷⁸, Y. Shimogama¹⁷⁴, J.D. Shinner⁹¹, I.P.J. Shipsey¹³⁰, S. Shirabe⁵², M. Shiyakova⁷⁷,
 J. Shlomi¹⁷⁵, M.J. Shochet³⁵, J. Shojaii¹⁰¹, D.R. Shope¹⁵⁰, S. Shrestha¹²³, E.M. Shrif^{31f}, M.J. Shroff¹⁷¹,
 E. Shulga¹⁷⁵, P. Sicho¹³⁶, A.M. Sickles¹⁶⁸, E. Sideras Haddad^{31f}, O. Sidiropoulou³⁴, A. Sidoti^{21b},
 F. Siegert⁴⁶, Dj. Sijacki¹⁴, J.M. Silva¹⁹, M.V. Silva Oliveira³⁴, S.B. Silverstein^{43a}, S. Simion⁶²,
 R. Simoniello³⁴, N.D. Simpson⁹⁴, S. Simsek^{11b}, P. Sinervo¹⁶², V. Sinetckii¹⁰⁹, S. Singh¹⁴⁸, S. Singh¹⁶²,
 S. Sinha⁴⁴, S. Sinha^{31f}, M. Sioli^{21b,21a}, I. Siral¹²⁷, S.Yu. Sivoklov¹⁰⁹, J. Sjölin^{43a,43b}, A. Skaf⁵¹,
 E. Skorda⁹⁴, P. Skubic¹²⁴, M. Slawinska⁸², K. Sliwa¹⁶⁵, V. Smakhtin¹⁷⁵, B.H. Smart¹³⁹, J. Smiesko¹³⁸,
 S.Yu. Smirnov¹⁰⁸, Y. Smirnov¹⁰⁸, L.N. Smirnova^{109,r}, O. Smirnova⁹⁴, E.A. Smith³⁵, H.A. Smith¹³⁰,
 M. Smizanska⁸⁷, K. Smolek¹³⁷, A. Smykiewicz⁸², A.A. Snesarev¹⁰⁷, H.L. Snoek¹¹⁵, S. Snyder²⁷,
 R. Sobie^{171,y}, A. Soffer¹⁵⁷, F. Sohns⁵¹, C.A. Solans Sanchez³⁴, E.Yu. Soldatov¹⁰⁸, U. Soldevila¹⁶⁹,
 A.A. Solodkov¹¹⁸, S. Solomon⁵⁰, A. Soloshenko⁷⁷, O.V. Solovyanov¹¹⁸, V. Solovyev¹³³, P. Sommer¹⁴⁵,
 H. Son¹⁶⁵, A. Sonay¹², W.Y. Song^{163b}, A. Sopczak¹³⁷, A.L. Sopio⁹², F. Sopkova^{26b}, S. Sottocornola^{68a,68b},
 R. Soualah^{64a,64c}, A.M. Soukharev^{117b,117a}, Z. Soumami^{33e}, D. South⁴⁴, S. Spagnolo^{65a,65b}, M. Spalla¹¹¹,
 M. Spangenberg¹⁷³, F. Spanò⁹¹, D. Sperlich⁵⁰, T.M. Spieker^{59a}, G. Spigo³⁴, M. Spina¹⁵², D.P. Spiteri⁵⁵,
 M. Spousta¹³⁸, A. Stabile^{66a,66b}, R. Stamen^{59a}, M. Stamenkovic¹¹⁵, A. Stampekis¹⁹, M. Standke²²,
 E. Stanecka⁸², B. Stanislaus³⁴, M.M. Stanitzki⁴⁴, M. Stankaityte¹³⁰, B. Stapf⁴⁴, E.A. Starchenko¹¹⁸,
 G.H. Stark¹⁴¹, J. Stark⁹⁸, D.M. Starke^{163b}, P. Staroba¹³⁶, P. Starovoitov^{59a}, S. Stärz¹⁰⁰, R. Staszewski⁸²,
 G. Stavropoulos⁴², P. Steinberg²⁷, A.L. Steinhebel¹²⁷, B. Stelzer^{148,163a}, H.J. Stelzer¹³⁴,
 O. Stelzer-Chilton^{163a}, H. Stenzel⁵⁴, T.J. Stevenson¹⁵², G.A. Stewart³⁴, M.C. Stockton³⁴, G. Stoicea^{25b},
 M. Stolarski^{135a}, S. Stonjek¹¹¹, A. Straessner⁴⁶, J. Strandberg¹⁵⁰, S. Strandberg^{43a,43b}, M. Strauss¹²⁴,
 T. Strebler⁹⁸, P. Strizenc^{26b}, R. Ströhmer¹⁷², D.M. Strom¹²⁷, L.R. Strom⁴⁴, R. Stroynowski⁴⁰,
 A. Strubig^{43a,43b}, S.A. Stucci²⁷, B. Stugu¹⁵, J. Stupak¹²⁴, N.A. Styles⁴⁴, D. Su¹⁴⁹, S. Su^{58a}, W. Su^{58d,144,58c},
 X. Su^{58a}, K. Sugizaki¹⁵⁹, V.V. Sulin¹⁰⁷, M.J. Sullivan⁸⁸, D.M.S. Sultan⁵², L. Sultanaliyeva¹⁰⁷,
 S. Sultansoy^{3c}, T. Sumida⁸³, S. Sun¹⁰², S. Sun¹⁷⁶, X. Sun⁹⁷, O. Sunneborn Gudnadottir¹⁶⁷,
 C.J.E. Suster¹⁵³, M.R. Sutton¹⁵², M. Svatos¹³⁶, M. Swiatlowski^{163a}, T. Swirski¹⁷², I. Sykora^{26a},
 M. Sykora¹³⁸, T. Sykora¹³⁸, D. Ta⁹⁶, K. Tackmann^{44,w}, A. Taffard¹⁶⁶, R. Tafirout^{163a}, R.H.M. Taibah¹³¹,
 R. Takashima⁸⁴, K. Takeda⁸⁰, T. Takeshita¹⁴⁶, E.P. Takeva⁴⁸, Y. Takubo⁷⁹, M. Talby⁹⁸,
 A.A. Talyshev^{117b,117a}, K.C. Tam^{60b}, N.M. Tamir¹⁵⁷, A. Tanaka¹⁵⁹, J. Tanaka¹⁵⁹, R. Tanaka⁶², J. Tang^{58c},
 Z. Tao¹⁷⁰, S. Tapia Araya⁷⁶, S. Tapprogge⁹⁶, A. Tarek Abouelfadl Mohamed¹⁰³, S. Tarem¹⁵⁶, K. Tariq^{58b},
 G. Tarna^{25b}, G.F. Tartarelli^{66a}, P. Tas¹³⁸, M. Tasevsky¹³⁶, E. Tassi^{39b,39a}, G. Tateno¹⁵⁹, Y. Tayalati^{33e},
 G.N. Taylor¹⁰¹, W. Taylor^{163b}, H. Teagle⁸⁸, A.S. Tee¹⁷⁶, R. Teixeira De Lima¹⁴⁹, P. Teixeira-Dias⁹¹,
 H. Ten Kate³⁴, J.J. Teoh¹¹⁵, K. Terashi¹⁵⁹, J. Terron⁹⁵, S. Terzo¹², M. Testa⁴⁹, R.J. Teuscher^{162,y},
 N. Themistokleous⁴⁸, T. Thevenaux-Pelzer¹⁷, O. Thielmann¹⁷⁷, D.W. Thomas⁹¹, J.P. Thomas¹⁹,
 E.A. Thompson⁴⁴, P.D. Thompson¹⁹, E. Thomson¹³², E.J. Thorpe⁹⁰, Y. Tian⁵¹, V. Tikhomirov^{107,af},
 Yu.A. Tikhonov^{117b,117a}, S. Timoshenko¹⁰⁸, P. Tipton¹⁷⁸, S. Tisserant⁹⁸, S.H. Tlou^{31f}, A. Tmourji³⁶,
 K. Todome^{21b,21a}, S. Todorova-Nova¹³⁸, S. Todt⁴⁶, M. Togawa⁷⁹, J. Tojo⁸⁵, S. Tokár^{26a}, K. Tokushuku⁷⁹,
 E. Tolley¹²³, R. Tombs³⁰, M. Tomoto^{79,112}, L. Tompkins¹⁴⁹, P. Tornambe⁹⁹, E. Torrence¹²⁷, H. Torres⁴⁶,
 E. Torró Pastor¹⁶⁹, M. Toscani²⁸, C. Toscirci³⁵, J. Toth^{98,x}, D.R. Tovey¹⁴⁵, A. Traeet¹⁵, C.J. Treado¹²¹,
 T. Trefzger¹⁷², A. Tricoli²⁷, I.M. Trigger^{163a}, S. Trincaz-Duvoid¹³¹, D.A. Trischuk¹⁷⁰, W. Trischuk¹⁶²,
 B. Trocmé⁵⁶, A. Trofymov⁶², C. Troncon^{66a}, F. Trovato¹⁵², L. Truong^{31c}, M. Trzebinski⁸², A. Trzupek⁸²,
 F. Tsai¹⁵¹, A. Tsiamis¹⁵⁸, P.V. Tsiareshka^{104,ad}, A. Tsirigotis^{158,u}, V. Tsiskaridze¹⁵¹, E.G. Tskhadadze^{155a},
 M. Tsopoulou¹⁵⁸, Y. Tsujikawa⁸³, I.I. Tsukerman¹¹⁹, V. Tsulaia¹⁶, S. Tsuno⁷⁹, O. Tsur¹⁵⁶, D. Tsybychev¹⁵¹,
 Y. Tu^{60b}, A. Tudorache^{25b}, V. Tudorache^{25b}, A.N. Tuna³⁴, S. Turchikhin⁷⁷, I. Turk Cakir^{3a}, R.J. Turner¹⁹,
 R. Turra^{66a}, P.M. Tuts³⁷, S. Tzamarias¹⁵⁸, P. Tzanis⁹, E. Tzovara⁹⁶, K. Uchida¹⁵⁹, F. Ukegawa¹⁶⁴,
 P.A. Ulloa Poblete^{142c}, G. Unal³⁴, M. Unal¹⁰, A. Undrus²⁷, G. Unel¹⁶⁶, F.C. Ungaro¹⁰¹, K. Uno¹⁵⁹,
 J. Urban^{26b}, P. Urquijo¹⁰¹, G. Usai⁷, R. Ushioda¹⁶⁰, M. Usman¹⁰⁶, Z. Uysal^{11d}, V. Vacek¹³⁷, B. Vachon¹⁰⁰,

K.O.H. Vadla¹²⁹, T. Vafeiadis³⁴, C. Valderanis¹¹⁰, E. Valdes Santurio^{43a,43b}, M. Valente^{163a},
 S. Valentinetti^{21b,21a}, A. Valero¹⁶⁹, R.A. Vallance¹⁹, A. Vallier⁹⁸, J.A. Valls Ferrer¹⁶⁹, T.R. Van Daalen¹⁴⁴,
 P. Van Gemmeren⁵, S. Van Stroud⁹², I. Van Vulpen¹¹⁵, M. Vanadia^{71a,71b}, W. Vandelli³⁴,
 M. Vandenbroucke¹⁴⁰, E.R. Vandewall¹²⁵, D. Vannicola¹⁵⁷, L. Vannoli^{53b,53a}, R. Vari^{70a}, E.W. Varnes⁶,
 C. Varni¹⁶, T. Varol¹⁵⁴, D. Varouchas⁶², K.E. Varvell¹⁵³, M.E. Vasile^{25b}, L. Vaslin³⁶, G.A. Vasquez¹⁷¹,
 F. Vazeille³⁶, D. Vazquez Furelos¹², T. Vazquez Schroeder³⁴, J. Veatch⁵¹, V. Vecchio⁹⁷, M.J. Veen¹¹⁵,
 I. Veliscek¹³⁰, L.M. Veloce¹⁶², F. Veloso^{135a,135c}, S. Veneziano^{70a}, A. Ventura^{65a,65b}, A. Verbytskyi¹¹¹,
 M. Verducci^{69a,69b}, C. Vergis²², M. Verissimo De Araujo^{78b}, W. Verkerke¹¹⁵, A.T. Vermeulen¹¹⁵,
 J.C. Vermeulen¹¹⁵, C. Vernieri¹⁴⁹, P.J. Verschuuren⁹¹, M. Vessella⁹⁹, M.L. Vesterbacka¹²¹,
 M.C. Vetterli^{148,aj}, A. Vgenopoulos¹⁵⁸, N. Viaux Maira^{142e}, T. Vickey¹⁴⁵, O.E. Vickey Boeriu¹⁴⁵,
 G.H.A. Viehhauser¹³⁰, L. Vignani^{59b}, M. Villa^{21b,21a}, M. Villaplana Perez¹⁶⁹, E.M. Villhauer⁴⁸,
 E. Vilucchi⁴⁹, M.G. Vincter³², G.S. Virdee¹⁹, A. Vishwakarma⁴⁸, C. Vittori^{21b,21a}, I. Vivarelli¹⁵²,
 V. Vladimirov¹⁷³, E. Voevodina¹¹¹, M. Vogel¹⁷⁷, P. Vokac¹³⁷, J. Von Ahnen⁴⁴, E. Von Toerne²²,
 V. Vorobel¹³⁸, K. Vorobev¹⁰⁸, M. Vos¹⁶⁹, J.H. Vosseveld⁸⁸, M. Vozak⁹⁷, L. Vozdecky⁹⁰, N. Vranjes¹⁴,
 M. Vranjes Milosavljevic¹⁴, V. Vrba^{137,*}, M. Vreeswijk¹¹⁵, N.K. Vu⁹⁸, R. Vuillermet³⁴, O.V. Vujanovic⁹⁶,
 I. Vukotic³⁵, S. Wada¹⁶⁴, C. Wagner⁹⁹, W. Wagner¹⁷⁷, S. Wahdan¹⁷⁷, H. Wahlberg⁸⁶, R. Wakasa¹⁶⁴,
 M. Wakida¹¹², V.M. Walbrecht¹¹¹, J. Walder¹³⁹, R. Walker¹¹⁰, S.D. Walker⁹¹, W. Walkowiak¹⁴⁷,
 A.M. Wang⁵⁷, A.Z. Wang¹⁷⁶, C. Wang^{58a}, C. Wang^{58c}, H. Wang¹⁶, J. Wang^{60a}, P. Wang⁴⁰, R.-J. Wang⁹⁶,
 R. Wang⁵⁷, R. Wang¹¹⁶, S.M. Wang¹⁵⁴, S. Wang^{58b}, T. Wang^{58a}, W.T. Wang⁷⁵, W.X. Wang^{58a}, X. Wang^{13c},
 X. Wang¹⁶⁸, X. Wang^{58c}, Y. Wang^{58a}, Z. Wang¹⁰², C. Wanotayaroj³⁴, A. Warburton¹⁰⁰, C.P. Ward³⁰,
 R.J. Ward¹⁹, N. Warrack⁵⁵, A.T. Watson¹⁹, M.F. Watson¹⁹, G. Watts¹⁴⁴, B.M. Waugh⁹², A.F. Webb¹⁰,
 C. Weber²⁷, M.S. Weber¹⁸, S.A. Weber³², S.M. Weber^{59a}, C. Wei^{58a}, Y. Wei¹³⁰, A.R. Weidberg¹³⁰,
 J. Weingarten⁴⁵, M. Weirich⁹⁶, C. Weiser⁵⁰, T. Wenaus²⁷, B. Wendland⁴⁵, T. Wengler³⁴, S. Wenig³⁴,
 N. Wermes²², M. Wessels^{59a}, K. Whalen¹²⁷, A.M. Wharton⁸⁷, A.S. White⁵⁷, A. White⁷, M.J. White¹,
 D. Whiteson¹⁶⁶, L. Wickremasinghe¹²⁸, W. Wiedenmann¹⁷⁶, C. Wiel⁴⁶, M. Wielers¹³⁹, N. Wieseotte⁹⁶,
 C. Wiglesworth³⁸, L.A.M. Wiik-Fuchs⁵⁰, D.J. Wilbern¹²⁴, H.G. Wilkens³⁴, L.J. Wilkins⁹¹,
 D.M. Williams³⁷, H.H. Williams¹³², S. Williams³⁰, S. Willocq⁹⁹, P.J. Windischhofer¹³⁰,
 I. Wingerter-Seez⁴, F. Winklmeier¹²⁷, B.T. Winter⁵⁰, M. Wittgen¹⁴⁹, M. Wobisch⁹³, A. Wolf⁹⁶,
 R. Wölker¹³⁰, J. Wollrath¹⁶⁶, M.W. Wolter⁸², H. Wolters^{135a,135c}, V.W.S. Wong¹⁷⁰, A.F. Wongel⁴⁴,
 S.D. Worm⁴⁴, B.K. Wosiek⁸², K.W. Woźniak⁸², K. Wraight⁵⁵, J. Wu^{13a,13d}, S.L. Wu¹⁷⁶, X. Wu⁵²,
 Y. Wu^{58a}, Z. Wu^{140,58a}, J. Wuerzinger¹³⁰, T.R. Wyatt⁹⁷, B.M. Wynne⁴⁸, S. Xella³⁸, L. Xia^{13c}, M. Xia^{13b},
 J. Xiang^{60c}, X. Xiao¹⁰², M. Xie^{58a}, X. Xie^{58a}, I. Xioidis¹⁵², D. Xu^{13a}, H. Xu^{58a}, H. Xu^{58a}, L. Xu^{58a},
 R. Xu¹³², T. Xu^{58a}, W. Xu¹⁰², Y. Xu^{13b}, Z. Xu^{58b}, Z. Xu¹⁴⁹, B. Yabsley¹⁵³, S. Yacoob^{31a}, N. Yamaguchi⁸⁵,
 Y. Yamaguchi¹⁶⁰, M. Yamatani¹⁵⁹, H. Yamauchi¹⁶⁴, T. Yamazaki¹⁶, Y. Yamazaki⁸⁰, J. Yan^{58c}, S. Yan¹³⁰,
 Z. Yan²³, H.J. Yang^{58c,58d}, H.T. Yang¹⁶, S. Yang^{58a}, T. Yang^{60c}, X. Yang^{58a}, X. Yang^{13a}, Y. Yang¹⁵⁹,
 Z. Yang^{102,58a}, W.-M. Yao¹⁶, Y.C. Yap⁴⁴, H. Ye^{13c}, J. Ye⁴⁰, S. Ye²⁷, I. Yeletsikh⁷⁷, M.R. Yexley⁸⁷,
 P. Yin³⁷, K. Yorita¹⁷⁴, K. Yoshihara⁷⁶, C.J.S. Young⁵⁰, C. Young¹⁴⁹, M. Yuan¹⁰², R. Yuan^{58b,i}, X. Yue^{59a},
 M. Zaazoua^{33e}, B. Zabinski⁸², G. Zacharis⁹, E. Zaid⁴⁸, A.M. Zaitsev^{118,ae}, T. Zakareishvili^{155b},
 N. Zakharchuk³², S. Zambito³⁴, D. Zanzi⁵⁰, S.V. Zeißner⁴⁵, C. Zeitnitz¹⁷⁷, J.C. Zeng¹⁶⁸, D.T. Zenger Jr²⁴,
 O. Zenin¹¹⁸, T. Ženiš^{26a}, S. Zenz⁹⁰, S. Zerradi^{33a}, D. Zerwas⁶², B. Zhang^{13c}, D.F. Zhang¹⁴⁵, G. Zhang^{13b},
 J. Zhang⁵, K. Zhang^{13a}, L. Zhang^{13c}, M. Zhang¹⁶⁸, R. Zhang¹⁷⁶, S. Zhang¹⁰², X. Zhang^{58c}, X. Zhang^{58b},
 Z. Zhang⁶², P. Zhao⁴⁷, T. Zhao^{58b}, Y. Zhao¹⁴¹, Z. Zhao^{58a}, A. Zhemchugov⁷⁷, Z. Zheng¹⁴⁹, D. Zhong¹⁶⁸,
 B. Zhou¹⁰², C. Zhou¹⁷⁶, H. Zhou⁶, N. Zhou^{58c}, Y. Zhou⁶, C.G. Zhu^{58b}, C. Zhu^{13a,13d}, H.L. Zhu^{58a},
 H. Zhu^{13a}, J. Zhu¹⁰², Y. Zhu^{58a}, X. Zhuang^{13a}, K. Zhukov¹⁰⁷, V. Zhulanov^{117b,117a}, D. Ziemska⁶³,
 N.I. Zimine⁷⁷, S. Zimmermann^{50,*}, J. Zinsser^{59b}, M. Ziolkowski¹⁴⁷, L. Živković¹⁴, A. Zoccoli^{21b,21a},
 K. Zoch⁵², T.G. Zorbas¹⁴⁵, O. Zormpa⁴², W. Zou³⁷, L. Zwalinski³⁴.

- ¹Department of Physics, University of Adelaide, Adelaide; Australia.
- ²Department of Physics, University of Alberta, Edmonton AB; Canada.
- ³(^a)Department of Physics, Ankara University, Ankara; (^b)Istanbul Aydin University, Application and Research Center for Advanced Studies, Istanbul; (^c)Division of Physics, TOBB University of Economics and Technology, Ankara; Turkey.
- ⁴LAPP, Univ. Savoie Mont Blanc, CNRS/IN2P3, Annecy ; France.
- ⁵High Energy Physics Division, Argonne National Laboratory, Argonne IL; United States of America.
- ⁶Department of Physics, University of Arizona, Tucson AZ; United States of America.
- ⁷Department of Physics, University of Texas at Arlington, Arlington TX; United States of America.
- ⁸Physics Department, National and Kapodistrian University of Athens, Athens; Greece.
- ⁹Physics Department, National Technical University of Athens, Zografou; Greece.
- ¹⁰Department of Physics, University of Texas at Austin, Austin TX; United States of America.
- ¹¹(^a)Bahcesehir University, Faculty of Engineering and Natural Sciences, Istanbul; (^b)Istanbul Bilgi University, Faculty of Engineering and Natural Sciences, Istanbul; (^c)Department of Physics, Bogazici University, Istanbul; (^d)Department of Physics Engineering, Gaziantep University, Gaziantep; Turkey.
- ¹²Institut de Física d'Altes Energies (IFAE), Barcelona Institute of Science and Technology, Barcelona; Spain.
- ¹³(^a)Institute of High Energy Physics, Chinese Academy of Sciences, Beijing; (^b)Physics Department, Tsinghua University, Beijing; (^c)Department of Physics, Nanjing University, Nanjing; (^d)University of Chinese Academy of Science (UCAS), Beijing; China.
- ¹⁴Institute of Physics, University of Belgrade, Belgrade; Serbia.
- ¹⁵Department for Physics and Technology, University of Bergen, Bergen; Norway.
- ¹⁶Physics Division, Lawrence Berkeley National Laboratory and University of California, Berkeley CA; United States of America.
- ¹⁷Institut für Physik, Humboldt Universität zu Berlin, Berlin; Germany.
- ¹⁸Albert Einstein Center for Fundamental Physics and Laboratory for High Energy Physics, University of Bern, Bern; Switzerland.
- ¹⁹School of Physics and Astronomy, University of Birmingham, Birmingham; United Kingdom.
- ²⁰(^a)Facultad de Ciencias y Centro de Investigaciones, Universidad Antonio Nariño, Bogotá; (^b)Departamento de Física, Universidad Nacional de Colombia, Bogotá; Colombia.
- ²¹(^a)Dipartimento di Fisica e Astronomia A. Righi, Università di Bologna, Bologna; (^b)INFN Sezione di Bologna; Italy.
- ²²Physikalisches Institut, Universität Bonn, Bonn; Germany.
- ²³Department of Physics, Boston University, Boston MA; United States of America.
- ²⁴Department of Physics, Brandeis University, Waltham MA; United States of America.
- ²⁵(^a)Transilvania University of Brasov, Brasov; (^b)Horia Hulubei National Institute of Physics and Nuclear Engineering, Bucharest; (^c)Department of Physics, Alexandru Ioan Cuza University of Iasi, Iasi; (^d)National Institute for Research and Development of Isotopic and Molecular Technologies, Physics Department, Cluj-Napoca; (^e)University Politehnica Bucharest, Bucharest; (^f)West University in Timisoara, Timisoara; Romania.
- ²⁶(^a)Faculty of Mathematics, Physics and Informatics, Comenius University, Bratislava; (^b)Department of Subnuclear Physics, Institute of Experimental Physics of the Slovak Academy of Sciences, Kosice; Slovak Republic.
- ²⁷Physics Department, Brookhaven National Laboratory, Upton NY; United States of America.
- ²⁸Departamento de Física (FCEN) and IFIBA, Universidad de Buenos Aires and CONICET, Buenos Aires; Argentina.
- ²⁹California State University, CA; United States of America.

- ³⁰Cavendish Laboratory, University of Cambridge, Cambridge; United Kingdom.
- ³¹(^a)Department of Physics, University of Cape Town, Cape Town; (^b)iThemba Labs, Western Cape; (^c)Department of Mechanical Engineering Science, University of Johannesburg, Johannesburg; (^d)National Institute of Physics, University of the Philippines Diliman (Philippines); (^e)University of South Africa, Department of Physics, Pretoria; (^f) School of Physics, University of the Witwatersrand, Johannesburg; South Africa.
- ³²Department of Physics, Carleton University, Ottawa ON; Canada.
- ³³(^a)Faculté des Sciences Ain Chock, Réseau Universitaire de Physique des Hautes Energies - Université Hassan II, Casablanca; (^b)Faculté des Sciences, Université Ibn-Tofail, Kénitra; (^c)Faculté des Sciences Semlalia, Université Cadi Ayyad, LPHEA-Marrakech; (^d)LPMR, Faculté des Sciences, Université Mohamed Premier, Oujda; (^e)Faculté des sciences, Université Mohammed V, Rabat; (^f) Mohammed VI Polytechnic University, Ben Guerir; Morocco.
- ³⁴CERN, Geneva; Switzerland.
- ³⁵Enrico Fermi Institute, University of Chicago, Chicago IL; United States of America.
- ³⁶LPC, Université Clermont Auvergne, CNRS/IN2P3, Clermont-Ferrand; France.
- ³⁷Nevis Laboratory, Columbia University, Irvington NY; United States of America.
- ³⁸Niels Bohr Institute, University of Copenhagen, Copenhagen; Denmark.
- ³⁹(^a)Dipartimento di Fisica, Università della Calabria, Rende; (^b)INFN Gruppo Collegato di Cosenza, Laboratori Nazionali di Frascati; Italy.
- ⁴⁰Physics Department, Southern Methodist University, Dallas TX; United States of America.
- ⁴¹Physics Department, University of Texas at Dallas, Richardson TX; United States of America.
- ⁴²National Centre for Scientific Research "Demokritos", Agia Paraskevi; Greece.
- ⁴³(^a)Department of Physics, Stockholm University; (^b)Oskar Klein Centre, Stockholm; Sweden.
- ⁴⁴Deutsches Elektronen-Synchrotron DESY, Hamburg and Zeuthen; Germany.
- ⁴⁵Fakultät Physik, Technische Universität Dortmund, Dortmund; Germany.
- ⁴⁶Institut für Kern- und Teilchenphysik, Technische Universität Dresden, Dresden; Germany.
- ⁴⁷Department of Physics, Duke University, Durham NC; United States of America.
- ⁴⁸SUPA - School of Physics and Astronomy, University of Edinburgh, Edinburgh; United Kingdom.
- ⁴⁹INFN e Laboratori Nazionali di Frascati, Frascati; Italy.
- ⁵⁰Physikalisches Institut, Albert-Ludwigs-Universität Freiburg, Freiburg; Germany.
- ⁵¹II. Physikalisches Institut, Georg-August-Universität Göttingen, Göttingen; Germany.
- ⁵²Département de Physique Nucléaire et Corpusculaire, Université de Genève, Genève; Switzerland.
- ⁵³(^a)Dipartimento di Fisica, Università di Genova, Genova; (^b)INFN Sezione di Genova; Italy.
- ⁵⁴II. Physikalisches Institut, Justus-Liebig-Universität Giessen, Giessen; Germany.
- ⁵⁵SUPA - School of Physics and Astronomy, University of Glasgow, Glasgow; United Kingdom.
- ⁵⁶LPSC, Université Grenoble Alpes, CNRS/IN2P3, Grenoble INP, Grenoble; France.
- ⁵⁷Laboratory for Particle Physics and Cosmology, Harvard University, Cambridge MA; United States of America.
- ⁵⁸(^a)Department of Modern Physics and State Key Laboratory of Particle Detection and Electronics, University of Science and Technology of China, Hefei; (^b)Institute of Frontier and Interdisciplinary Science and Key Laboratory of Particle Physics and Particle Irradiation (MOE), Shandong University, Qingdao; (^c)School of Physics and Astronomy, Shanghai Jiao Tong University, Key Laboratory for Particle Astrophysics and Cosmology (MOE), SKLPPC, Shanghai; (^d)Tsungh-Dao Lee Institute, Shanghai; China.
- ⁵⁹(^a)Kirchhoff-Institut für Physik, Ruprecht-Karls-Universität Heidelberg, Heidelberg; (^b)Physikalisches Institut, Ruprecht-Karls-Universität Heidelberg, Heidelberg; Germany.
- ⁶⁰(^a)Department of Physics, Chinese University of Hong Kong, Shatin, N.T., Hong Kong; (^b)Department of Physics, University of Hong Kong, Hong Kong; (^c)Department of Physics and Institute for Advanced

- Study, Hong Kong University of Science and Technology, Clear Water Bay, Kowloon, Hong Kong; China.
- ⁶¹Department of Physics, National Tsing Hua University, Hsinchu; Taiwan.
- ⁶²IJCLab, Université Paris-Saclay, CNRS/IN2P3, 91405, Orsay; France.
- ⁶³Department of Physics, Indiana University, Bloomington IN; United States of America.
- ⁶⁴(^a)INFN Gruppo Collegato di Udine, Sezione di Trieste, Udine; (^b)ICTP, Trieste; (^c)Dipartimento Politecnico di Ingegneria e Architettura, Università di Udine, Udine; Italy.
- ⁶⁵(^a)INFN Sezione di Lecce; (^b)Dipartimento di Matematica e Fisica, Università del Salento, Lecce; Italy.
- ⁶⁶(^a)INFN Sezione di Milano; (^b)Dipartimento di Fisica, Università di Milano, Milano; Italy.
- ⁶⁷(^a)INFN Sezione di Napoli; (^b)Dipartimento di Fisica, Università di Napoli, Napoli; Italy.
- ⁶⁸(^a)INFN Sezione di Pavia; (^b)Dipartimento di Fisica, Università di Pavia, Pavia; Italy.
- ⁶⁹(^a)INFN Sezione di Pisa; (^b)Dipartimento di Fisica E. Fermi, Università di Pisa, Pisa; Italy.
- ⁷⁰(^a)INFN Sezione di Roma; (^b)Dipartimento di Fisica, Sapienza Università di Roma, Roma; Italy.
- ⁷¹(^a)INFN Sezione di Roma Tor Vergata; (^b)Dipartimento di Fisica, Università di Roma Tor Vergata, Roma; Italy.
- ⁷²(^a)INFN Sezione di Roma Tre; (^b)Dipartimento di Matematica e Fisica, Università Roma Tre, Roma; Italy.
- ⁷³(^a)INFN-TIFPA; (^b)Università degli Studi di Trento, Trento; Italy.
- ⁷⁴Institut für Astro- und Teilchenphysik, Leopold-Franzens-Universität, Innsbruck; Austria.
- ⁷⁵University of Iowa, Iowa City IA; United States of America.
- ⁷⁶Department of Physics and Astronomy, Iowa State University, Ames IA; United States of America.
- ⁷⁷Joint Institute for Nuclear Research, Dubna; Russia.
- ⁷⁸(^a)Departamento de Engenharia Elétrica, Universidade Federal de Juiz de Fora (UFJF), Juiz de Fora; (^b)Universidade Federal do Rio De Janeiro COPPE/EE/IF, Rio de Janeiro; (^c)Instituto de Física, Universidade de São Paulo, São Paulo; Brazil.
- ⁷⁹KEK, High Energy Accelerator Research Organization, Tsukuba; Japan.
- ⁸⁰Graduate School of Science, Kobe University, Kobe; Japan.
- ⁸¹(^a)AGH University of Science and Technology, Faculty of Physics and Applied Computer Science, Krakow; (^b)Marian Smoluchowski Institute of Physics, Jagiellonian University, Krakow; Poland.
- ⁸²Institute of Nuclear Physics Polish Academy of Sciences, Krakow; Poland.
- ⁸³Faculty of Science, Kyoto University, Kyoto; Japan.
- ⁸⁴Kyoto University of Education, Kyoto; Japan.
- ⁸⁵Research Center for Advanced Particle Physics and Department of Physics, Kyushu University, Fukuoka ; Japan.
- ⁸⁶Instituto de Física La Plata, Universidad Nacional de La Plata and CONICET, La Plata; Argentina.
- ⁸⁷Physics Department, Lancaster University, Lancaster; United Kingdom.
- ⁸⁸Oliver Lodge Laboratory, University of Liverpool, Liverpool; United Kingdom.
- ⁸⁹Department of Experimental Particle Physics, Jožef Stefan Institute and Department of Physics, University of Ljubljana, Ljubljana; Slovenia.
- ⁹⁰School of Physics and Astronomy, Queen Mary University of London, London; United Kingdom.
- ⁹¹Department of Physics, Royal Holloway University of London, Egham; United Kingdom.
- ⁹²Department of Physics and Astronomy, University College London, London; United Kingdom.
- ⁹³Louisiana Tech University, Ruston LA; United States of America.
- ⁹⁴Fysiska institutionen, Lunds universitet, Lund; Sweden.
- ⁹⁵Departamento de Física Teórica C-15 and CIAFF, Universidad Autónoma de Madrid, Madrid; Spain.
- ⁹⁶Institut für Physik, Universität Mainz, Mainz; Germany.
- ⁹⁷School of Physics and Astronomy, University of Manchester, Manchester; United Kingdom.
- ⁹⁸CPPM, Aix-Marseille Université, CNRS/IN2P3, Marseille; France.

- ⁹⁹Department of Physics, University of Massachusetts, Amherst MA; United States of America.
- ¹⁰⁰Department of Physics, McGill University, Montreal QC; Canada.
- ¹⁰¹School of Physics, University of Melbourne, Victoria; Australia.
- ¹⁰²Department of Physics, University of Michigan, Ann Arbor MI; United States of America.
- ¹⁰³Department of Physics and Astronomy, Michigan State University, East Lansing MI; United States of America.
- ¹⁰⁴B.I. Stepanov Institute of Physics, National Academy of Sciences of Belarus, Minsk; Belarus.
- ¹⁰⁵Research Institute for Nuclear Problems of Byelorussian State University, Minsk; Belarus.
- ¹⁰⁶Group of Particle Physics, University of Montreal, Montreal QC; Canada.
- ¹⁰⁷P.N. Lebedev Physical Institute of the Russian Academy of Sciences, Moscow; Russia.
- ¹⁰⁸National Research Nuclear University MEPhI, Moscow; Russia.
- ¹⁰⁹D.V. Skobel'syn Institute of Nuclear Physics, M.V. Lomonosov Moscow State University, Moscow; Russia.
- ¹¹⁰Fakultät für Physik, Ludwig-Maximilians-Universität München, München; Germany.
- ¹¹¹Max-Planck-Institut für Physik (Werner-Heisenberg-Institut), München; Germany.
- ¹¹²Graduate School of Science and Kobayashi-Maskawa Institute, Nagoya University, Nagoya; Japan.
- ¹¹³Department of Physics and Astronomy, University of New Mexico, Albuquerque NM; United States of America.
- ¹¹⁴Institute for Mathematics, Astrophysics and Particle Physics, Radboud University/Nikhef, Nijmegen; Netherlands.
- ¹¹⁵Nikhef National Institute for Subatomic Physics and University of Amsterdam, Amsterdam; Netherlands.
- ¹¹⁶Department of Physics, Northern Illinois University, DeKalb IL; United States of America.
- ¹¹⁷(^a) Budker Institute of Nuclear Physics and NSU, SB RAS, Novosibirsk; (^b) Novosibirsk State University Novosibirsk; Russia.
- ¹¹⁸Institute for High Energy Physics of the National Research Centre Kurchatov Institute, Protvino; Russia.
- ¹¹⁹Institute for Theoretical and Experimental Physics named by A.I. Alikhanov of National Research Centre "Kurchatov Institute", Moscow; Russia.
- ¹²⁰(^a) New York University Abu Dhabi, Abu Dhabi; (^b) United Arab Emirates University, Al Ain; (^c) University of Sharjah, Sharjah; United Arab Emirates.
- ¹²¹Department of Physics, New York University, New York NY; United States of America.
- ¹²²Ochanomizu University, Otsuka, Bunkyo-ku, Tokyo; Japan.
- ¹²³Ohio State University, Columbus OH; United States of America.
- ¹²⁴Homer L. Dodge Department of Physics and Astronomy, University of Oklahoma, Norman OK; United States of America.
- ¹²⁵Department of Physics, Oklahoma State University, Stillwater OK; United States of America.
- ¹²⁶Palacký University, Joint Laboratory of Optics, Olomouc; Czech Republic.
- ¹²⁷Institute for Fundamental Science, University of Oregon, Eugene, OR; United States of America.
- ¹²⁸Graduate School of Science, Osaka University, Osaka; Japan.
- ¹²⁹Department of Physics, University of Oslo, Oslo; Norway.
- ¹³⁰Department of Physics, Oxford University, Oxford; United Kingdom.
- ¹³¹LPNHE, Sorbonne Université, Université Paris Cité, CNRS/IN2P3, Paris; France.
- ¹³²Department of Physics, University of Pennsylvania, Philadelphia PA; United States of America.
- ¹³³Konstantinov Nuclear Physics Institute of National Research Centre "Kurchatov Institute", PNPI, St. Petersburg; Russia.
- ¹³⁴Department of Physics and Astronomy, University of Pittsburgh, Pittsburgh PA; United States of America.

- ¹³⁵(*a*) Laboratório de Instrumentação e Física Experimental de Partículas - LIP, Lisboa; (*b*) Departamento de Física, Faculdade de Ciências, Universidade de Lisboa, Lisboa; (*c*) Departamento de Física, Universidade de Coimbra, Coimbra; (*d*) Centro de Física Nuclear da Universidade de Lisboa, Lisboa; (*e*) Departamento de Física, Universidade do Minho, Braga; (*f*) Departamento de Física Teórica y del Cosmos, Universidad de Granada, Granada (Spain); (*g*) Instituto Superior Técnico, Universidade de Lisboa, Lisboa; Portugal.
- ¹³⁶Institute of Physics of the Czech Academy of Sciences, Prague; Czech Republic.
- ¹³⁷Czech Technical University in Prague, Prague; Czech Republic.
- ¹³⁸Charles University, Faculty of Mathematics and Physics, Prague; Czech Republic.
- ¹³⁹Particle Physics Department, Rutherford Appleton Laboratory, Didcot; United Kingdom.
- ¹⁴⁰IRFU, CEA, Université Paris-Saclay, Gif-sur-Yvette; France.
- ¹⁴¹Santa Cruz Institute for Particle Physics, University of California Santa Cruz, Santa Cruz CA; United States of America.
- ¹⁴²(*a*) Departamento de Física, Pontificia Universidad Católica de Chile, Santiago; (*b*) Instituto de Investigación Multidisciplinario en Ciencia y Tecnología, y Departamento de Física, Universidad de La Serena; (*c*) Universidad Andres Bello, Department of Physics, Santiago; (*d*) Instituto de Alta Investigación, Universidad de Tarapacá, Arica; (*e*) Departamento de Física, Universidad Técnica Federico Santa María, Valparaíso; Chile.
- ¹⁴³Universidade Federal de São João del Rei (UFSJ), São João del Rei; Brazil.
- ¹⁴⁴Department of Physics, University of Washington, Seattle WA; United States of America.
- ¹⁴⁵Department of Physics and Astronomy, University of Sheffield, Sheffield; United Kingdom.
- ¹⁴⁶Department of Physics, Shinshu University, Nagano; Japan.
- ¹⁴⁷Department Physik, Universität Siegen, Siegen; Germany.
- ¹⁴⁸Department of Physics, Simon Fraser University, Burnaby BC; Canada.
- ¹⁴⁹SLAC National Accelerator Laboratory, Stanford CA; United States of America.
- ¹⁵⁰Department of Physics, Royal Institute of Technology, Stockholm; Sweden.
- ¹⁵¹Departments of Physics and Astronomy, Stony Brook University, Stony Brook NY; United States of America.
- ¹⁵²Department of Physics and Astronomy, University of Sussex, Brighton; United Kingdom.
- ¹⁵³School of Physics, University of Sydney, Sydney; Australia.
- ¹⁵⁴Institute of Physics, Academia Sinica, Taipei; Taiwan.
- ¹⁵⁵(*a*) E. Andronikashvili Institute of Physics, Iv. Javakhishvili Tbilisi State University, Tbilisi; (*b*) High Energy Physics Institute, Tbilisi State University, Tbilisi; Georgia.
- ¹⁵⁶Department of Physics, Technion, Israel Institute of Technology, Haifa; Israel.
- ¹⁵⁷Raymond and Beverly Sackler School of Physics and Astronomy, Tel Aviv University, Tel Aviv; Israel.
- ¹⁵⁸Department of Physics, Aristotle University of Thessaloniki, Thessaloniki; Greece.
- ¹⁵⁹International Center for Elementary Particle Physics and Department of Physics, University of Tokyo, Tokyo; Japan.
- ¹⁶⁰Department of Physics, Tokyo Institute of Technology, Tokyo; Japan.
- ¹⁶¹Tomsk State University, Tomsk; Russia.
- ¹⁶²Department of Physics, University of Toronto, Toronto ON; Canada.
- ¹⁶³(*a*) TRIUMF, Vancouver BC; (*b*) Department of Physics and Astronomy, York University, Toronto ON; Canada.
- ¹⁶⁴Division of Physics and Tomonaga Center for the History of the Universe, Faculty of Pure and Applied Sciences, University of Tsukuba, Tsukuba; Japan.
- ¹⁶⁵Department of Physics and Astronomy, Tufts University, Medford MA; United States of America.
- ¹⁶⁶Department of Physics and Astronomy, University of California Irvine, Irvine CA; United States of America.

- ¹⁶⁷Department of Physics and Astronomy, University of Uppsala, Uppsala; Sweden.
- ¹⁶⁸Department of Physics, University of Illinois, Urbana IL; United States of America.
- ¹⁶⁹Instituto de Física Corpuscular (IFIC), Centro Mixto Universidad de Valencia - CSIC, Valencia; Spain.
- ¹⁷⁰Department of Physics, University of British Columbia, Vancouver BC; Canada.
- ¹⁷¹Department of Physics and Astronomy, University of Victoria, Victoria BC; Canada.
- ¹⁷²Fakultät für Physik und Astronomie, Julius-Maximilians-Universität Würzburg, Würzburg; Germany.
- ¹⁷³Department of Physics, University of Warwick, Coventry; United Kingdom.
- ¹⁷⁴Waseda University, Tokyo; Japan.
- ¹⁷⁵Department of Particle Physics and Astrophysics, Weizmann Institute of Science, Rehovot; Israel.
- ¹⁷⁶Department of Physics, University of Wisconsin, Madison WI; United States of America.
- ¹⁷⁷Fakultät für Mathematik und Naturwissenschaften, Fachgruppe Physik, Bergische Universität Wuppertal, Wuppertal; Germany.
- ¹⁷⁸Department of Physics, Yale University, New Haven CT; United States of America.
- ^a Also at Borough of Manhattan Community College, City University of New York, New York NY; United States of America.
- ^b Also at Bruno Kessler Foundation, Trento; Italy.
- ^c Also at Center for High Energy Physics, Peking University; China.
- ^d Also at Centro Studi e Ricerche Enrico Fermi; Italy.
- ^e Also at CERN, Geneva; Switzerland.
- ^f Also at Département de Physique Nucléaire et Corpusculaire, Université de Genève, Genève; Switzerland.
- ^g Also at Departament de Física de la Universitat Autònoma de Barcelona, Barcelona; Spain.
- ^h Also at Department of Financial and Management Engineering, University of the Aegean, Chios; Greece.
- ⁱ Also at Department of Physics and Astronomy, Michigan State University, East Lansing MI; United States of America.
- ^j Also at Department of Physics and Astronomy, University of Louisville, Louisville, KY; United States of America.
- ^k Also at Department of Physics, Ben Gurion University of the Negev, Beer Sheva; Israel.
- ^l Also at Department of Physics, California State University, East Bay; United States of America.
- ^m Also at Department of Physics, California State University, Fresno; United States of America.
- ⁿ Also at Department of Physics, California State University, Sacramento; United States of America.
- ^o Also at Department of Physics, King's College London, London; United Kingdom.
- ^p Also at Department of Physics, St. Petersburg State Polytechnical University, St. Petersburg; Russia.
- ^q Also at Department of Physics, University of Fribourg, Fribourg; Switzerland.
- ^r Also at Faculty of Physics, M.V. Lomonosov Moscow State University, Moscow; Russia.
- ^s Also at Faculty of Physics, Sofia University, 'St. Kliment Ohridski', Sofia; Bulgaria.
- ^t Also at Graduate School of Science, Osaka University, Osaka; Japan.
- ^u Also at Hellenic Open University, Patras; Greece.
- ^v Also at Institutio Catalana de Recerca i Estudis Avancats, ICREA, Barcelona; Spain.
- ^w Also at Institut für Experimentalphysik, Universität Hamburg, Hamburg; Germany.
- ^x Also at Institute for Particle and Nuclear Physics, Wigner Research Centre for Physics, Budapest; Hungary.
- ^y Also at Institute of Particle Physics (IPP); Canada.
- ^z Also at Institute of Physics, Azerbaijan Academy of Sciences, Baku; Azerbaijan.
- ^{aa} Also at Institute of Theoretical Physics, Ilia State University, Tbilisi; Georgia.
- ^{ab} Also at Instituto de Física Teórica, IFT-UAM/CSIC, Madrid; Spain.
- ^{ac} Also at Istanbul University, Dept. of Physics, Istanbul; Turkey.

- ad* Also at Joint Institute for Nuclear Research, Dubna; Russia.
- ae* Also at Moscow Institute of Physics and Technology State University, Dolgoprudny; Russia.
- af* Also at National Research Nuclear University MEPhI, Moscow; Russia.
- ag* Also at Physics Department, An-Najah National University, Nablus; Palestine.
- ah* Also at Physikalisches Institut, Albert-Ludwigs-Universität Freiburg, Freiburg; Germany.
- ai* Also at The City College of New York, New York NY; United States of America.
- aj* Also at TRIUMF, Vancouver BC; Canada.
- ak* Also at Università di Napoli Parthenope, Napoli; Italy.
- al* Also at University of Chinese Academy of Sciences (UCAS), Beijing; China.
- am* Also at Yeditepe University, Physics Department, Istanbul; Turkey.
- * Deceased